SPARC4

Simultaneous Polarimeter and Rapid Camera in 4 bands

Claudia Vilega Rodrigues

claudia.rodrigues@inpe.br

Instituto Nacional de Pesquisas Espaciais

Divisão de Astrofísica

Laboratório Nacional de Astrofísica
4 de maio 2018

Objetivo deste seminário

- Apresentar o instrumento SPARC4 para o LNA: **corpo técnico** e de pesquisadores

- Dirimir dúvidas sobre o instrumento e o projeto

- Receber comentários sobre o instrumento e o projeto

O que é a SPARC4?

- Simultaneous Polarimeter And Rapid Camera in 4 bands
  - ✓ imageamento simultâneo em 4 bandas largas (griz SDSS)
  - ✓ polarimetria é uma opção do usuário
  - ✓ resolução temporal inferior a 1 segundo

- será instalada no telescópio de 1,6 m do **Observatório do Pico dos Dias/LNA**

O que é a SPARC4?

- Simultaneous Polarimeter And Rapid Camera in 4 bands
  - ✓ imageamento simultâneo em 4 bandas largas (griz SDSS)
  - ✓ polarimetria é uma opção do usuário
  - ✓ resolução temporal inferior a 1 segundo

- será instalada no telescópio de 1,6 m do **Observatório do Pico dos Dias/LNA**

O objetivo é que seja uma **facilidade** do observatório.

SPARC4 para quê?

- SPARC4 é um instrumento talhado para técnicas diferenciais:
  - ✓ fotometria diferencial;
  - ✓ polarimetria.

- O objetivo desse desenvolvimento é:
  - ✓ aumentar a eficiência do observatório, levando em consideração as condições atmosféricas do sítio;
  - ✓ produzir ciência competitiva no contexto mundial.

Atualmente - Dados de 4 noites

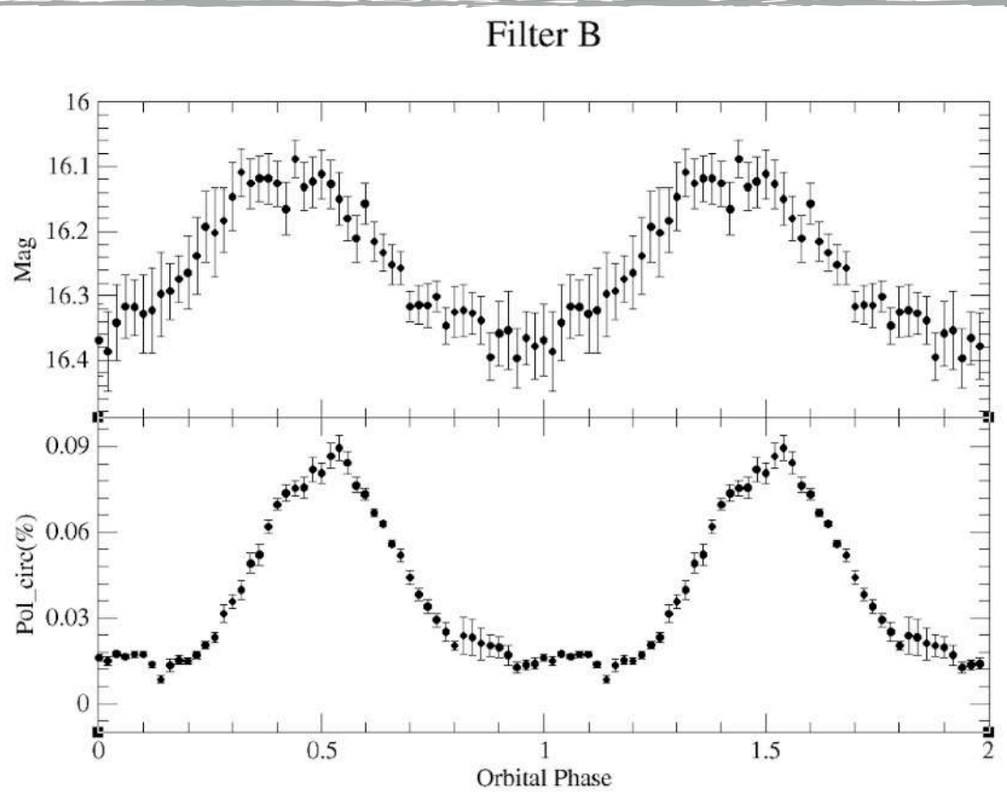

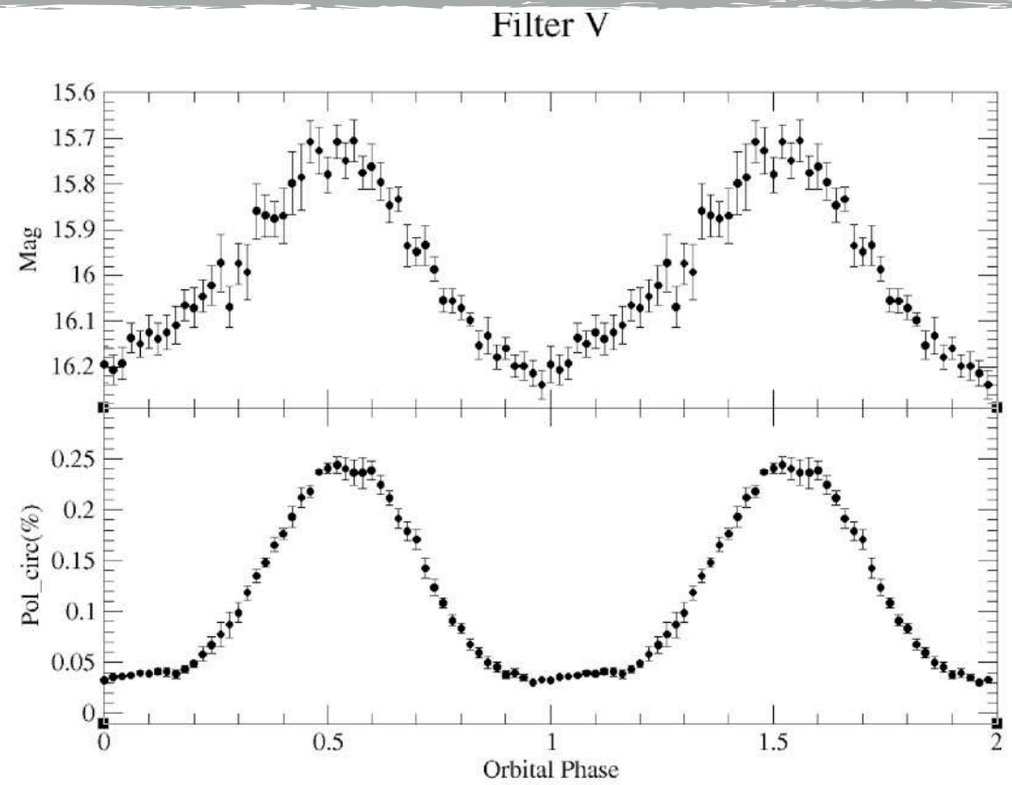

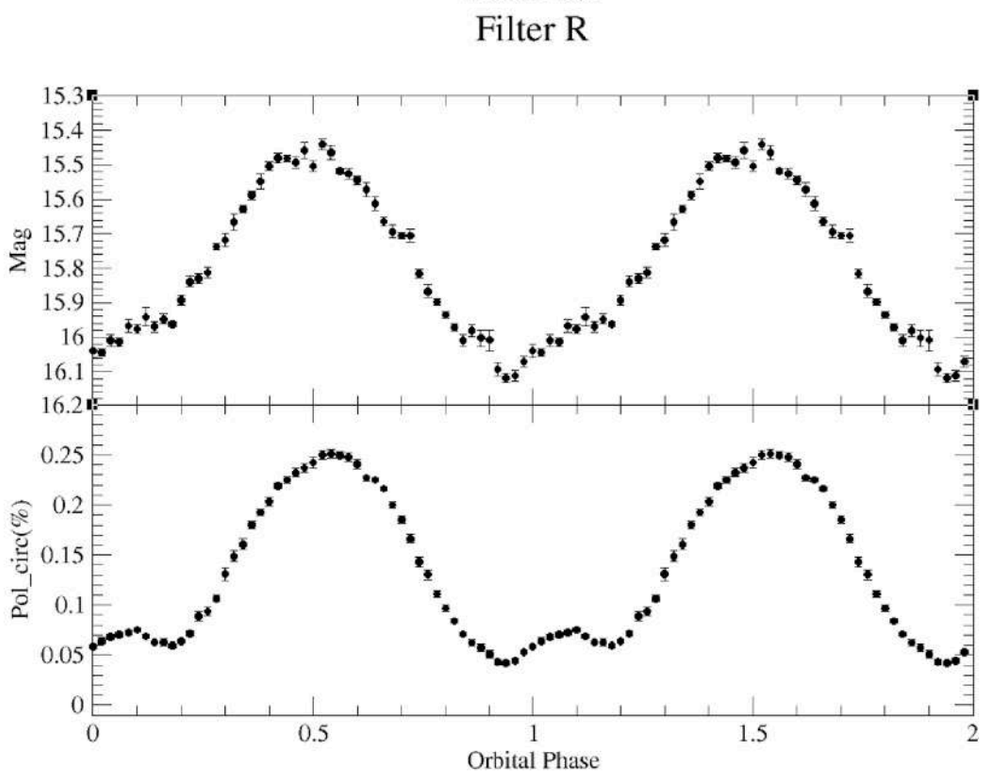

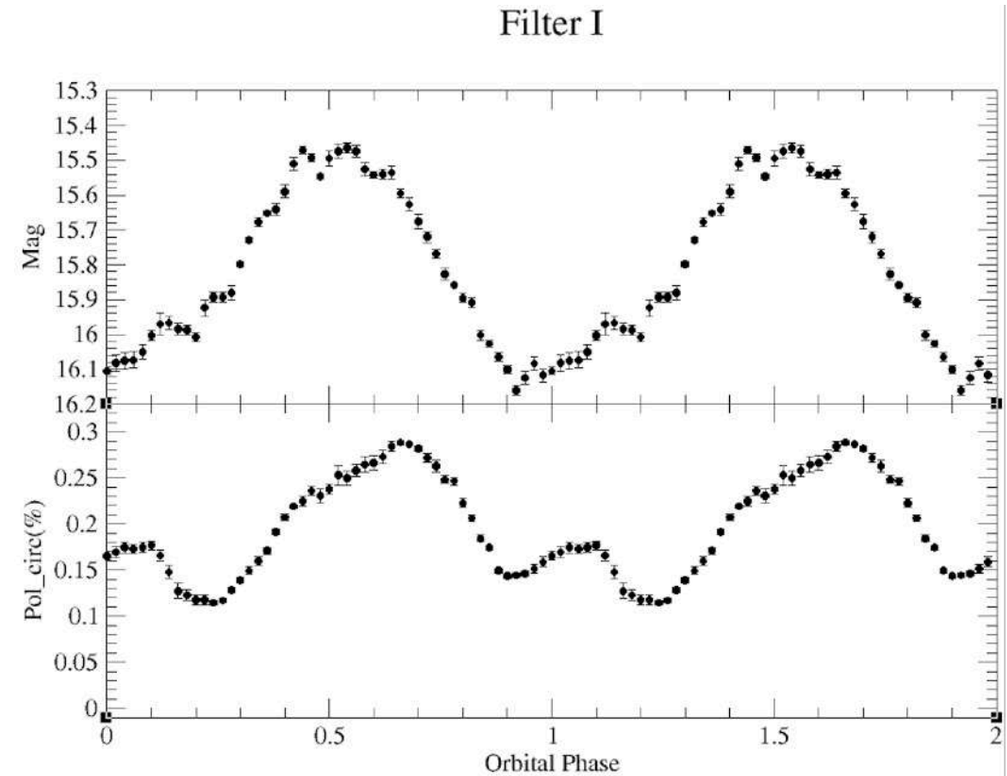

SPARC4


Filter B
Mag
Pol_circ(%)
Orbital Phase
Filter R
Filter I
Uma noite equivalente
a quatro!
Dados simultâneos!

Produtividade do OPD

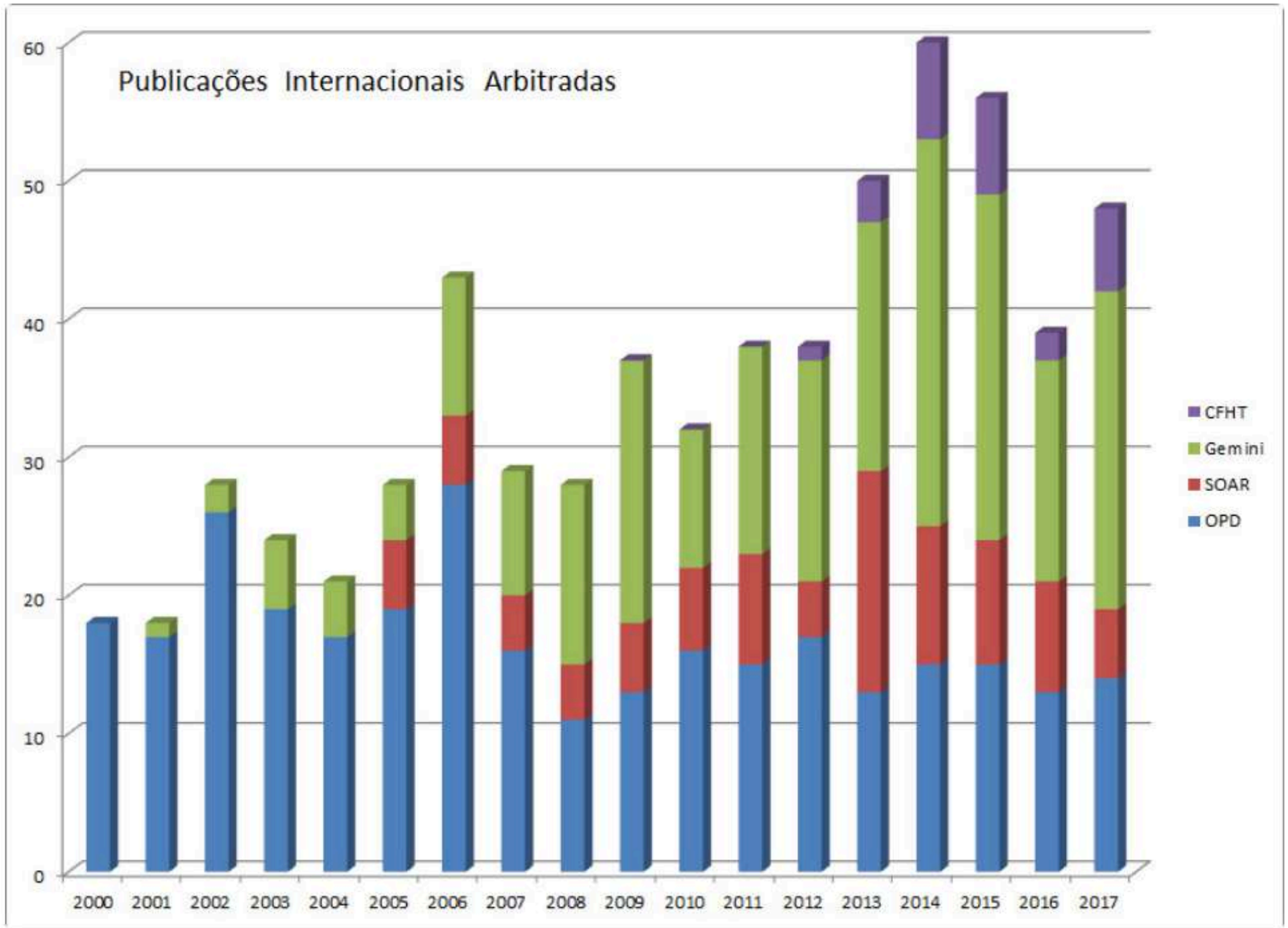

www.lna.br

OPD

- O OPD contribui com uma parcela não desprezível da produção dos observatórios gerenciados pelo LNA.

- A maioria dos artigos do OPD (da ordem de 70%) referem-se a dados de fotometria diferencial e/ou polarimetria.

Características SPARC4

Telescópio f#	f/10
Telescópio abertura	1.6m
Detetores científicos	Andor Ultra 888 (EMCCD)
Pixels	1024 x 1024
Tamanho do Pixel	13 µm
Final f#	f/5
Campo	5.7 arcmin x 5.7 arcmin
Escala de placa	0.35 arcsec/pixel
Detetor do autoguider (AG)	Andor Luca®
AG #Pixels	1000 x 1000
AG pixel size	8 µm
AG final f#	f/5
AG campo	3.4 arcmin x 3.4 arcmin
AG Escala de placa	0.20 arcsec/pixel
Bandas naturais	SDSS griz
Resolução temporal	<1 s (detector inteiro - readout mais rápido)

O projeto SPARC4

- O projeto SPARC4 tem por objetivo:
  - ✓ construir um instrumento;
  - ✓ desenvolver uma interface de controle com um front-end amigável;
  - ✓ produzir documentação para manutenção e uso;
  - ✓ entregar um instrumento testado;
  - ✓ entregar uma pipeline de redução.

Histórico

- **2009 Nov: Proposta de instrumento para LNA -** CVR e Francisco Jablonski
- 2011 Mai: Concessão de fundos pela Fapesp para realização do projeto conceitual
- **2012 Ago: Revisão do projeto conceitual**
- 2015 Mar: Primeira compra - dicróicos chegam no LNA (verba LNA + INPE)
- 2015 Jul: Entrega dos detetores científicos - INPE
- 2016 Jan: Computadores e data storage (Fapemig e INCT-A)
- **2016 Nov: Aprovação de projeto Finep suficiente para conclusão do instrumento**
- 2017 Mar: Óptica principal chega ao INPE
- 2017 Nov: Óptica polarimétrica chega ao INPE

Custo total estimado

US$ 700k

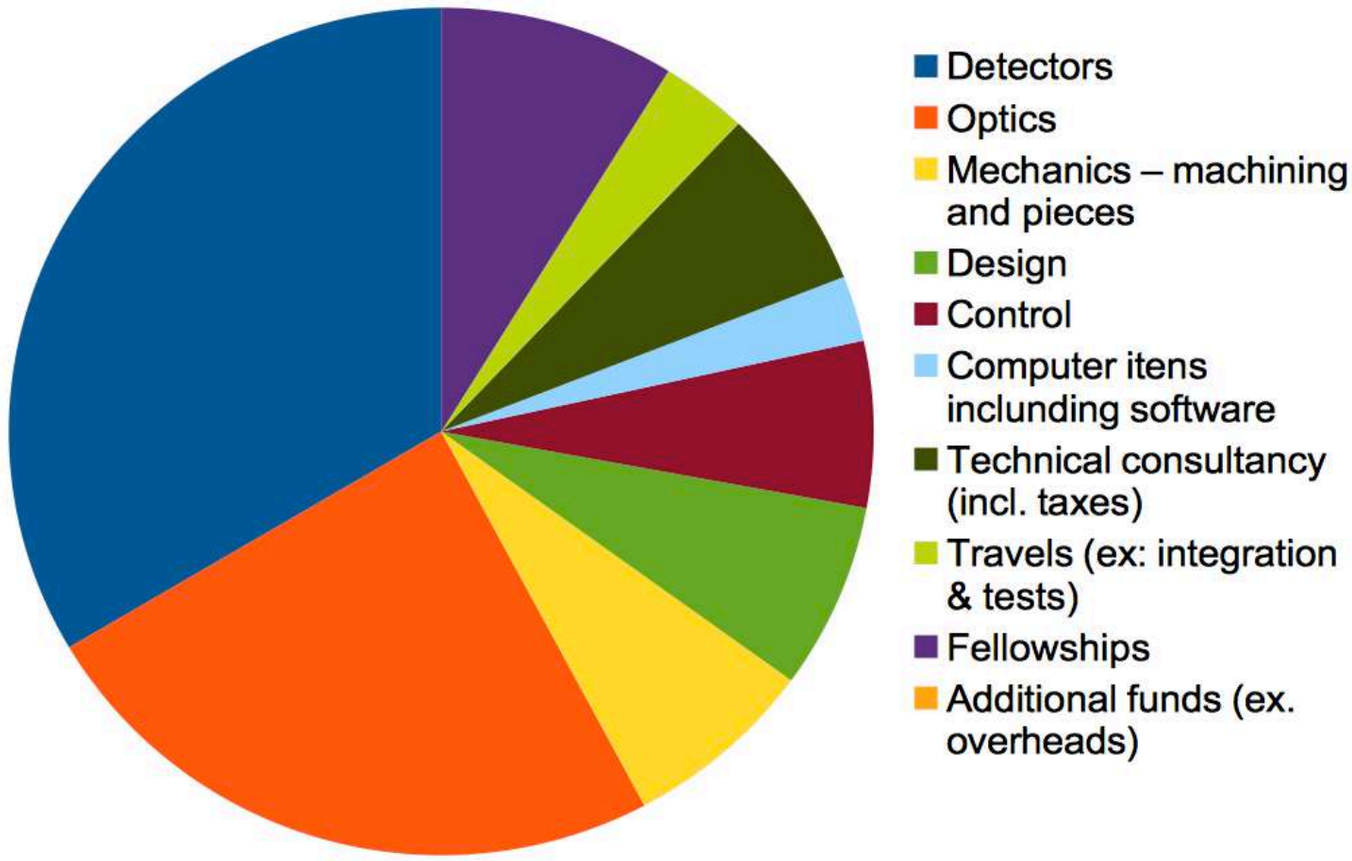

Financiamento

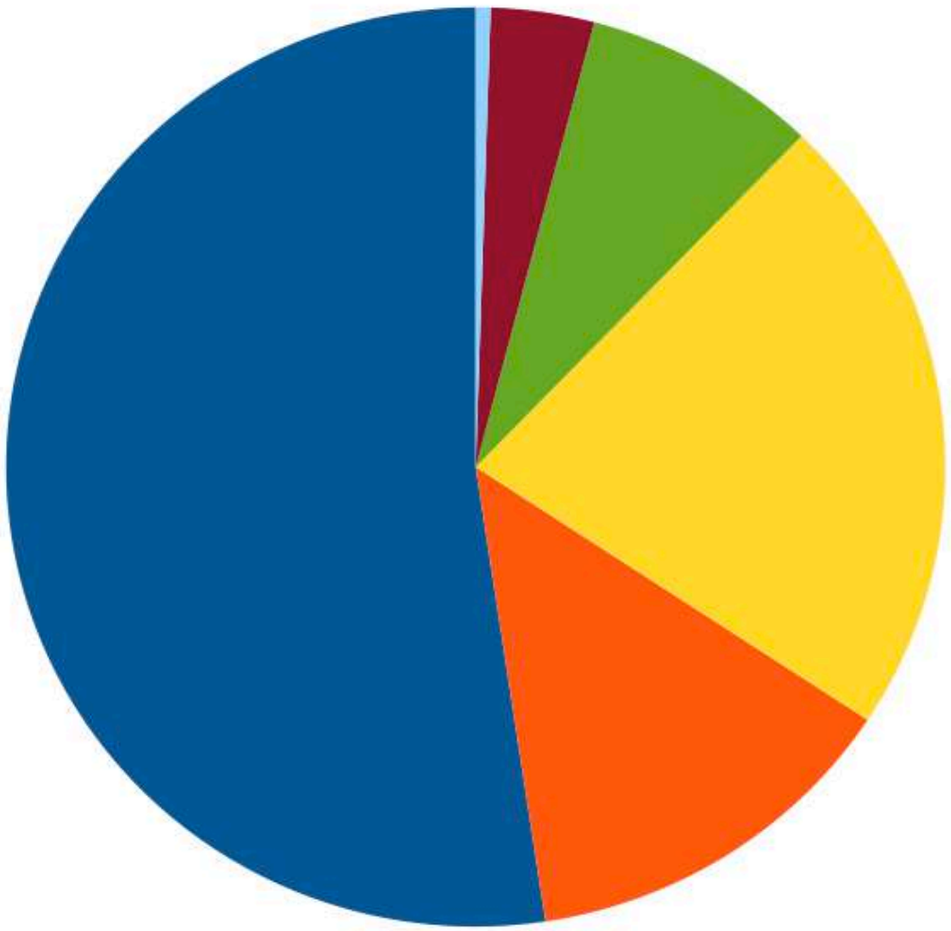

- Verba aprovada pela Finep é suficiente para completar o projeto, mas…
  - ✓ apenas parte foi liberada
    - suficiente para construção! :-)
  - ✓ liberação do restante da verba é incerta

Unidades da SPARC4

- A partir da flange do telescópio, o instrumento possui as seguintes unidades:
  - ✓ módulo de autoguiagem e autofocalização
  - ✓ unidade polarimétrica
  - ✓ colimador
  - ✓ caixa óptica
    - divisores de feixe dicróicos
    - suporte para filtros
    - câmeras redutoras
  - ✓ detectores

Unidades da SPARC4

- A partir da flange do telescópio, o instrumento possui as seguintes unidades:
  - ✓ módulo de autoguiagem e autofocalização
  - ✓ unidade polarimétrica
  - ✓ colimador
  - ✓ caixa óptica
    - divisores de feixe dicróicos
    - suporte para filtros
    - câmeras redutoras
  - ✓ detectores

No módulo de autoguiagem, haverá uma gaveta com um alimentador para o Echarpe.

Detetores científicos

Andor Ultra 888

Andor Ultra 888

- Detetores
  - ✓ Frame-transfer
  - ✓ EMCCDs
    - multiplicação de elétrons que possibilita utilização de alto ganho

- Aquisição: orçamento INPE

- Cada câmera possui janelas e coatings escolhidos para maximizar resposta espectral em cada banda

- Caracterização das câmeras feita por
  - ✓ Denis V. Bernandes e Eder Martioli

Excelente cosmética

Propriedades dentro da especificação

Characterization of the SPARC4 CCDs

D V Bernardes[1]; E Martioli[1]; C V Rodrigues[2].

[1]Laboratório Nacional de Astrofísica, Rua dos Estados Unidos, 154, Itajubá-MG, Brasil
[2]Instituto Nacional de Pesquisas Espaciais, Avenida dos Astronautas, 1758, São José dos Campos-SP, Brasil.

E-mail: dbernardes@lna.br, emartioli@lna.br, claudia.rodrigues@inpe.br.

Abstract. We present the photometric characterization of the four iXon Ultra 888 CCD cameras of the SPARC4 instrument, which will be installed on the 1.6 m telescope of the *Pico dos Dias* Observatory in Brazil. We applied experimental methodologies for a systematic characterization of the read noise, electronic gain, dark current, and quantum efficiency of the CCDs. We have analyzed the statistical distribution of the read noise, and also its spatial gradient and temporal variability, where we obtained an average value of the read noise of 6.33 electrons. We applied the Janesick method to determine the electronic gain, where we obtained an average value of 3.35 e-/ADU. We have also obtained an average dark current of 0.00014 e-/pix/s for CCD internal temperature of -70 °C. We have inspected the dependency of the dark current with temperature and the spatial distribution of the dark current, where we found a variable profile in the CCD 9917. We developed an experiment using a bench mounted monochromator to obtain the spectral dependency of the quantum efficiency in the spectral range between 350 nm and 1100 nm, where we measured the quantum efficiency for each camera. The camera 9915 presents the highest quantum efficiency of 95.8 %. Our results are compared with those from the manufacturer. These experiments allow us to diagnose the performance of these CCD cameras, an important sub-system of the SPARC4 instrument. It also provides a systematic way for monitoring the aging of the CCDs.

Keywords: instrumentation: detectors - methods: data analysis - techniques: image processing.

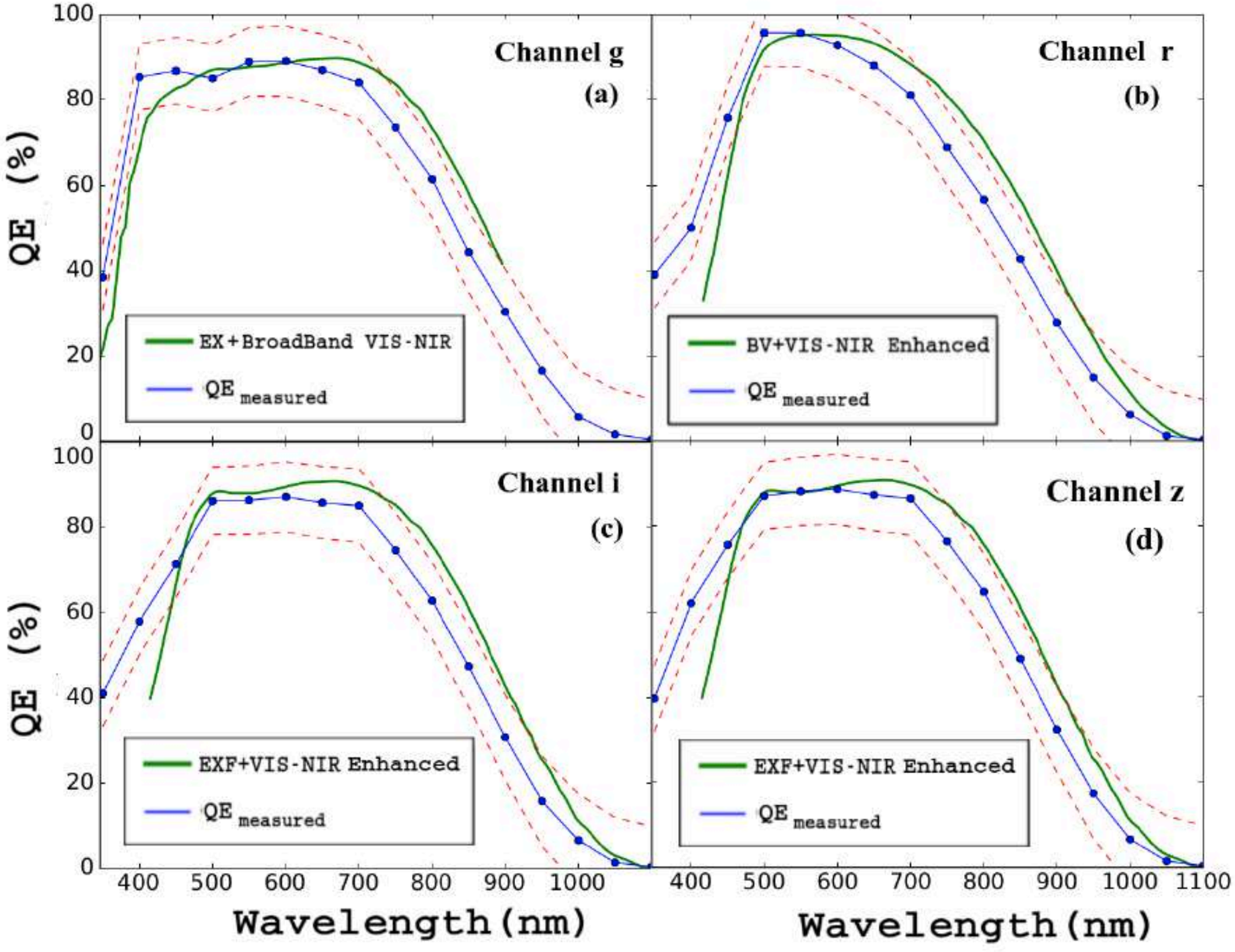

Figure 20: Quantum efficiency for CCDs 9914 (a), 9915 (b), 9916 (c) and 9917 (d). Blue line shows the measured quantum efficiency and red dashed lines show the estimated uncertainty from mechanical misalignment and light source stabilization. Green line presents the manufacturer's quantum efficiency. The legend presents the detector and coating specifications.

Acknowledgments

We want to thank Rodrigo Prates Campos, Saulo Roberly Gargaglioni and Adriano Messala Coimbra for their technical support with the equipments. We want to thank the LNA's mechanics workshop staff for machining the parts

Controle das câmeras

- Computadores de aquisição
  - ✓ verba garantida - Fapemig
  - ✓ Luciano Fraga (LNA)

- Sincronização das câmeras
  - ✓ equipamento - em compra via Finep (?)
  - ✓ desenvolvimento: Denis V. Bernardes, Luciano Fraga e Eder Martioli

Optica

Conceito óptico

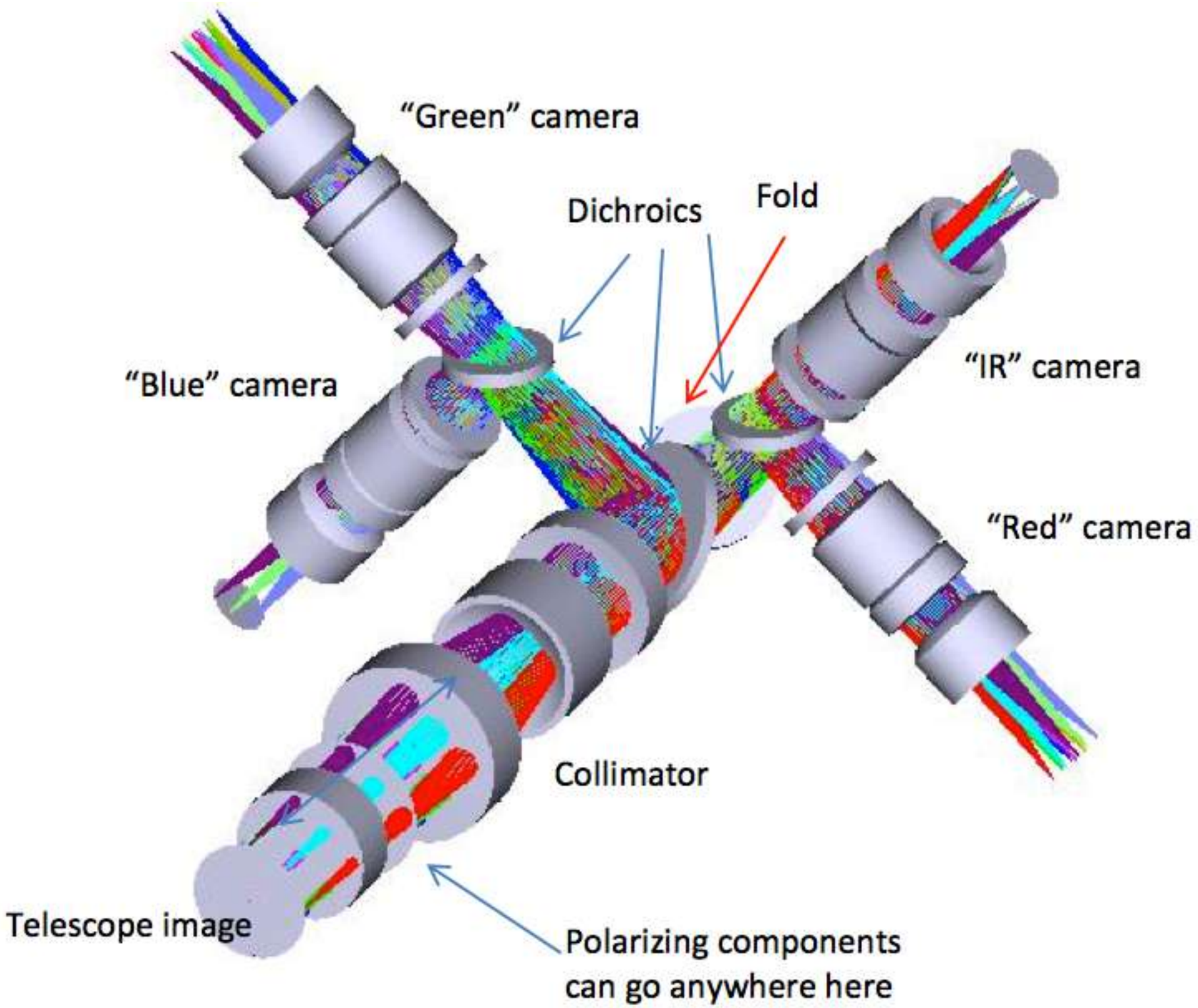

Projeto óptico

- Damien Jones (Prime Optics/Australia) e Rene Laporte (INPE)
- Inclui
  - ✓ Sistema do autoguider e autofocalização
    - espelhos, câmera focalizadora e prismas para autofocalização
  - ✓ Colimador
  - ✓ Dicróicos
  - ✓ Espelho
  - ✓ Câmeras focalizadoras

Dicróicos

- Aquisição: LNA e INPE

- Fabricante: Materion Barr

- Medidas feitas no LNA
  - ✓ Clemens Gneiding - LNA
  - ✓ Flavio Ribeiro - LNA
  - ✓ Luidhy Santana da Silva - UFRJ
  - ✓ Rodrigo Prates Campos - LNA

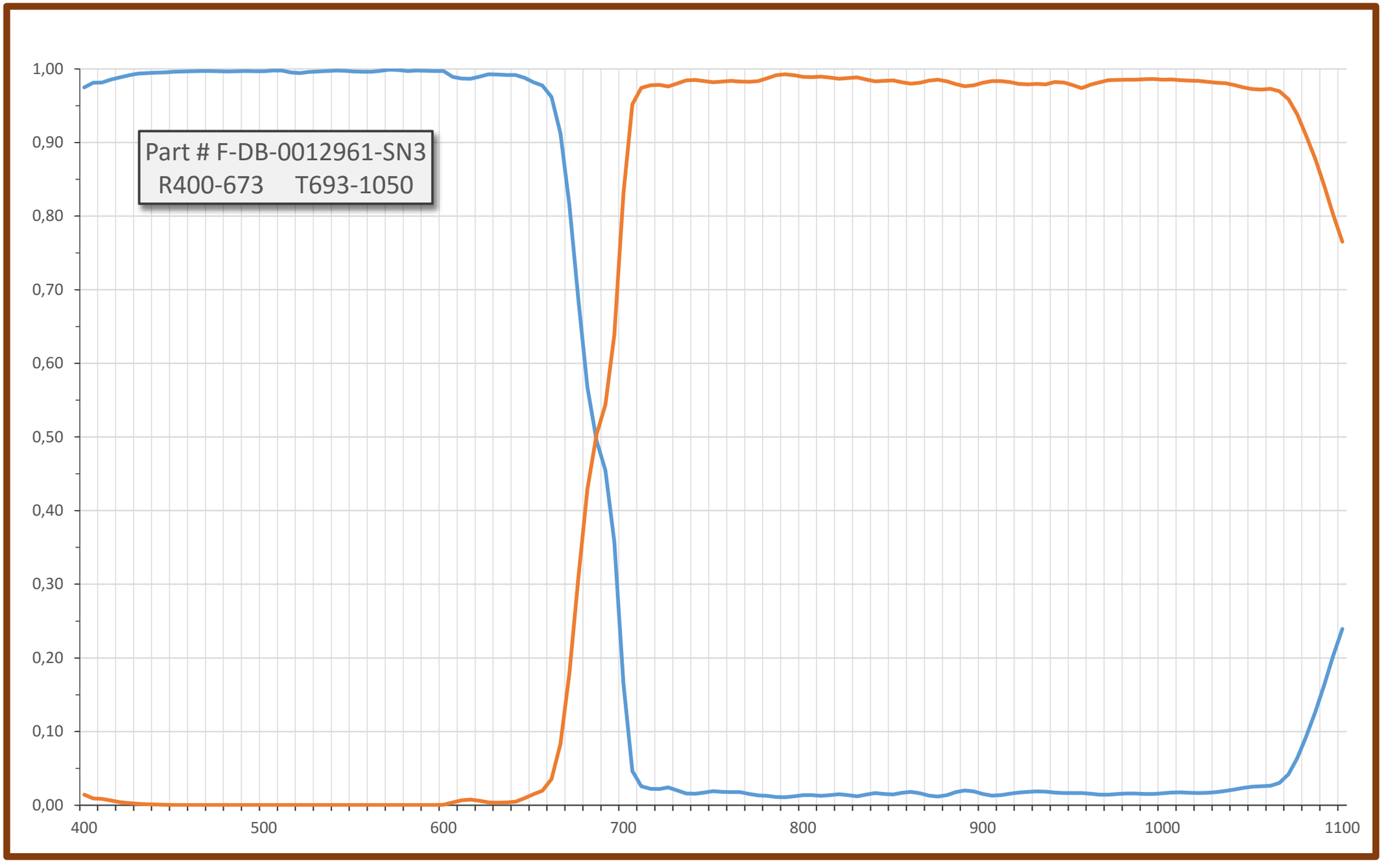
Part # F-DB-0012961-SN3
R400-673 T693-1050
1,00
0,90
0,80
0,70
0,60
0,50
0,40
0,30
0,20
0,10
0,00
400
500
600
700
800
900
1000
1100

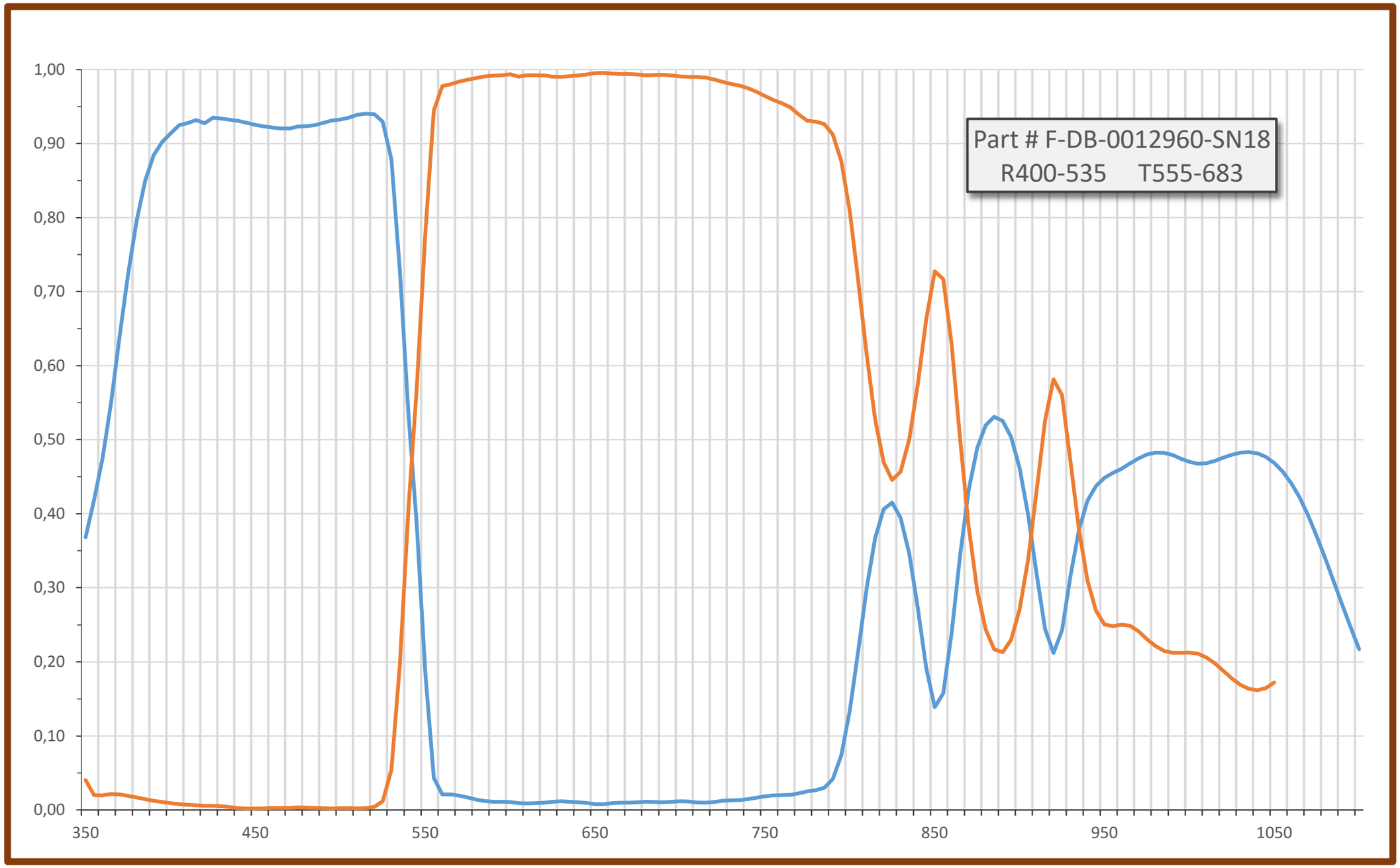
Part # F-DB-0012960-SN18
R400-535 T555-683
1,00
0,90
0,80
0,70
0,60
0,50
0,40
0,30
0,20
0,10
0,00
350
450
550
650
750
850
950
1050

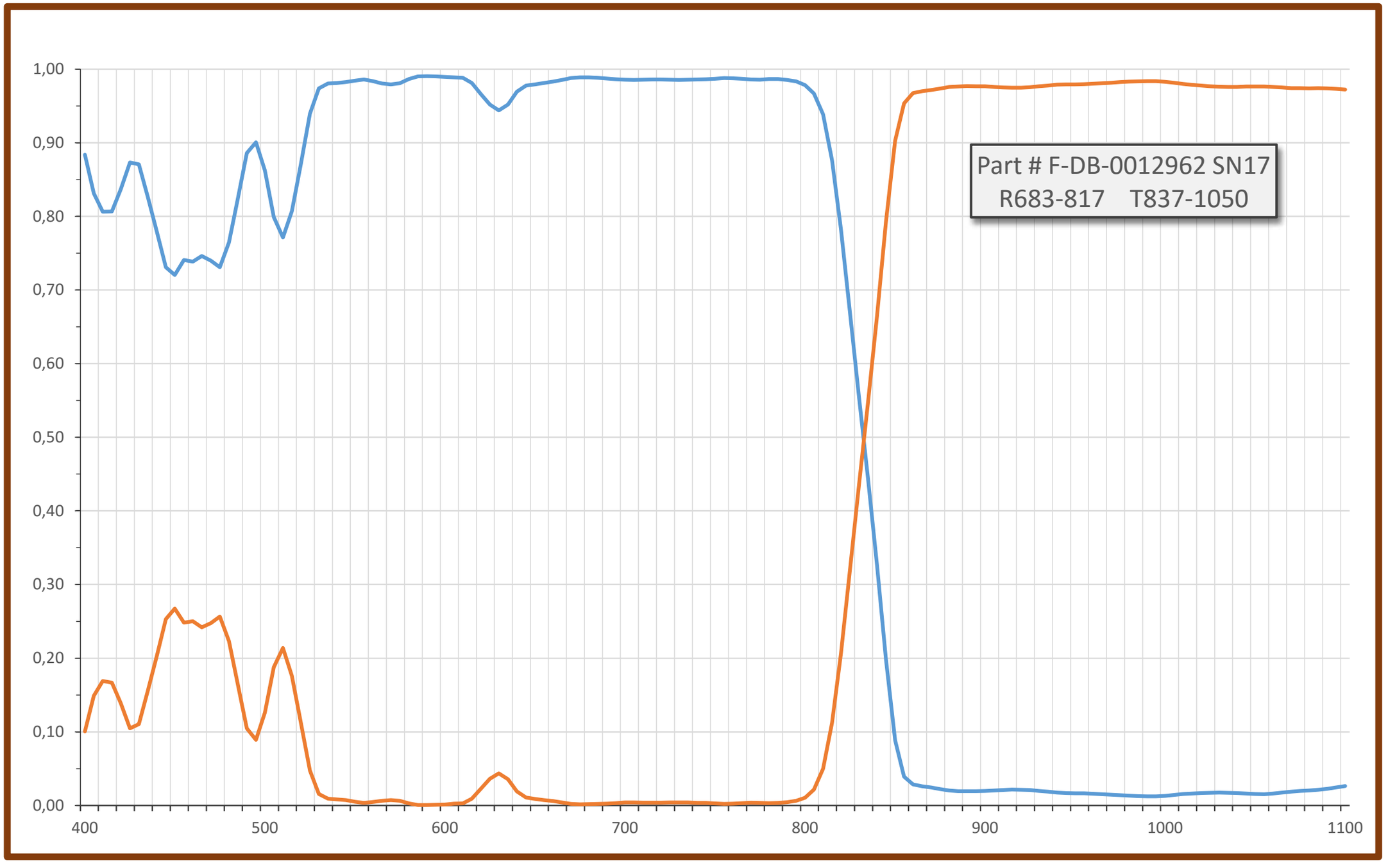
Part # F-DB-0012962 SN17
R683-817 T837-1050
1,00
0,90
0,80
0,70
0,60
0,50
0,40
0,30
0,20
0,10
0,00
400
500
600
700
800
900
1000
1100

Colimador e focalizadores

Rainbow Research Optics - EUA

Aquisição: INPE

Lentes individuais

- As lentes individuais estão dentro das especificações

- Medidas feitas no LNA e no INPE
  - ✓ Braulio Albuquerque (INPE)
  - ✓ Clemens Gneiding (LNA)
  - ✓ Flavio Ribeiro (LNA)
  - ✓ Jesulino Bispo (LNA)
  - ✓ Rene Laporte (INPE)

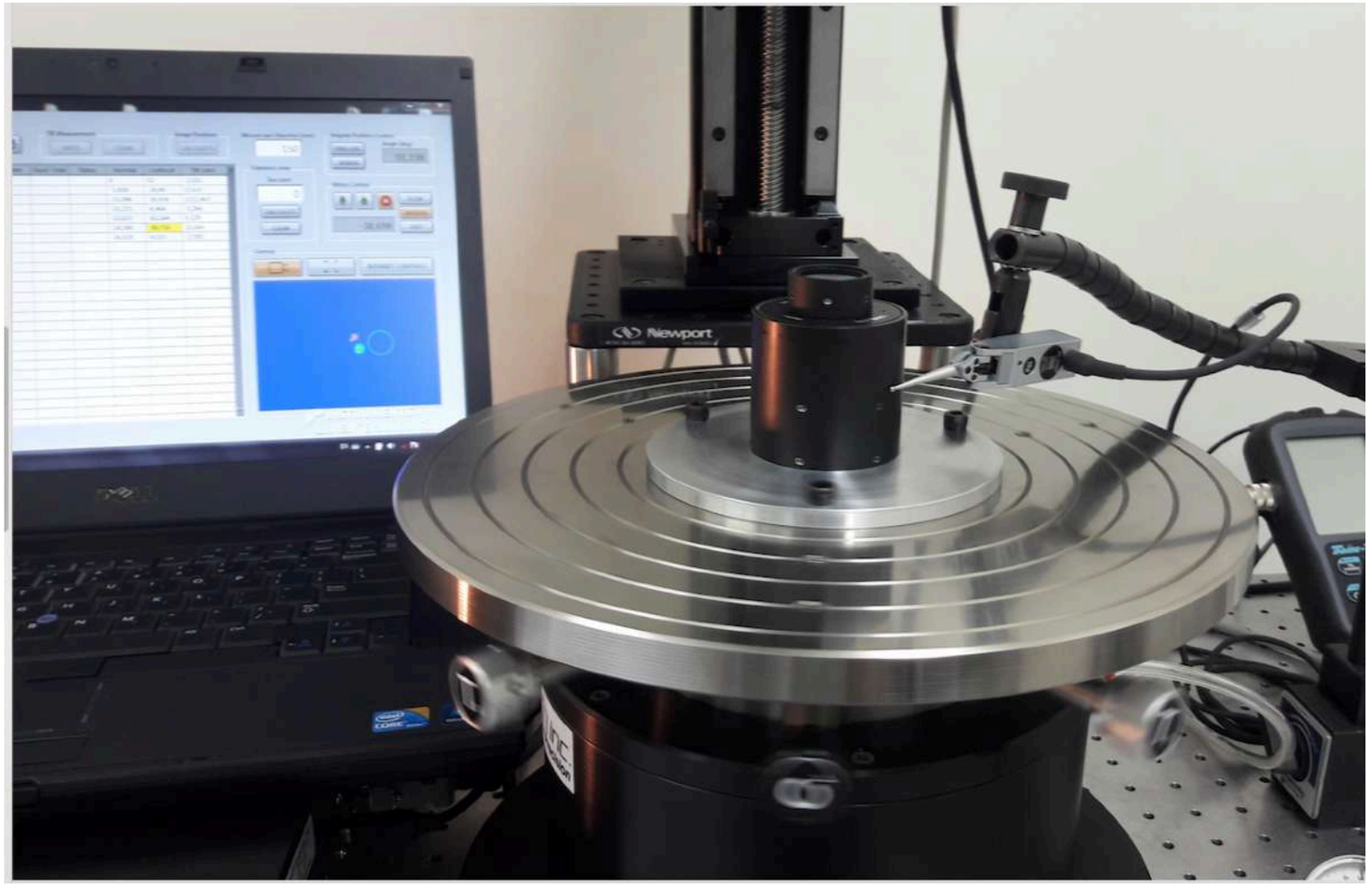

Barris e montagem

Primeira versão: Usinagem Metalcard - Brasil

Montagem

- Montagem dos barris ópticos
  - ✓ Tolerância muito pequena no posicionamento das lentes - Desafio

- Primeira versão dos barris
  - ✓ Usinagem pela Metalcard (Verba Finep) e oficina mecânica do LNA
  - ✓ Não permitiu posicionamento adequado das lentes nos barris

- Segunda versão
  - ✓ Modificação do conceito de ajuste das lentes
  - ✓ Sendo usinada no LNA
  - ✓ Teste de montagem em maio

Óptica polarimétrica

- Definição
  - ✓ Antonio Mario Magalhães (IAG/USP), Antonio Pereyra (IGP/Peru), CVR

- Itens
  - ✓ 2 lâminas retardoras: meia-onda e quarto-de-onda
  - ✓ prisma de Savart
  - ✓ polarizador
  - ✓ depolarizador

- Todos itens adquiridos
  - ✓ Fabricantes Karl Lambrecht (EUA) e Meadowlark (EUA)
  - ✓ Verba INPE

- Conferência de dimensão e qualidade da superfície feita no LNA
  - ✓ Flavio Ribeiro

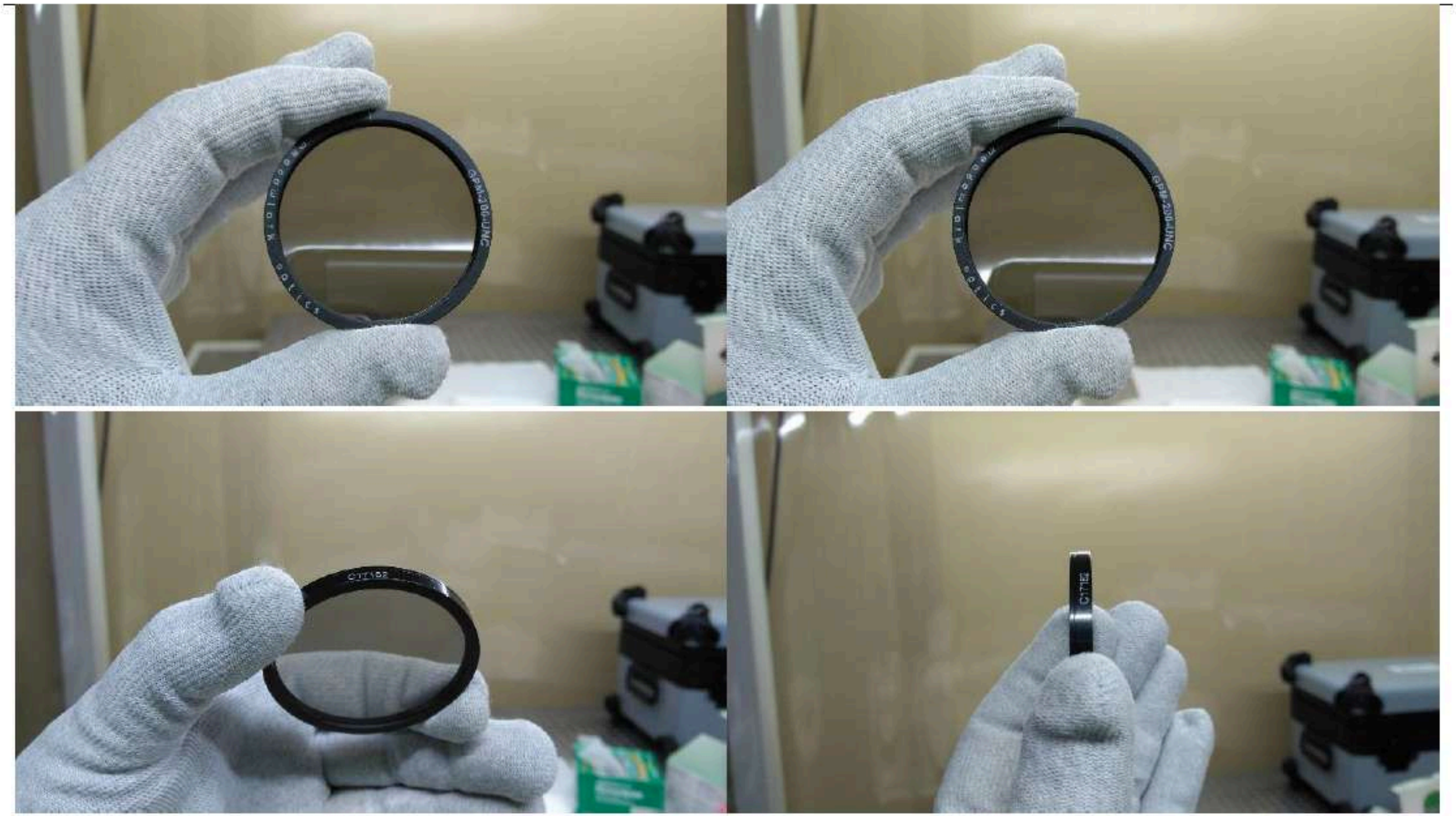

Figura 2.1 – Fotos de C17182

Depolarizador

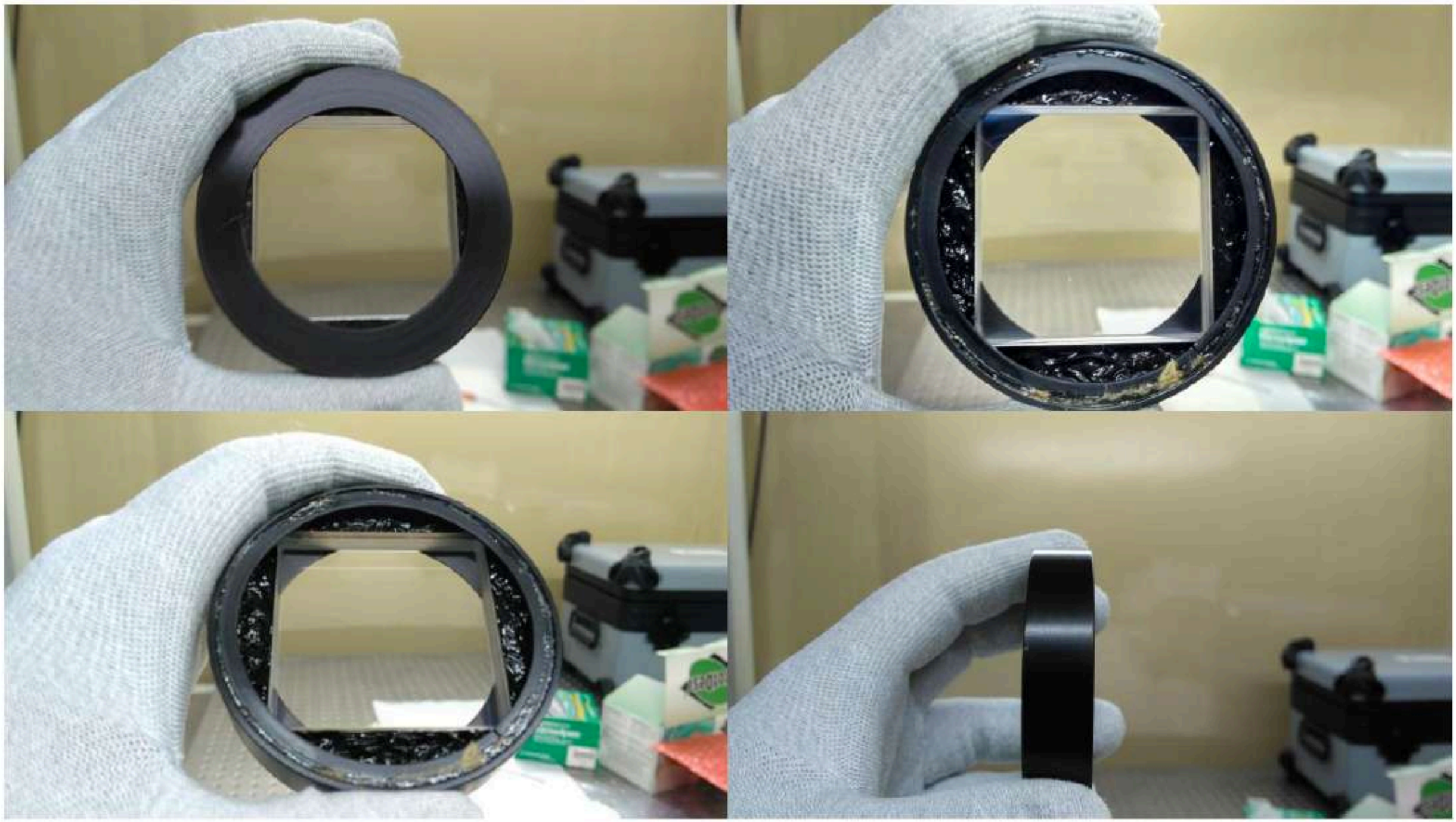

Figura 2.16 – Fotos de F17087

Prisma de Savart

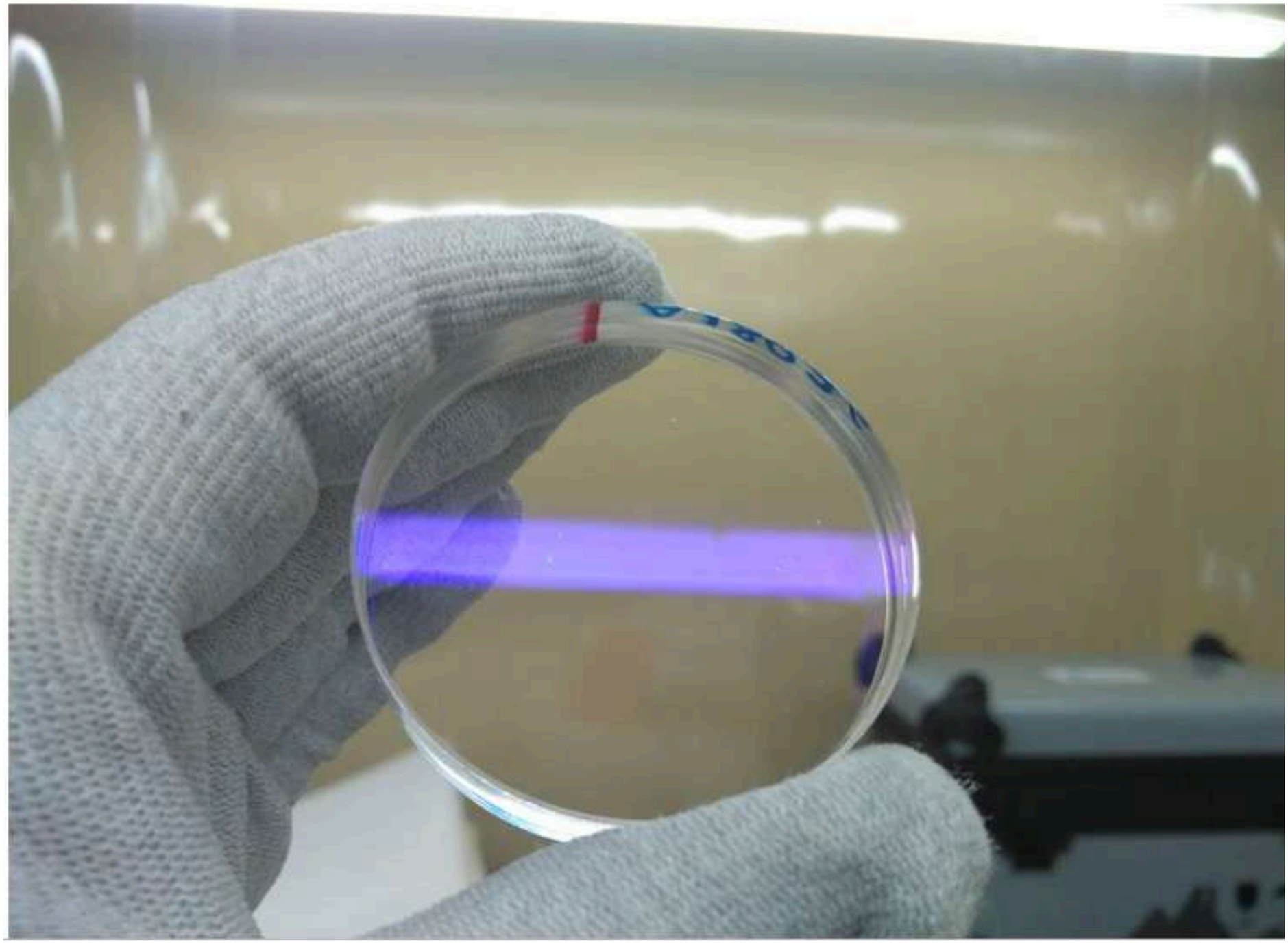

Projeto mecânico

Projeto mecânico

- Desenvolvido por Rene Laporte (INPE) e Ruben Dominguez (Univ. of Arizona)
  - ✓ Revisão crítica por Vanessa Bawden Macanhan (LNA)
  - ✓ Consistência com projeto óptico revisada por Clemens Gneiding (LNA)
  - ✓ Consistência com projeto de controle revisada por Francisco Rodrigues (LNA)
- Projeto finalizado
- Análise de flexão realizada
  - ✓ Valentino Lau (INPE)
- Impacto da flexão na óptica
  - ✓ sendo avaliada - Clemens Gneiding
- Próxima etapa - detalhamento de projeto
  - ✓ Analysis Engenharia - serviço terceirizado com verba Finep
    - árvore de produto, desenhos 2D
- Usinagem será realizada na oficina mecânica do LNA

Visão geral

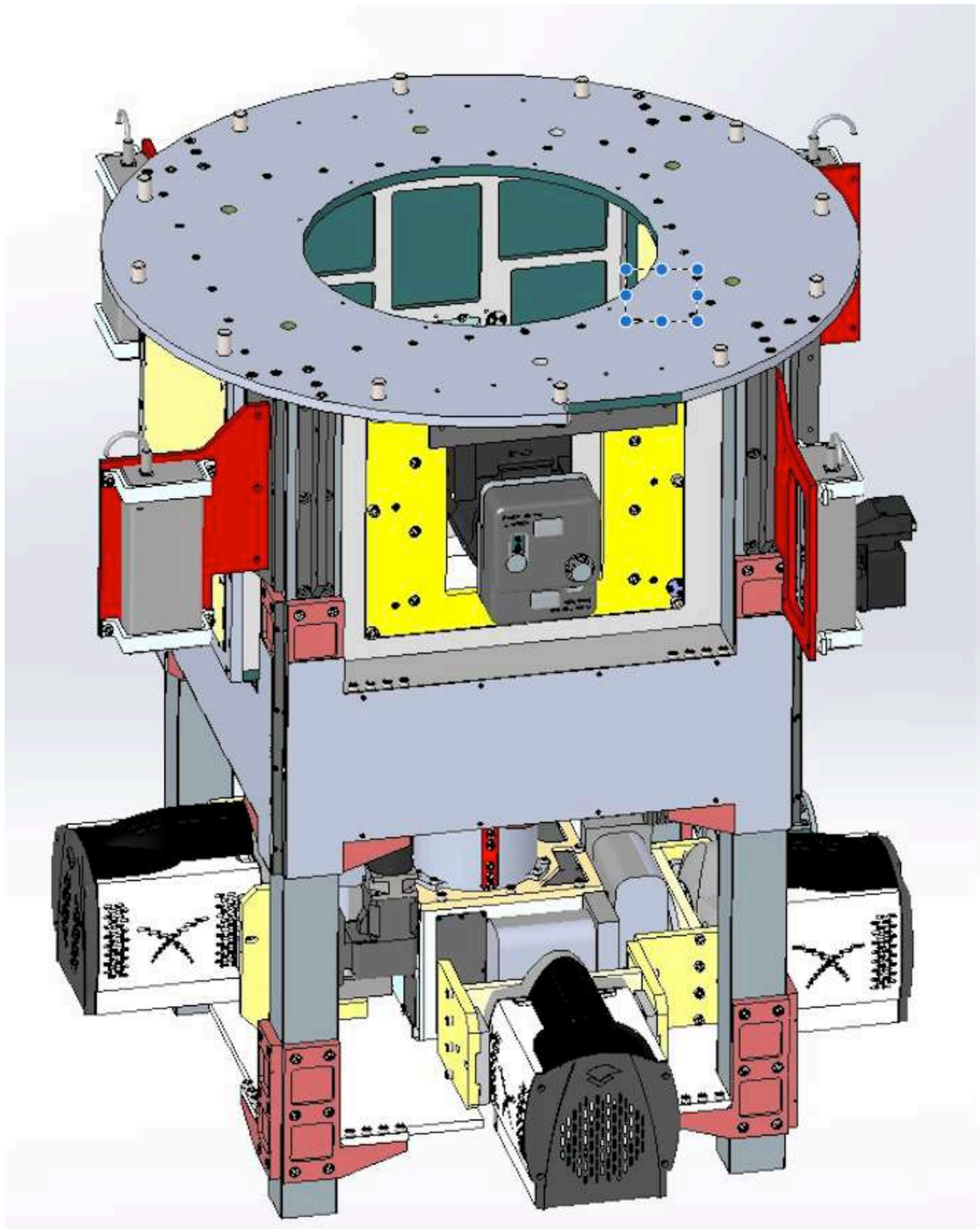

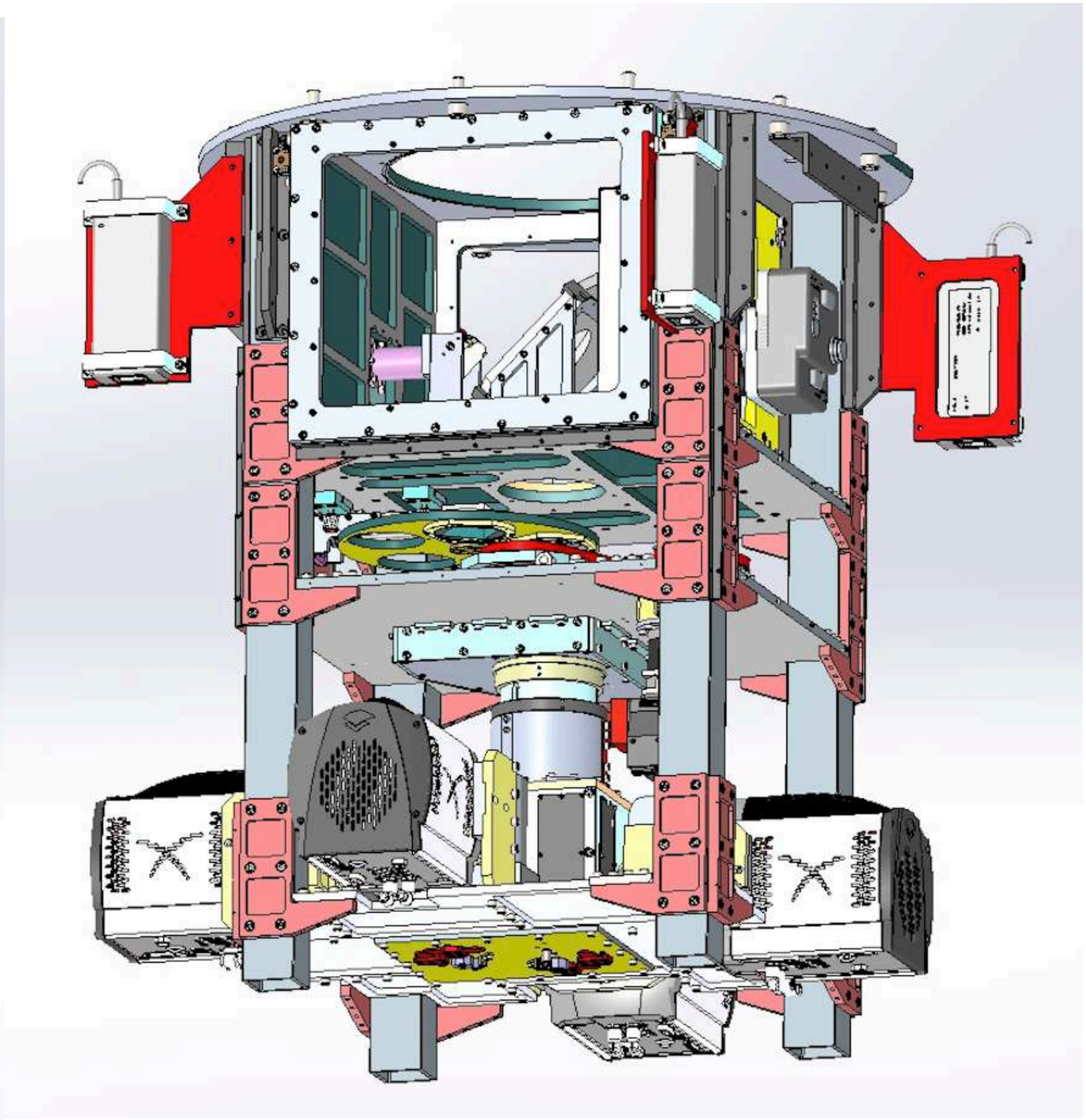

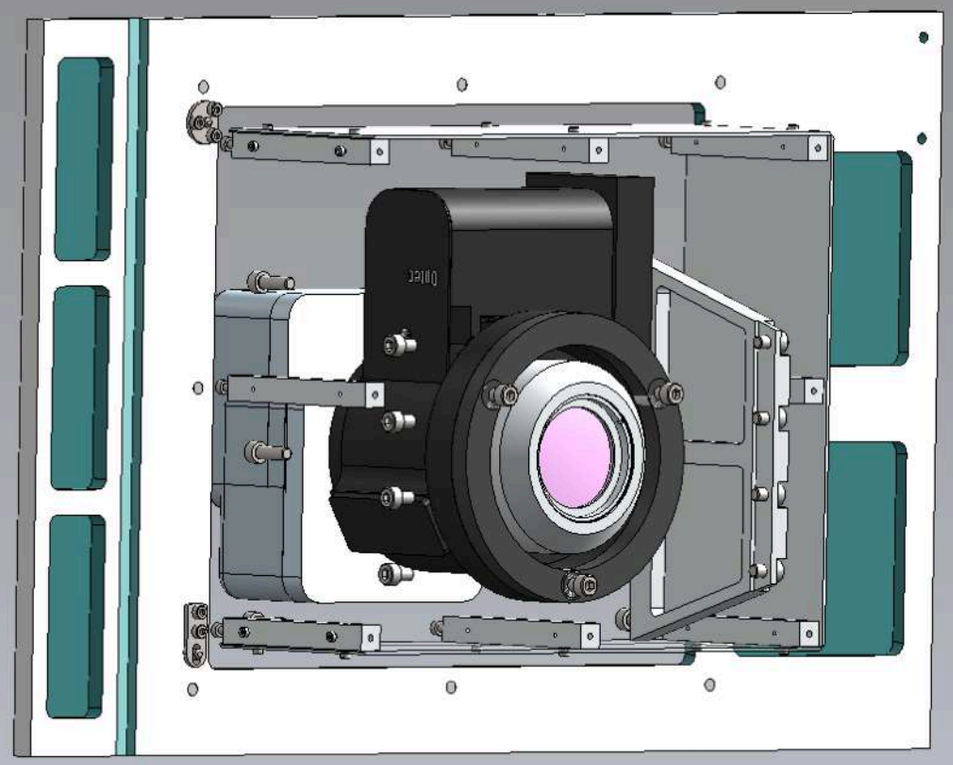

Autoguider

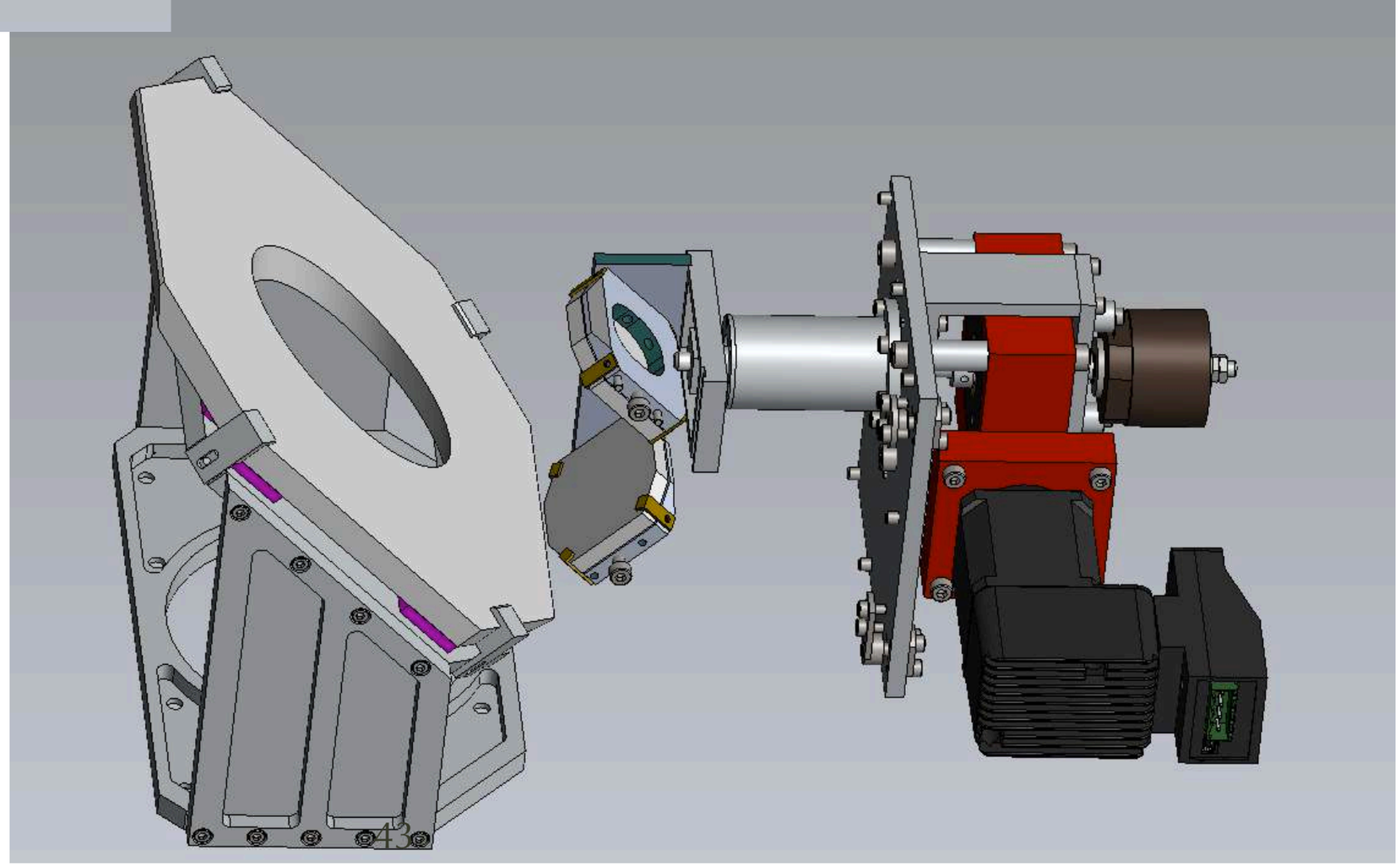

Polarimetria

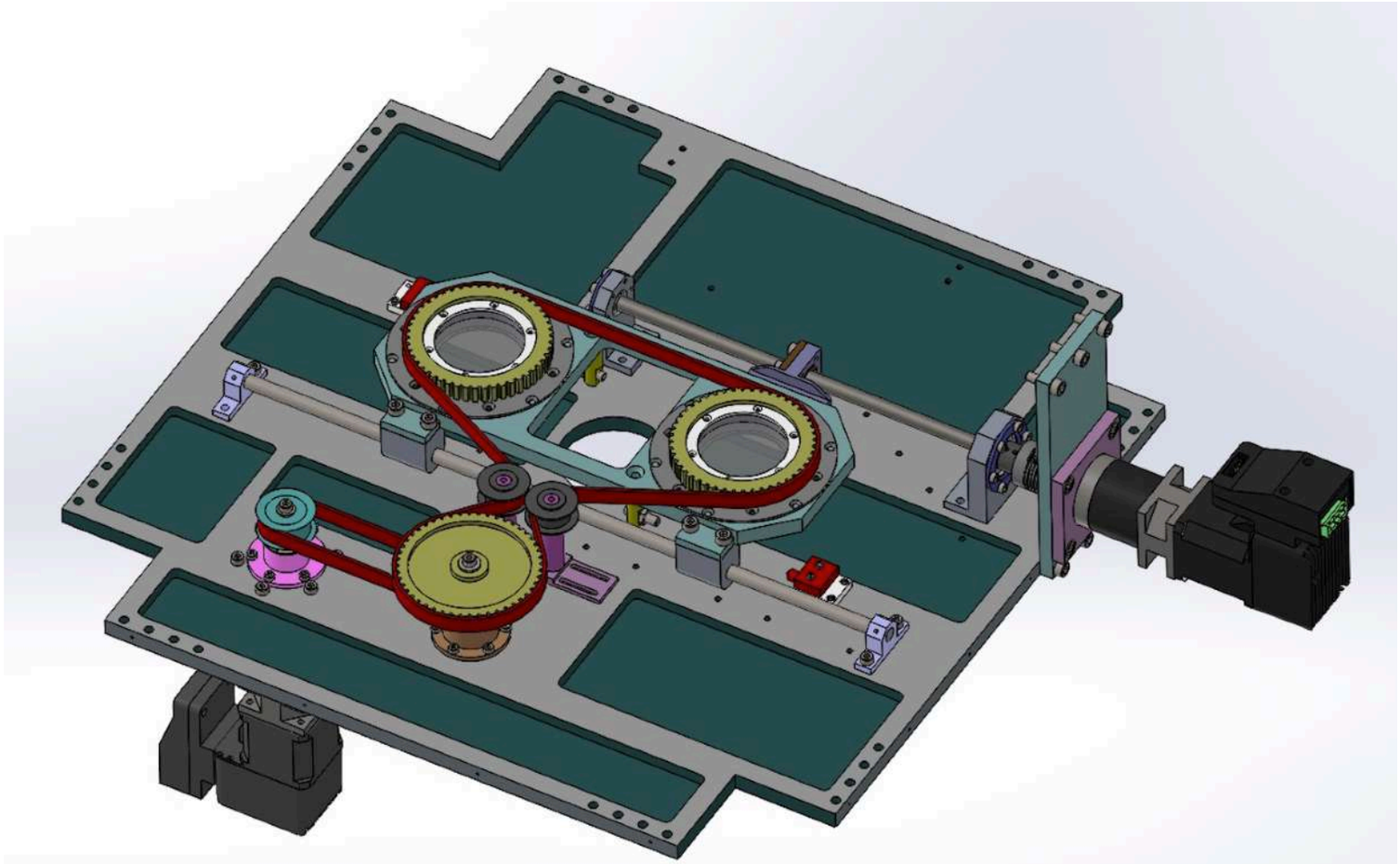

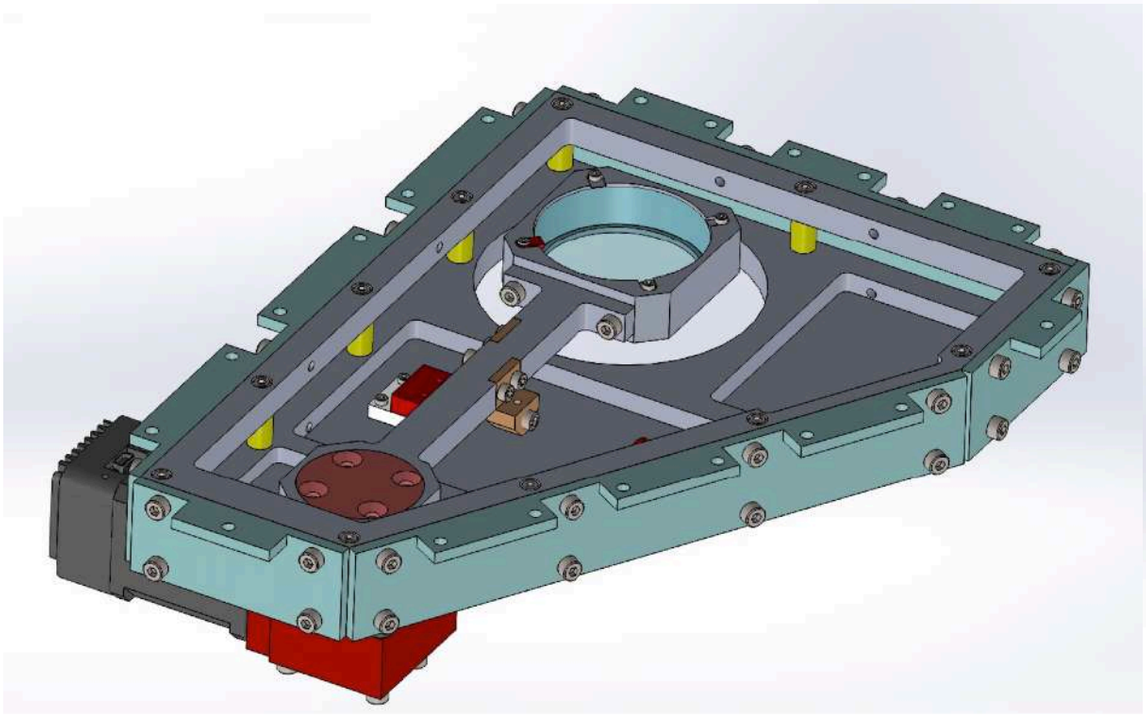

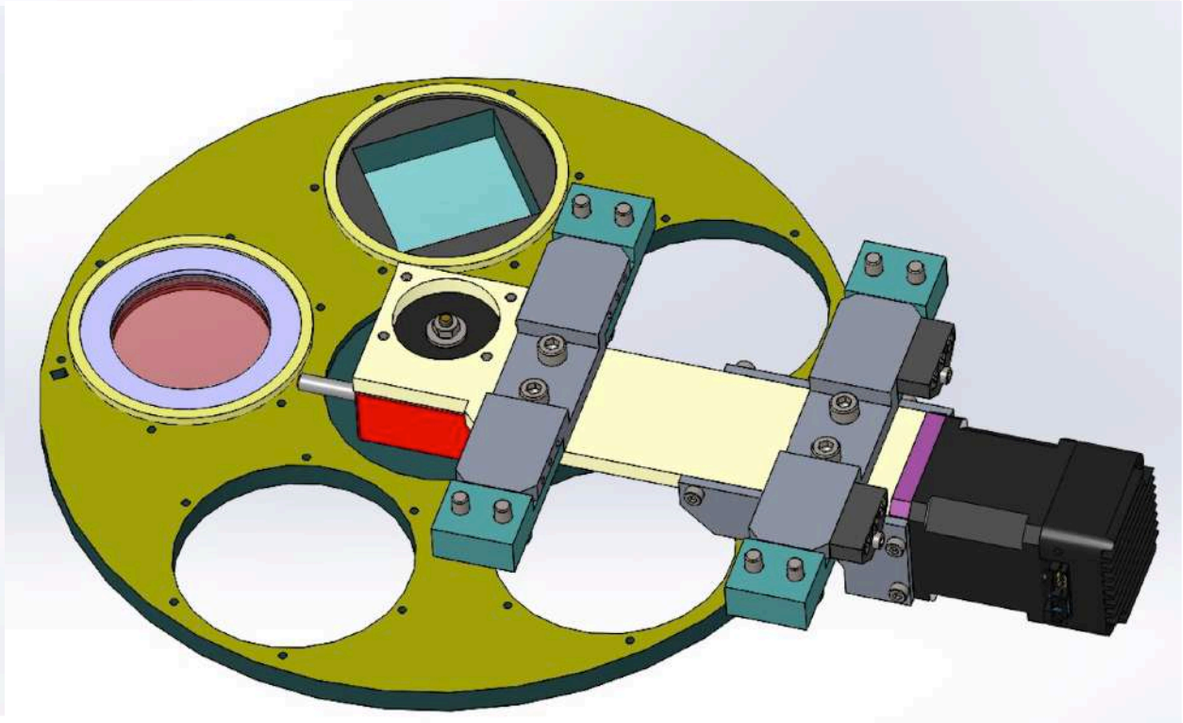

Optical box

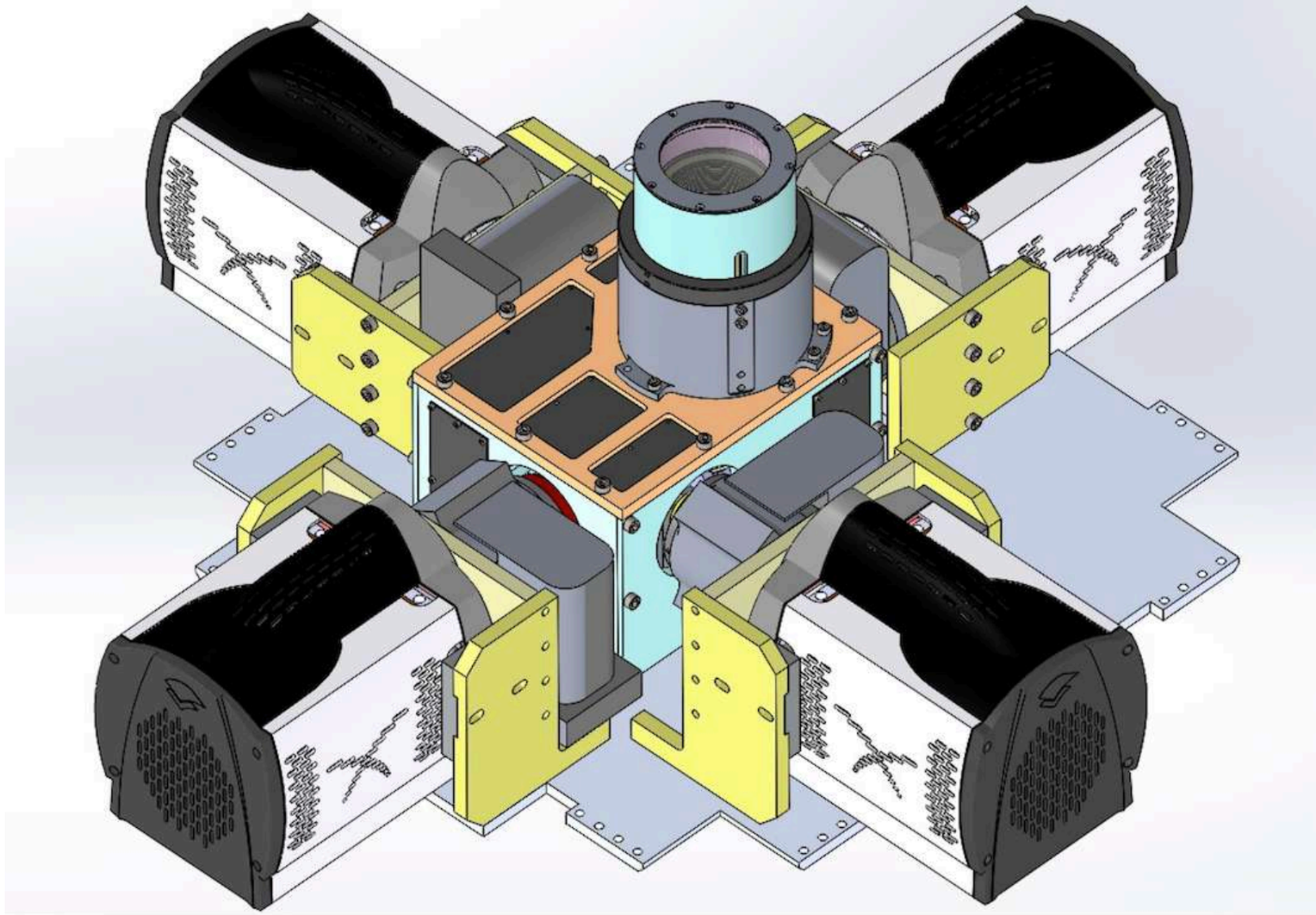

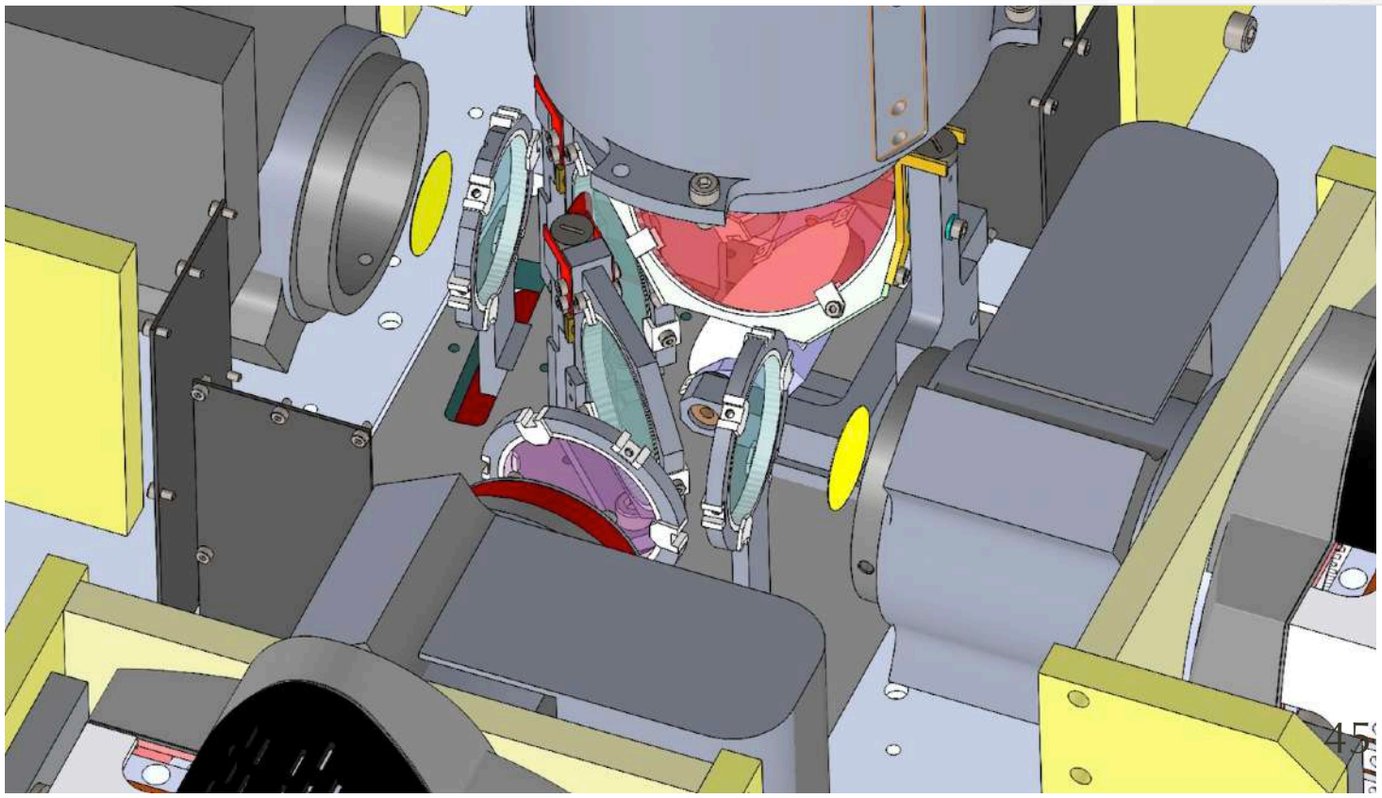

Echarpe feeder

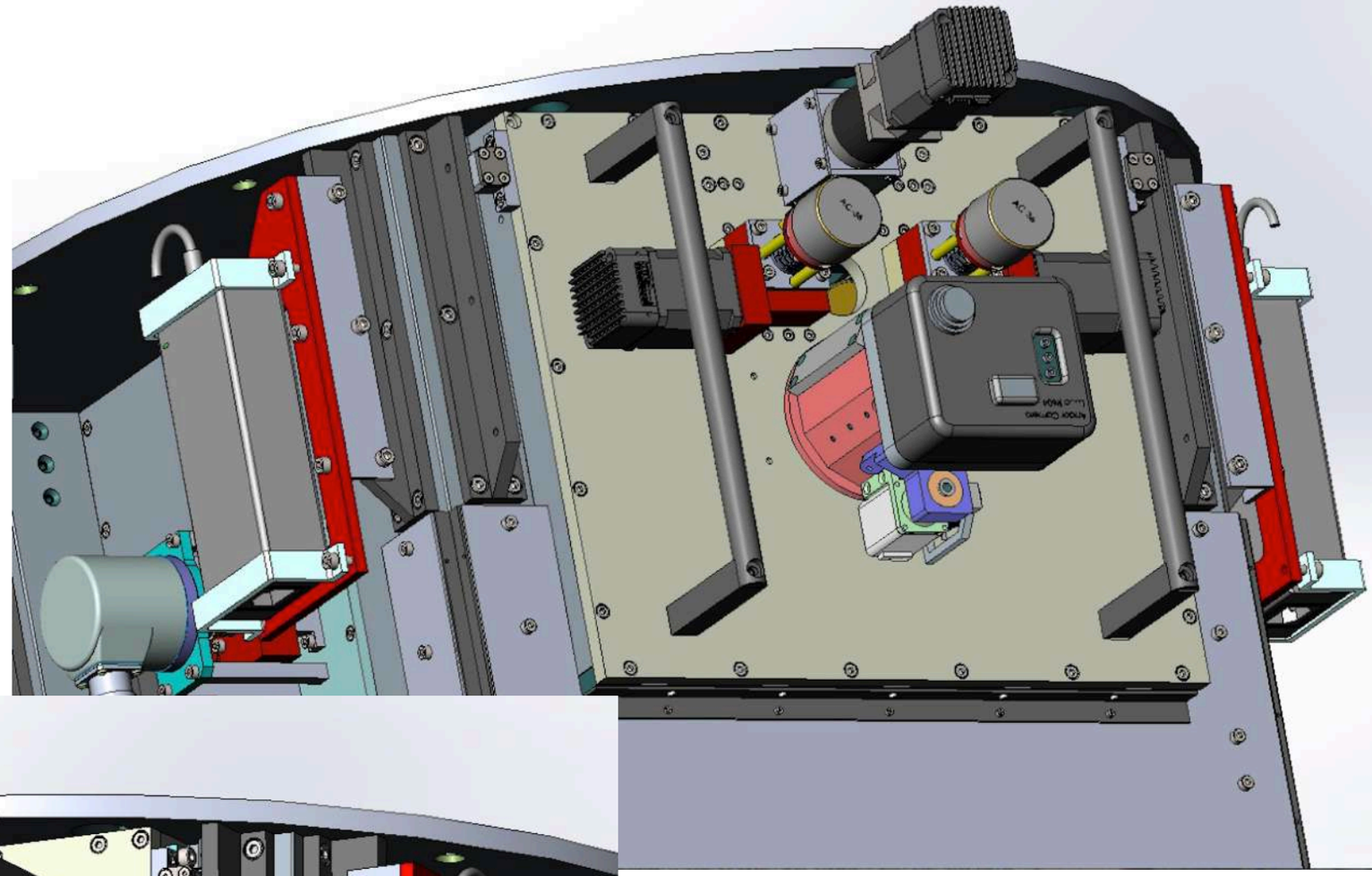

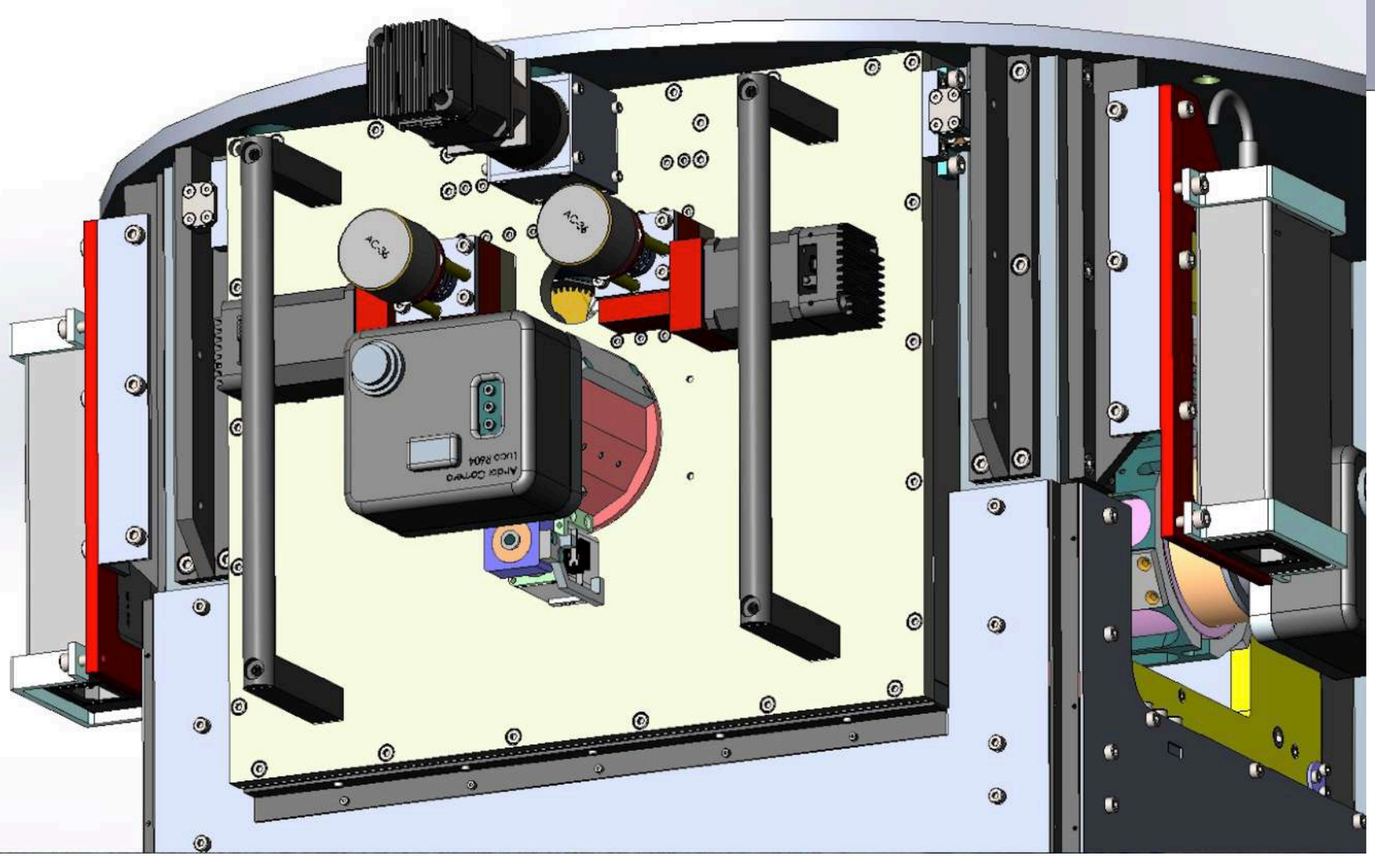

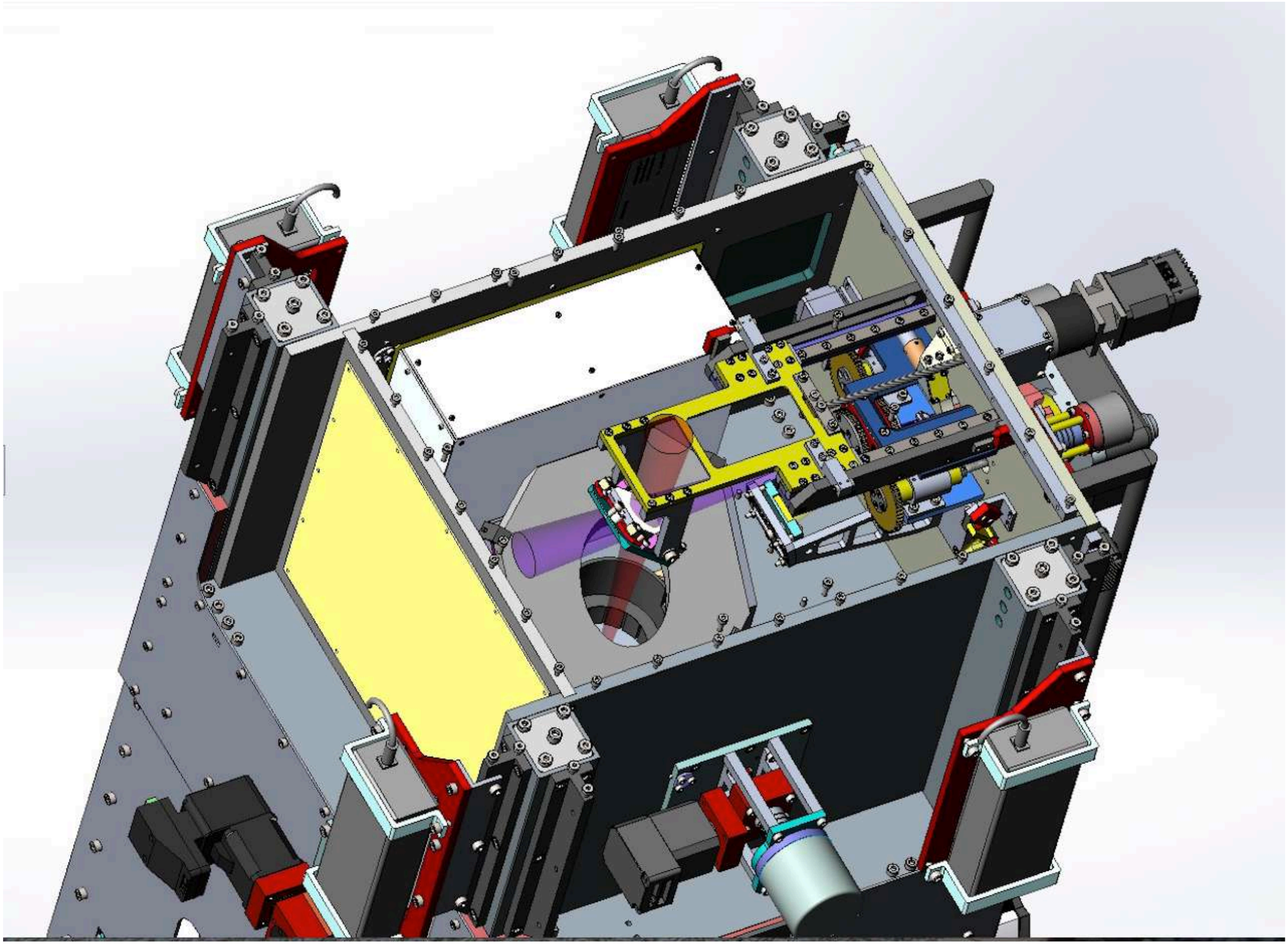

Análise de flexão

MODELO MOD v65

/: Untitled

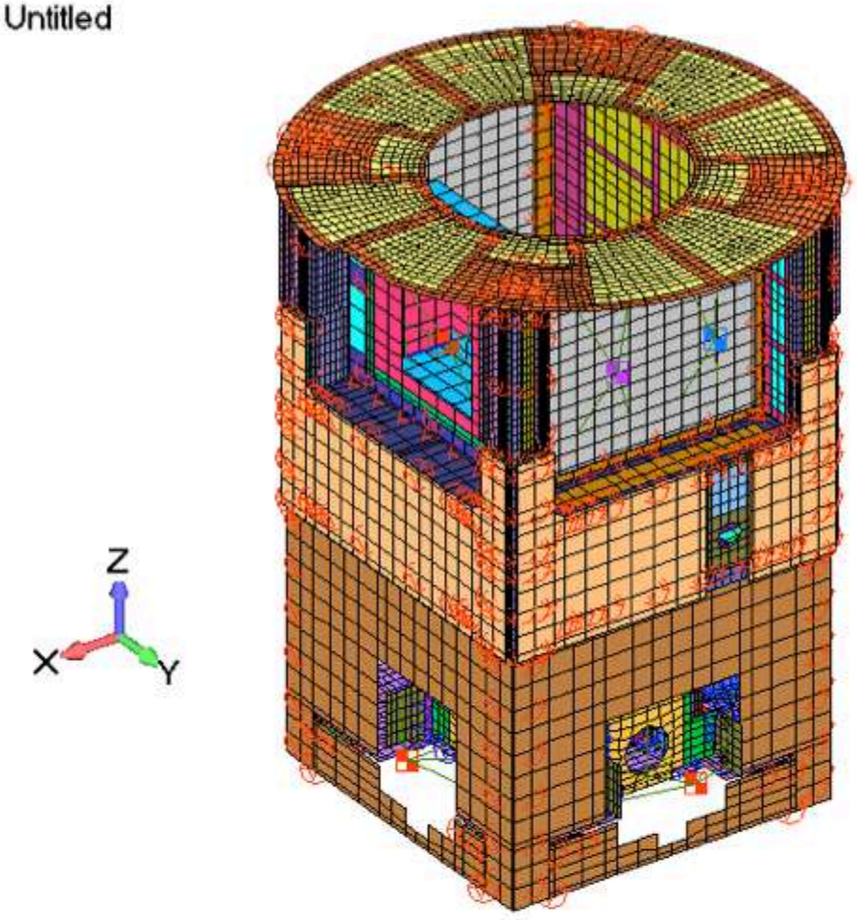

V: Untitled
G: Platina

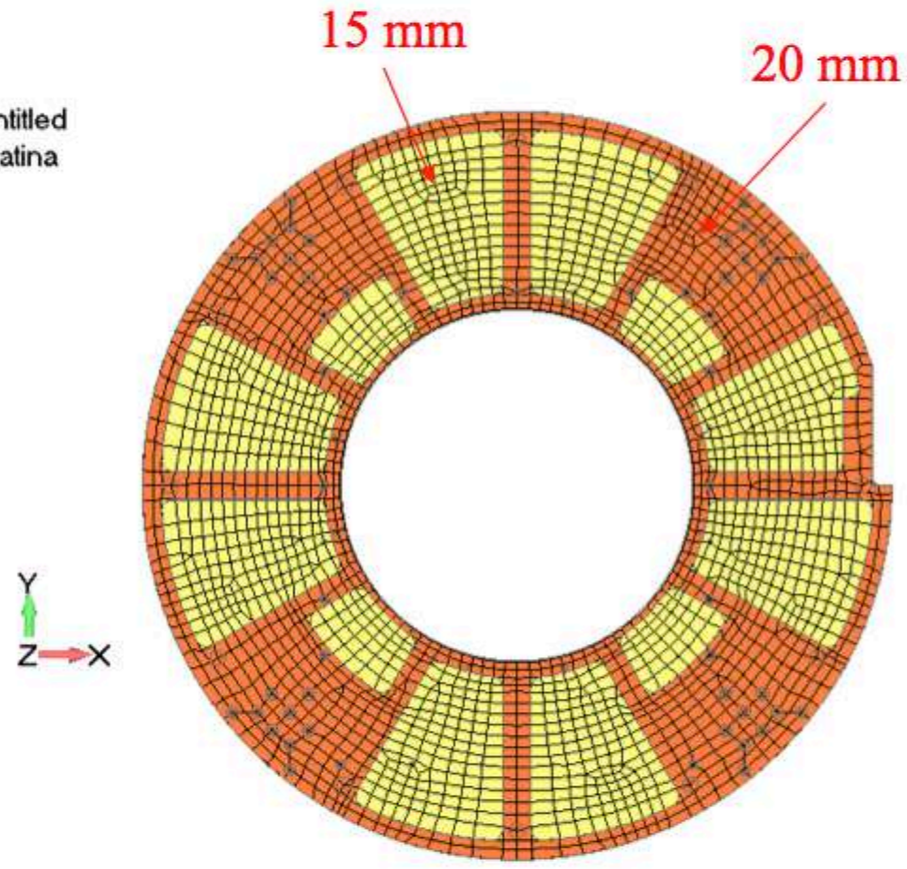

Massa total
do modelo 126.4 kg

Mass		Center of Gravity in CSys 0					
Structural =	110.6919	X=	392.1822	Y=	472.2713	Z=	196.7802
NonStructural=	15.74176	X=	393.3615	Y=	481.4712	Z=	38.61672
Total Mass =	126.4336	X=	392.329	Y=	473.4168	Z=	177.0879

3

DESLOCAMENTOS

Envelope Máximo

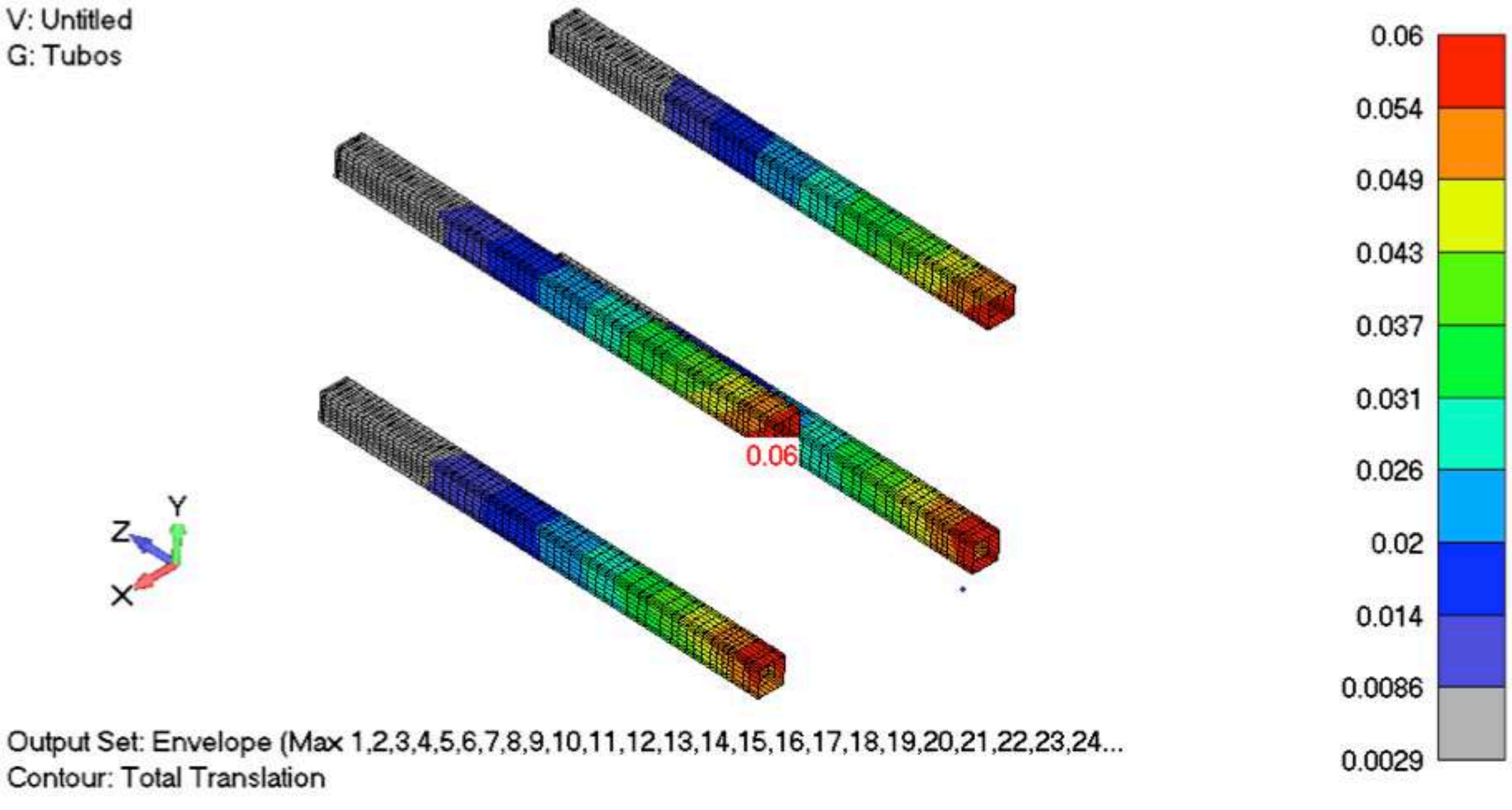

Output Set: Envelope (Max 1,2,3,4,5,6,7,8,9,10,11,12,13,14,15,16,17,18,19,20,21,22,23,24...
Contour: Total Translation

Caso 999 – Vertical 1G

V: Untitled
L: Vertical 1G
G: Laterais Removidas

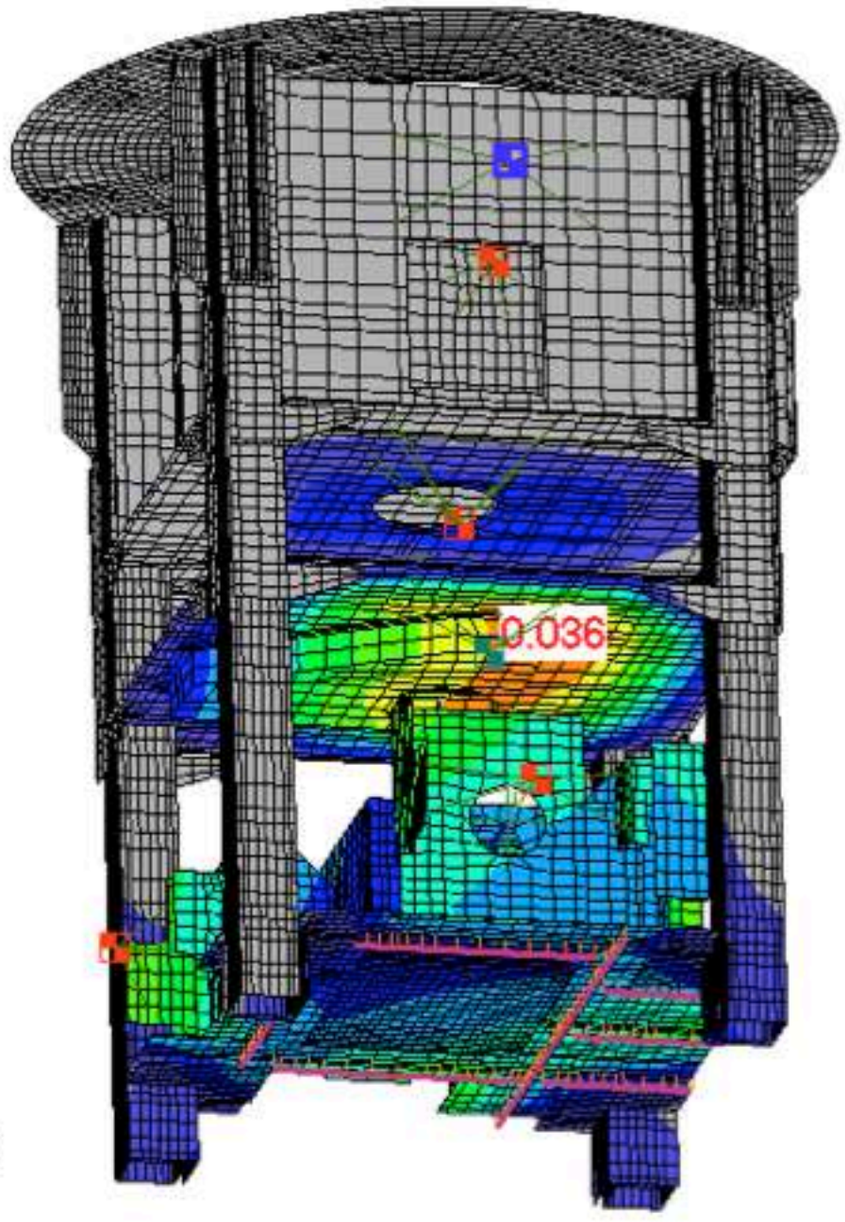

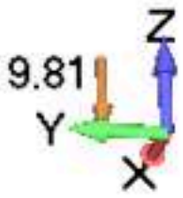

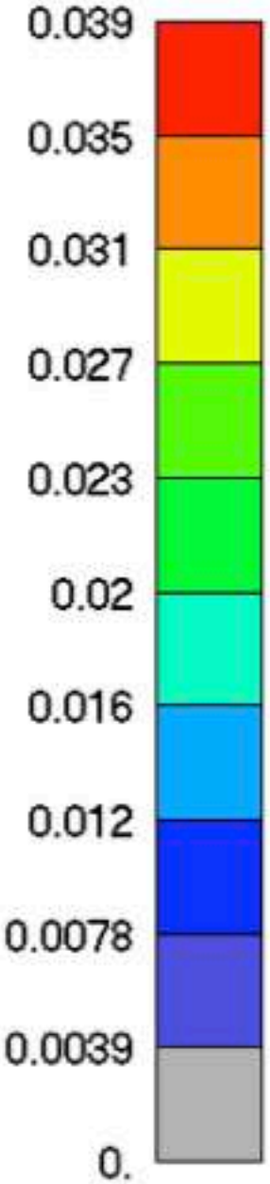

Output Set: MSC/NASTRAN Case 999
Contour: Total Translation

Caso 3 - Posição 1, 60°, RotZ=180°

V: Untitled
L: Posição 1, 60°, RotZ=180°
G: Laterais Removidas

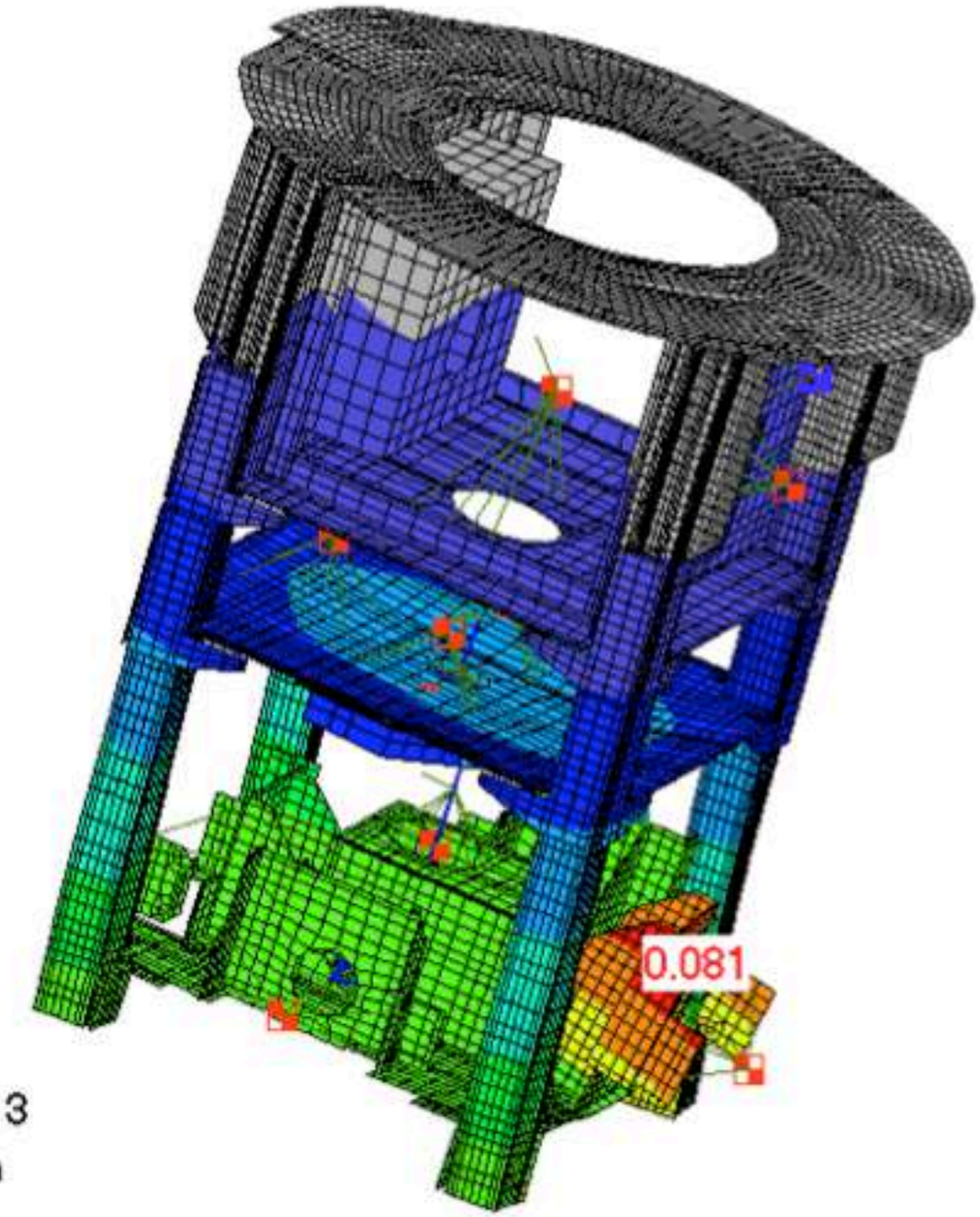

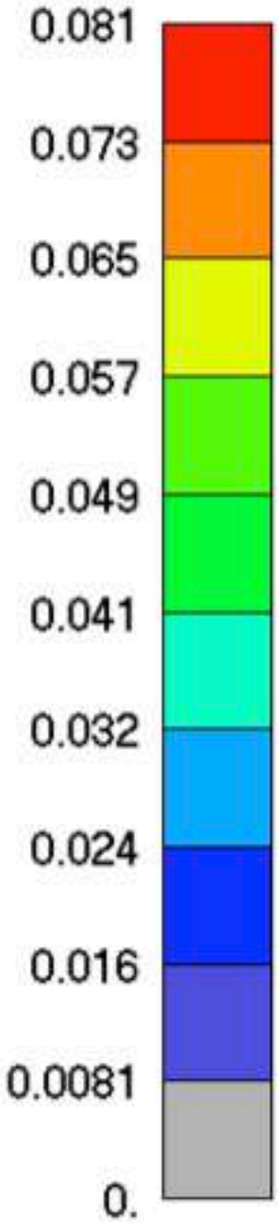

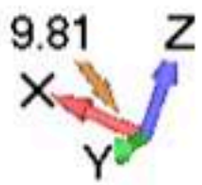

Output Set: MSC/NASTRAN Case 3
Deformed(0.106): Total Translation
Contour: Total Translation

Focalizador

- LNA está desenvolvendo um focalizador
  - ✓ Marcio Vital de Arruda (mecânica)
  - ✓ Francisco Rodrigues (controle)
  - ✓ Usinagem e testes - equipe do LNA

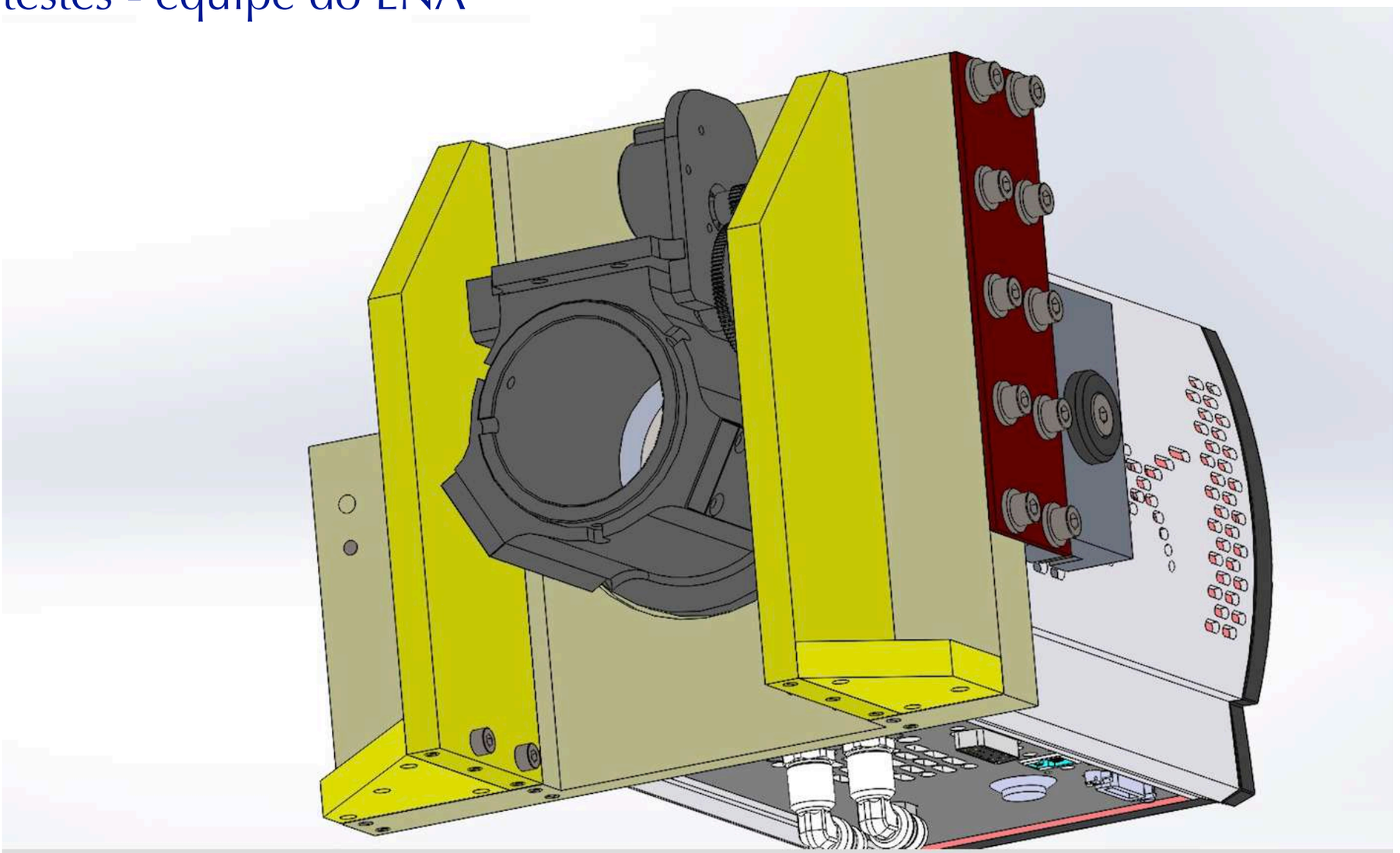

Focalizador

- LNA está desenvolvendo um focalizador

ica)

LNA

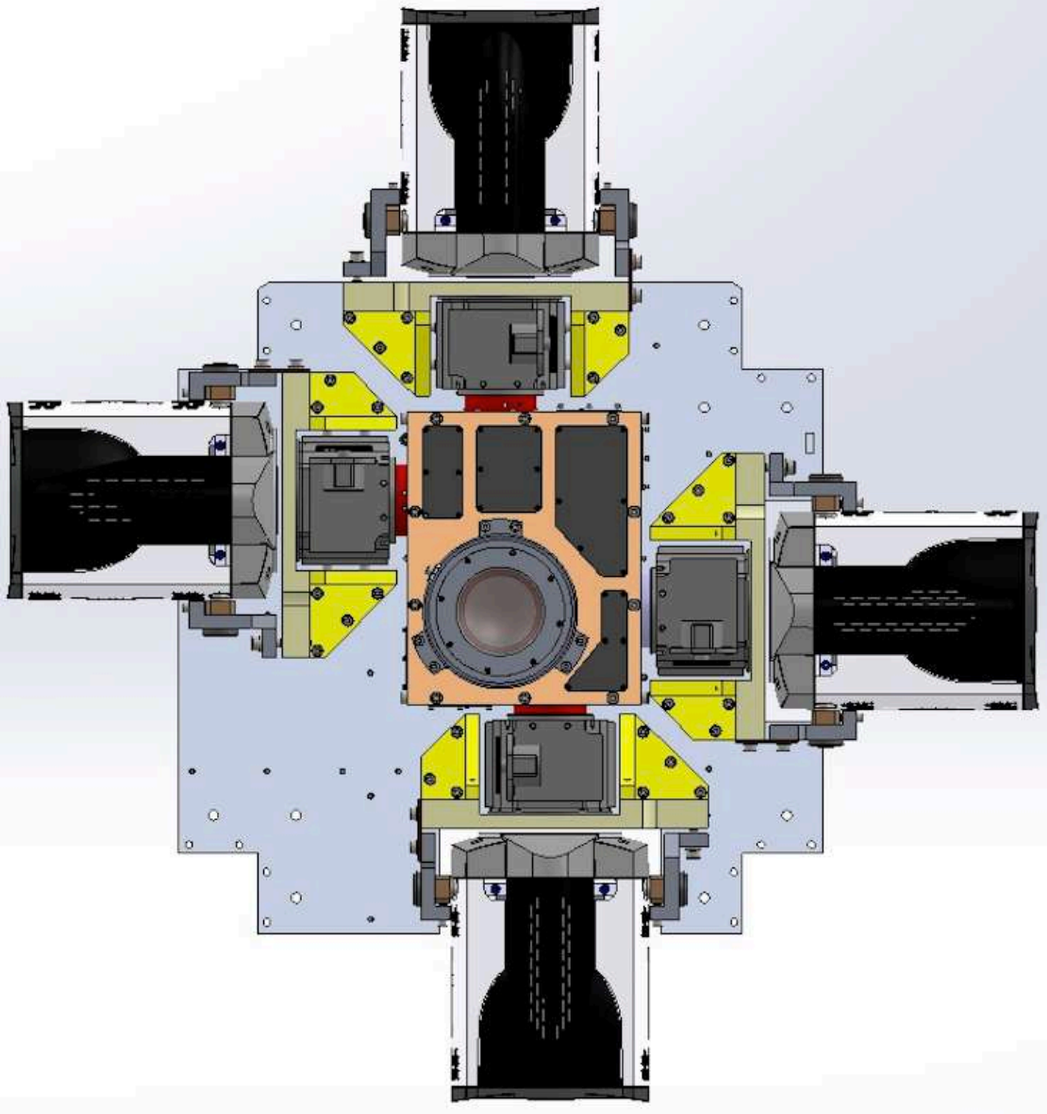

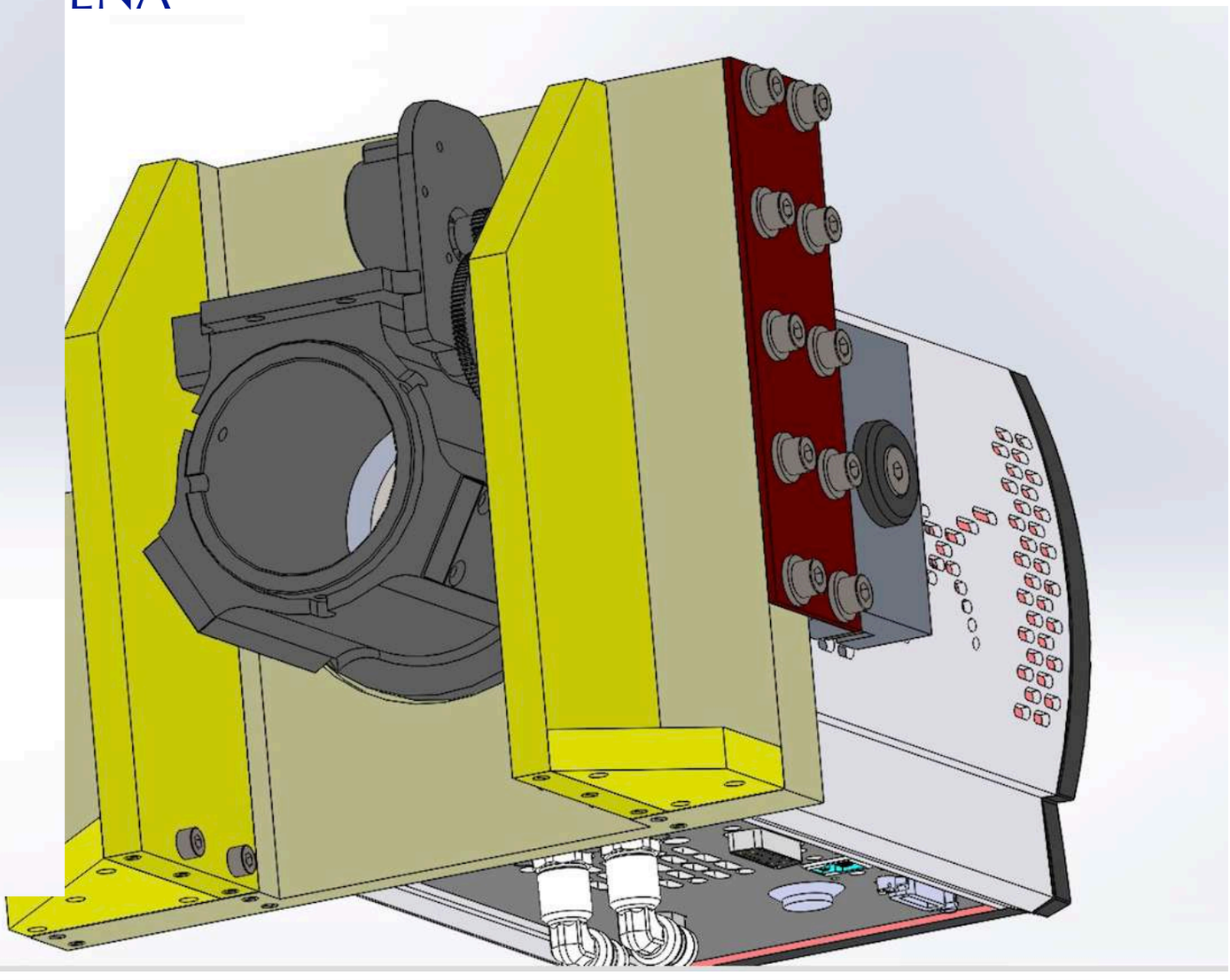

Projeto de controle

Projeto de controle

- Desenvolvimento feito no LNA
  - ✓ Francisco Rodrigues

- Compra em curso de componentes para construção de protótipos e testes (Finep)

- Finalização do projeto

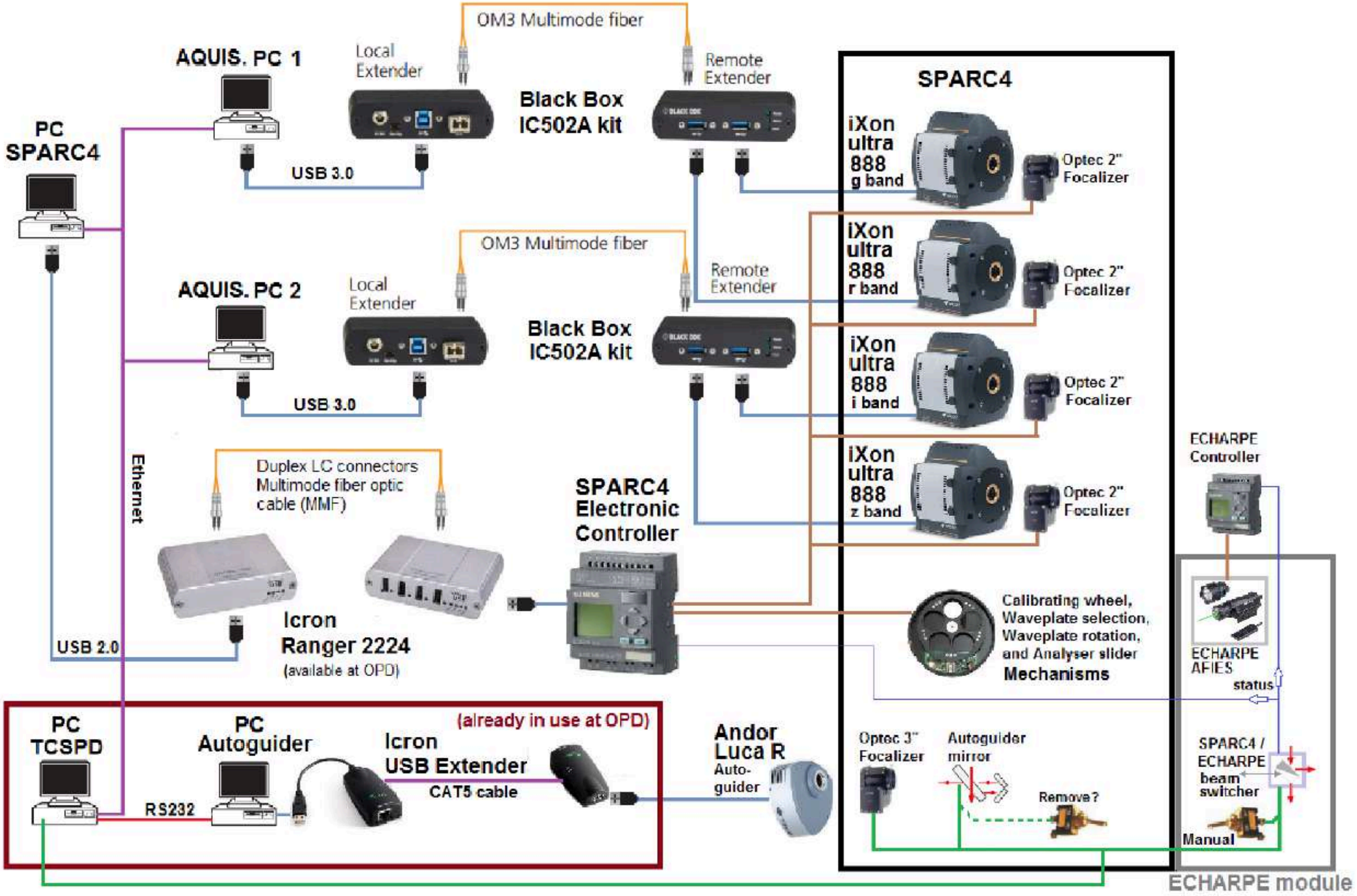
OM3 Multimode fiber
AQUIS. PC 1
Local Extender
Remote Extender
Black Box IC502A kit
PC SPARC4
USB 3.0
SPARC4
iXon ultra 888 g band
Optec 2" Focalizer
OM3 Multimode fiber
AQUIS. PC 2
Local Extender
Remote Extender
Black Box IC502A kit
iXon ultra 888 r band
Optec 2" Focalizer
USB 3.0
iXon ultra 888 i band
Optec 2" Focalizer
Ethernet
Duplex LC connectors Multimode fiber optic cable (MMF)
SPARC4 Electronic Controller
iXon ultra 888 z band
Optec 2" Focalizer
ECHARPE Controller
Icron Ranger 2224
(available at OPD)
USB 2.0
Calibrating wheel, Waveplate selection, Waveplate rotation, and Analyser slider
Mechanisms
ECHARPE AFIES
status
(already in use at OPD)
PC TCSPD
PC Autoguider
Icron USB Extender
CAT5 cable
Andor Luca R
Auto-guider
Optec 3" Focalizer
Autoguider mirror
Remove?
SPARC4 / ECHARPE beam switcher
RS232
Manual
ECHARPE module

GUI

- Luciano Fraga
- Conceito ainda precisa ser finalizado
- Definição do responsável pelo desenvolvimento

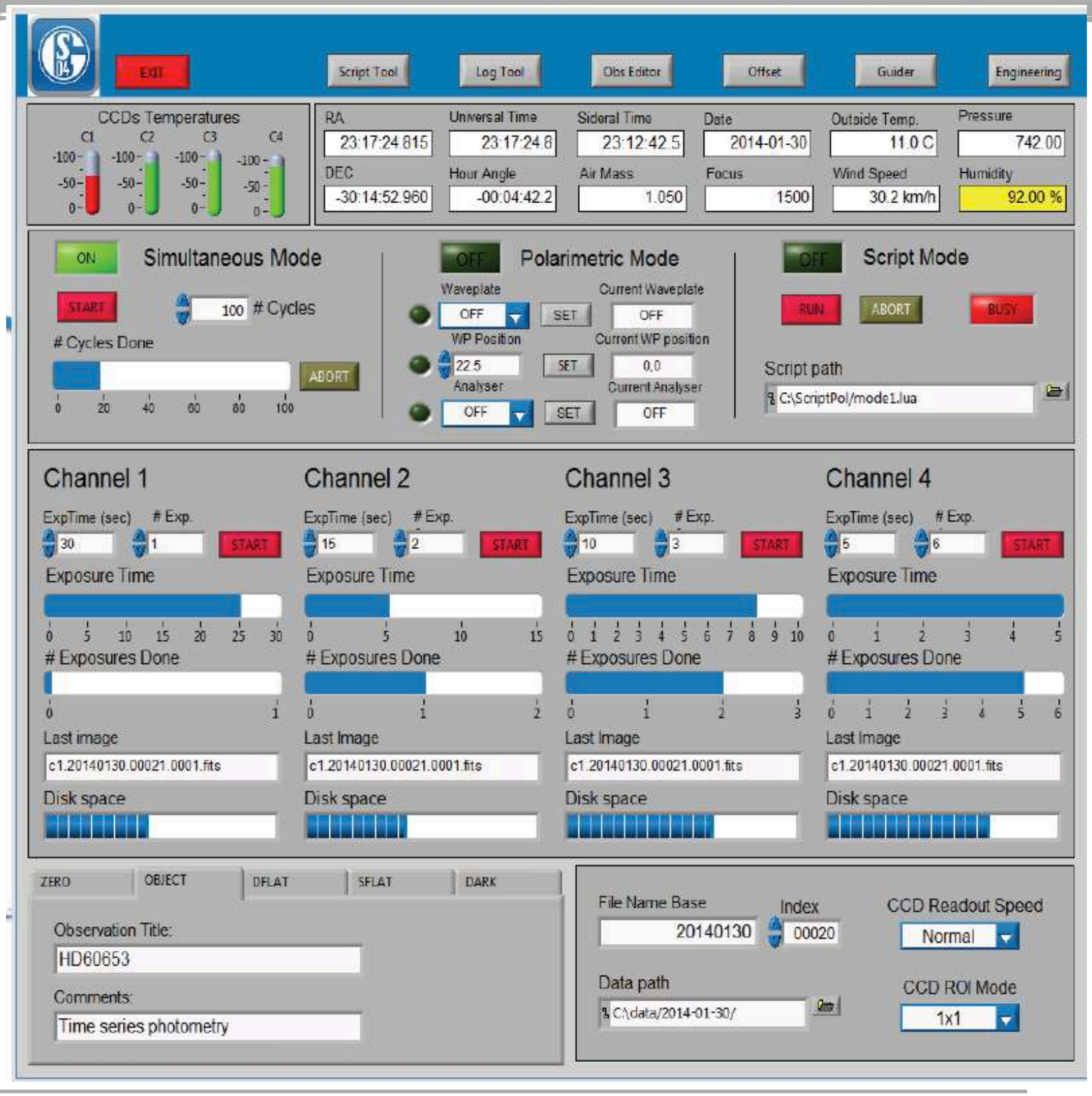

Software de redução de dados

- Software de redução de dados
  - ✓ quick view durante a noite
  - ✓ pipeline propriamente dito para produzir produtos finais de redução

- Solicitação de bolsa PNPD sendo avaliada no INPE

- Início depende de bolsista

Equipe técnica

Alessandro da S. Paula (LNA)
Antonio M. Magalhães (USP)
Antonio Pereyra (IGP/Peru)
Braulio de Albuquerque (INPE)
Cláudia V. Rodrigues (INPE)
Clemens Gneiding (LNA)
Damien Jones (Prime Optics)
Denis V. Bernardes (LNA)
Eder Martioli (LNA)
Flavio Ribeiro (LNA)
Francisco Rodrigues (LNA)
Francisco J. Jablonski (INPE)
Jesulino Bispo (LNA)
Keith Taylor (Instruments4)
Luciano Fraga (LNA)
Luiz Antonio Reitano (INPE)
Marcio Vital de Arruda (LNA)
Rene Laporte (INPE)

Equipe científica

Alex Carciofi (USP)
André de C. Milone (INPE)
Antonio M. Magalhães (USP)
Antonio Pereyra (IGP/Peru)
Cláudia V. Rodrigues (INPE)
Deonisio Cieslinski (INPE)
Eder Martioli (LNA)
Francisco J. Jablonski (INPE)
Gabriel Franco (UFMG)
Joaquim E. R. Costa (INPE)
Karleyne M. G. da Silva (ESO)
Leonardo A. de Almeida (USP)
Luciano Fraga (LNA)
Marcelo Borges (ON)
Marcelo Assafin (UFRJ)

Futuro

- 2018
  - ✓ montagem dos barris e aferição da qualidade óptica
  - ✓ usinagem
  - ✓ início da montagem e testes de subsistemas
  - ✓ início da integração
  - ✓ início da GUI e do software de aquisição
  - ✓ início do software de reduçao
- 2019
  - ✓ integração e testes
  - ✓ primeira luz
  - ✓ comissionamento
- 2020
  - ✓ entrega do instrumento para o OPD/LNA

Obrigada!

Agradecimentos (CVR)

CNPq : Proc. 306701/2015-4

Fapesp: 2013/26258-4

Some examples of present OPD science that can be benefited from SPARC4

Science cases

- **Binaries, including interacting binaries**
  - ✓ multi-band light and polarization curves
- **Solar system studies**
  - ✓ multi-band light curves
- **Exoplanets**
  - ✓ multi-band light and polarization curves
- **Pulsating stars**
  - ✓ multi-band light curves
- **Circumstellar envelopes**
  - ✓ multi-band polarimetry
- **Star forming regions**
  - ✓ multi-band polarimetry
- **Stellar populations and open cluster**
  - ✓ multi-band photometry

Multicolor time-series: photometry and polarimetry

Interacting binaries

- Interacting binaries is one science case that can benefit from SPARC4/OPD and SOAR complementary capabilities.

- An specific example is the study of magnetic cataclysmic variables. Scientific goals:
  - ✓ study the magnetic accretion
  - ✓ understand the evolution of compact binaries having highly magnetic stars

- Method
  - ✓ candidates selected from Catalina Real Time Survey
  - ✓ first verification by snapshot spectroscopy (SOAR Goodman)
  - ✓ time-resolved spectroscopy, photometry, and/or polarimetry follow-up using SOAR or OPD telescopes
    - final classification
    - modelling/physical insight

HS 2231+2441: an HW Vir system composed by a low-mass white dwarf and a brown dwarf ⋆

L. A. Almeida[1]†, A. Damineli[1], C. V. Rodrigues[2], M. G. Pereira[3] and F. Jablonski[2]

2017 MNRAS

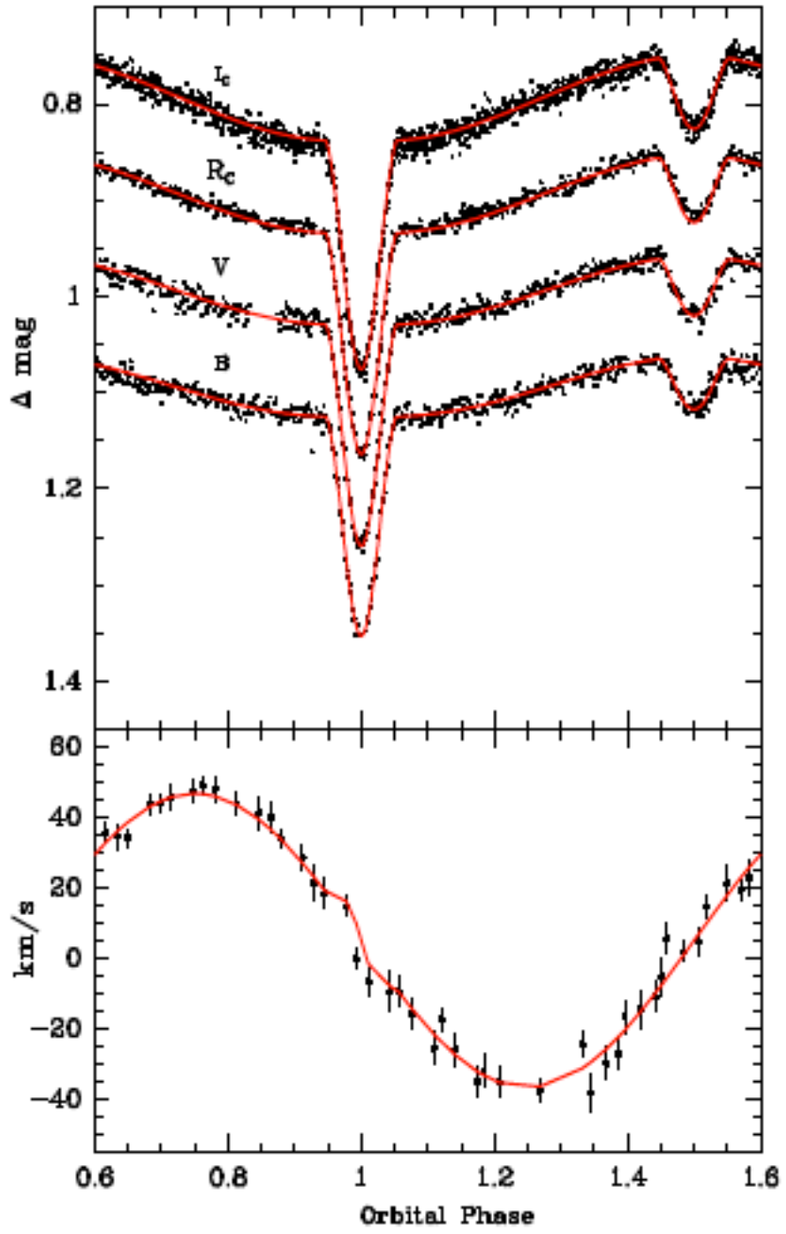

Figure 7. The best simultaneous fit to the light curves in the B, V, R_C, and I_C bands and primary radial velocity curve performed with the Wilson-Devinney code.

Table 4. System parameters of the best model fit to photometric light curves in the B, V, R_C, I_C bands and the primary star radial velocity curve of HS 2231+2441.

Parameter	Value	
Fixed Parameters	Solution 1	Solution 2
$q(M_2/M_1)$	0.190	0.160
T_1(K)	28500	28500
α_1^a(B)	0.290	0.290
α_1^a(V)	0.256	0.256
$\alpha_1^a(R_C)$	0.222	0.222
$\alpha_1^a(I_C)$	0.188	0.188
α_2^a(B)	0.727	0.677
α_2^a(V)	0.742	0.651
$\alpha_2^a(R_C)$	0.705	0.624
$\alpha_2^a(I_C)$	0.594	0.527
β_1^b	1	1
β_2^b	0.3	0.3
A_1^c	1	1
Adjusted Parameters	Solution 1	Solution 2
Ω_1^d	4.31±0.05	4.24±0.06
Ω_2^d	2.91±0.03	2.68±0.02
T_2(K)	3010±460	3410±500
i (°)	79.4±0.2	79.6±0.1
a^e ($R_\odot$)	0.59±0.01	0.67±0.02
A_2^c(B)	1.243±0.07	1.39±0.09
A_2^c(V)	1.305±0.06	1.28±0.08
$A_2^c(R_C)$	1.574±0.05	1.76±0.06
$A_2^c(I_C)$	1.797±0.05	1.87±0.05
Derived parameters		
M_1 ($M_\odot$)	0.190±0.006	0.288±0.005
M_2 ($M_\odot$)	0.036±0.004	0.046±0.004
R_1 ($R_\odot$)	0.144±0.004	0.165±0.005
R_2 ($R_\odot$)	0.074±0.004	0.086±0.004
log g_1 (cm s^{-2})	5.40±0.03	5.46±0.03
log g_2 (cm s^{-2})	5.25±0.07	5.23±0.006
$v_{rot;1}^f$	65.9±1.9	75.5±2.3
$v_{rot;2}^f$	33.9±1.9	39.4±1.9

[a] Linear limb darkening coefficient from Claret & Bloemen (2011);
[b] Gravity darkening exponent;
[c] Bolometric albedo;
[d] Adimensional potential;
[e] Components separation;
[f] Rotational velocity adopting synchronised rotation ($P_{orb} = P_{rot}$).

A new polar = magnetic cataclysmic variable

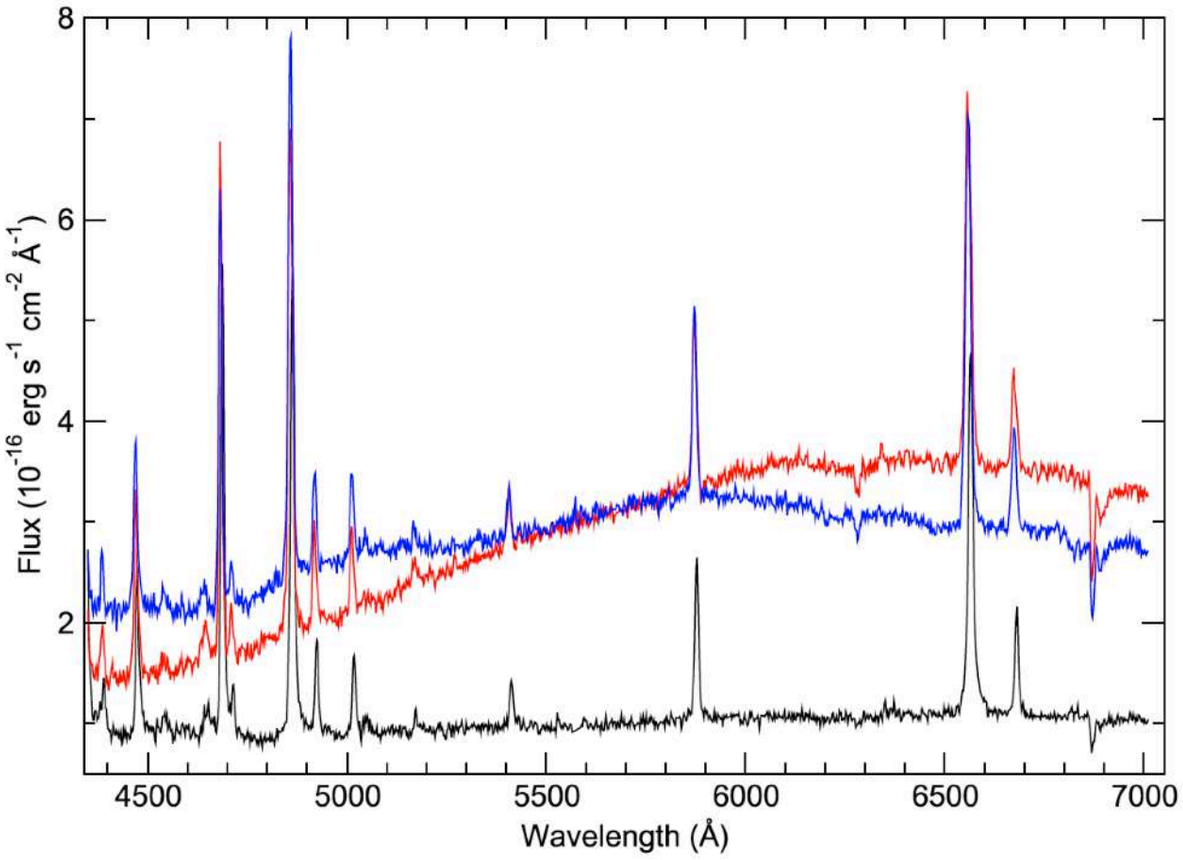

Figure 3. Three consecutive (black, red, blue) spectra of MLS1690-10 obtained with 20 minute intervals.

Goodman spectra

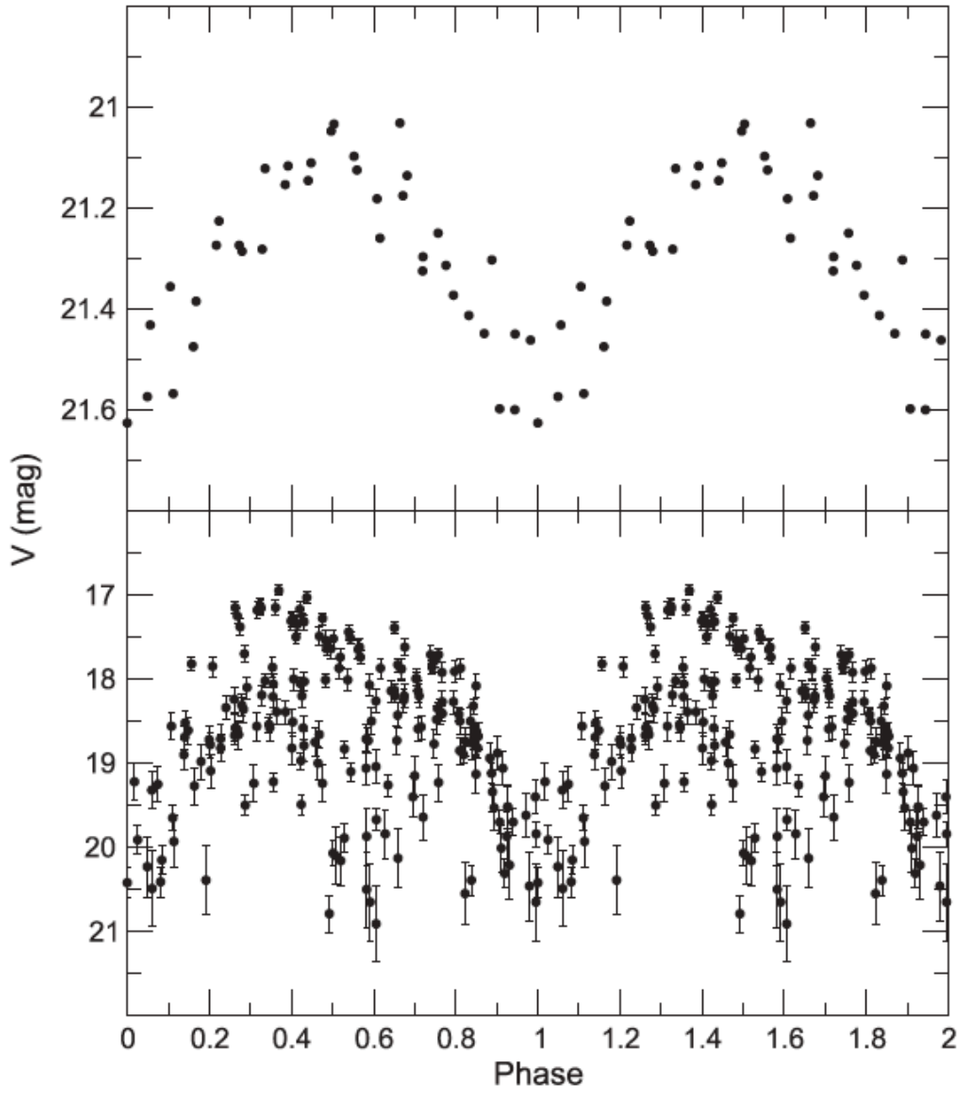

Figure 4. OPD (upper panel) and CRTS (lower panel) light curves of MLS1609-10, both folded with the period of 0.075439 days.

OPD photometry (upper panel)

Oliveira+2017

Photometry

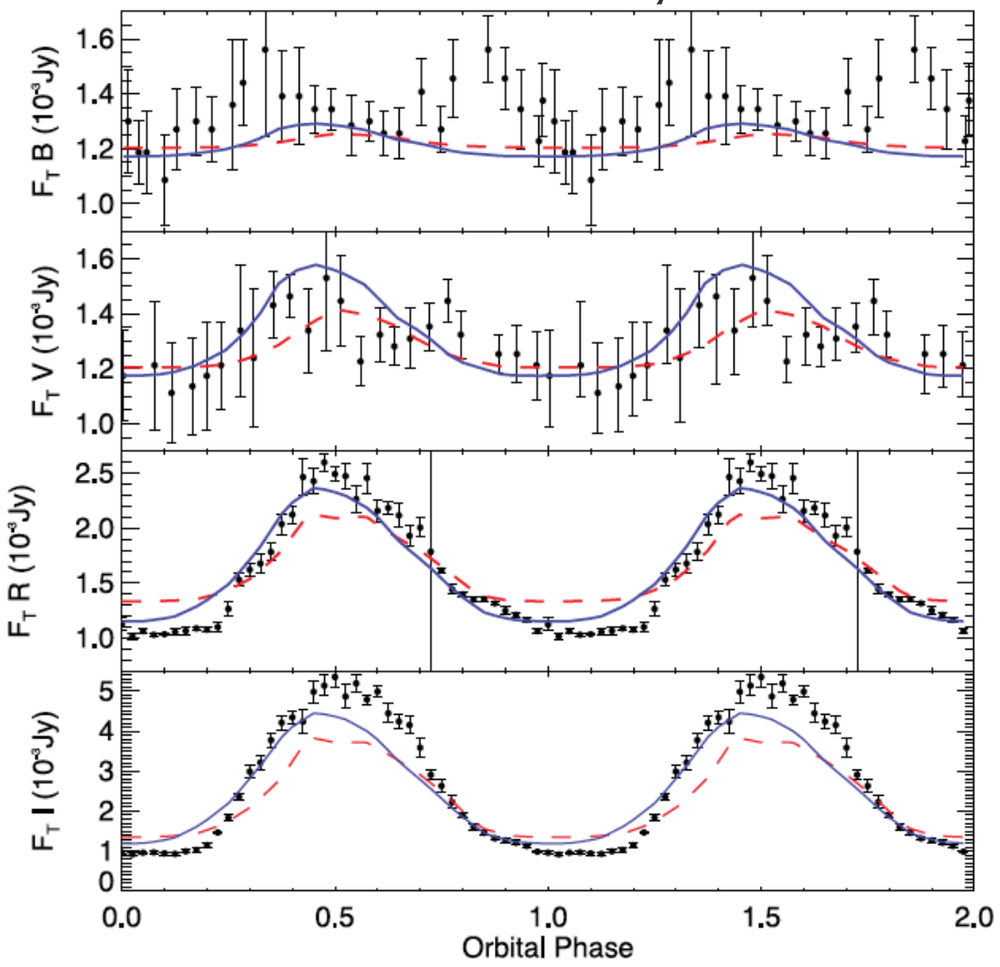

Polarimetry

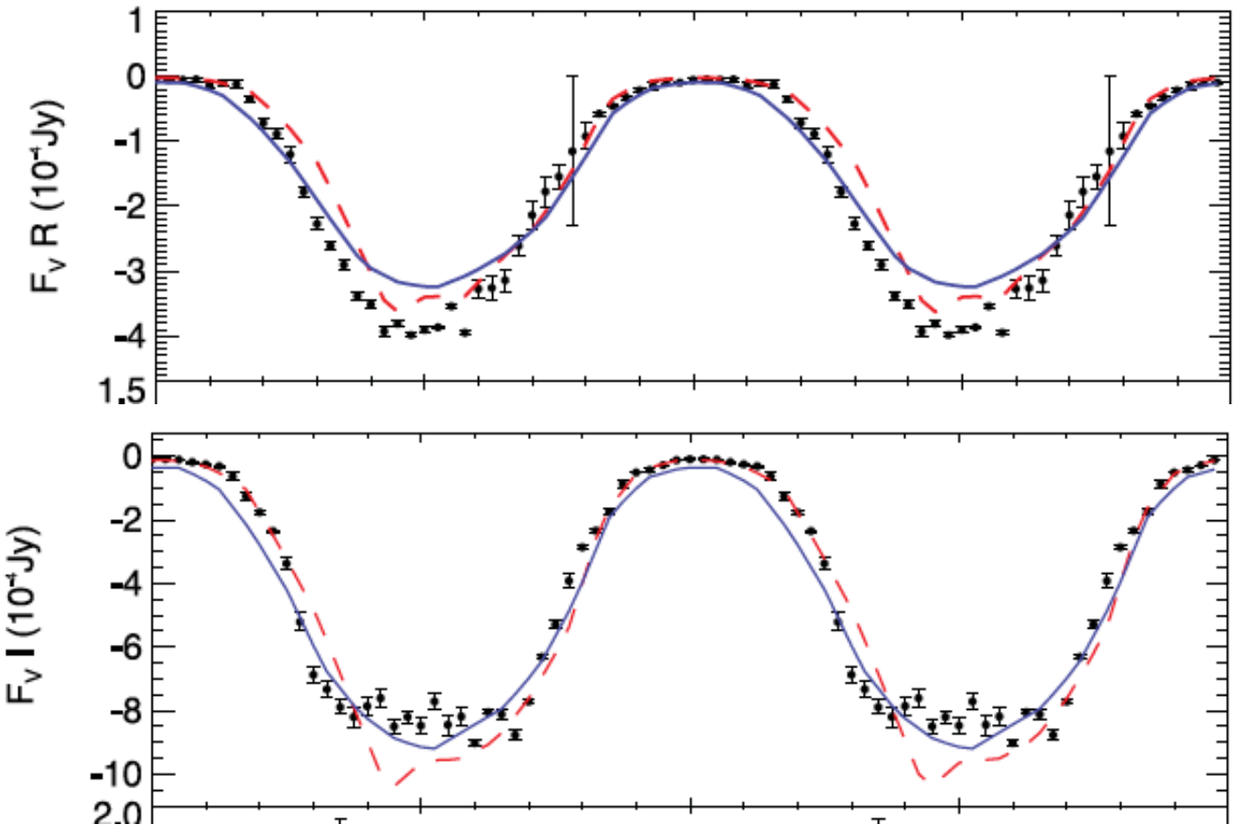

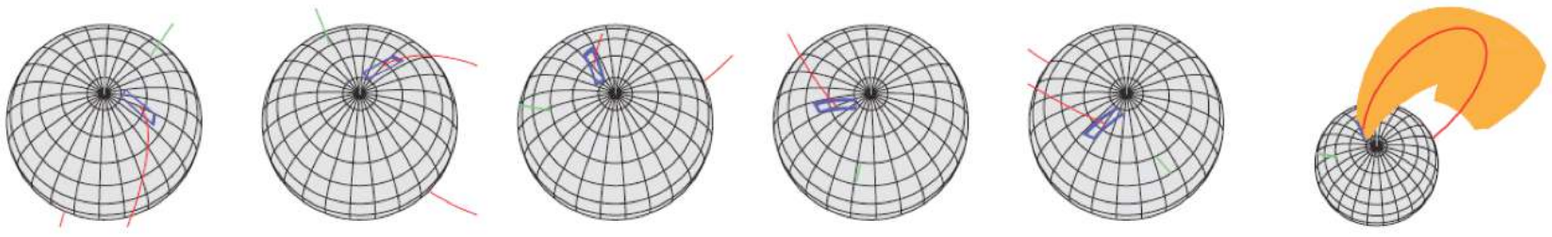

0.2 0.4 0.6 0.8 0.9

Orbital phase

Title: Stokes imaging of AM Her systems using 3D inhomogeneous models - II. Modelling X-ray and optical data of CP Tucanae

Authors: Silva, K. M. G.; Rodrigues, C. V.; Costa, J. E. R.; de Souza, C. A.; Cieslinski, D.; Hickel, G. R.

Bibliographic 2013MNRAS.432.1587S

Flickering in CVs

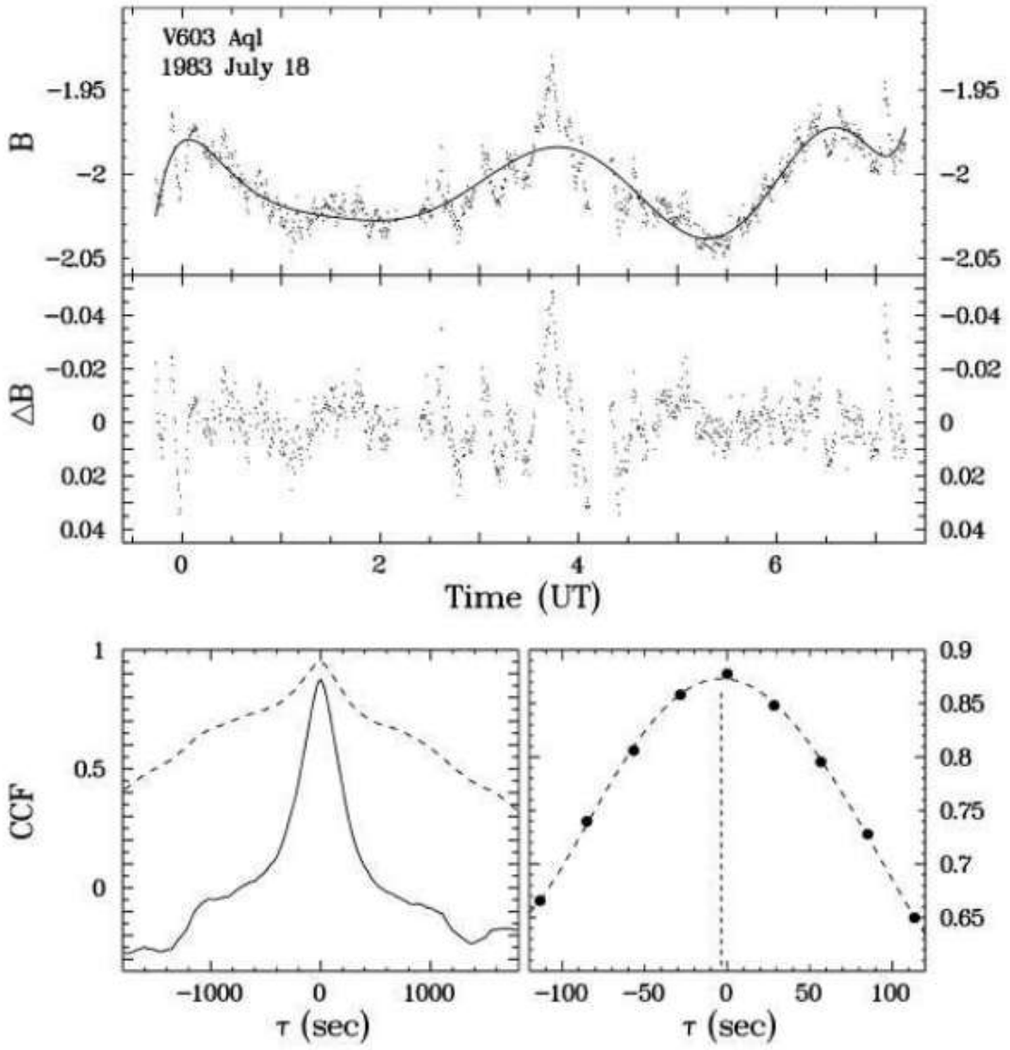

Fig. 1. Example of a light curve and the CCF of the brightness variations in two photometric bands. *Top: B*-band light curve of V603 Aql observed on 1983 July 18. The solid line is a fit of a high-order polynomial to the data. *Centre:* Residuals between the original light curve and the polynomial fit. *Bottom left:* CCF of the light curve shown in the top panel with the simultaneously observed light curve in the *U*-band (broken line) and of the residuals between the original data and the polynomial fit (solid line). *Bottom right:* Enlarged section of the maximum of the CCF shown as a solid line in the lower left panel (dots) together with a fit of a high-order polynomial to the data (broken curve). The broken vertical line indicates the location of the maximum of the fitted polynomial.

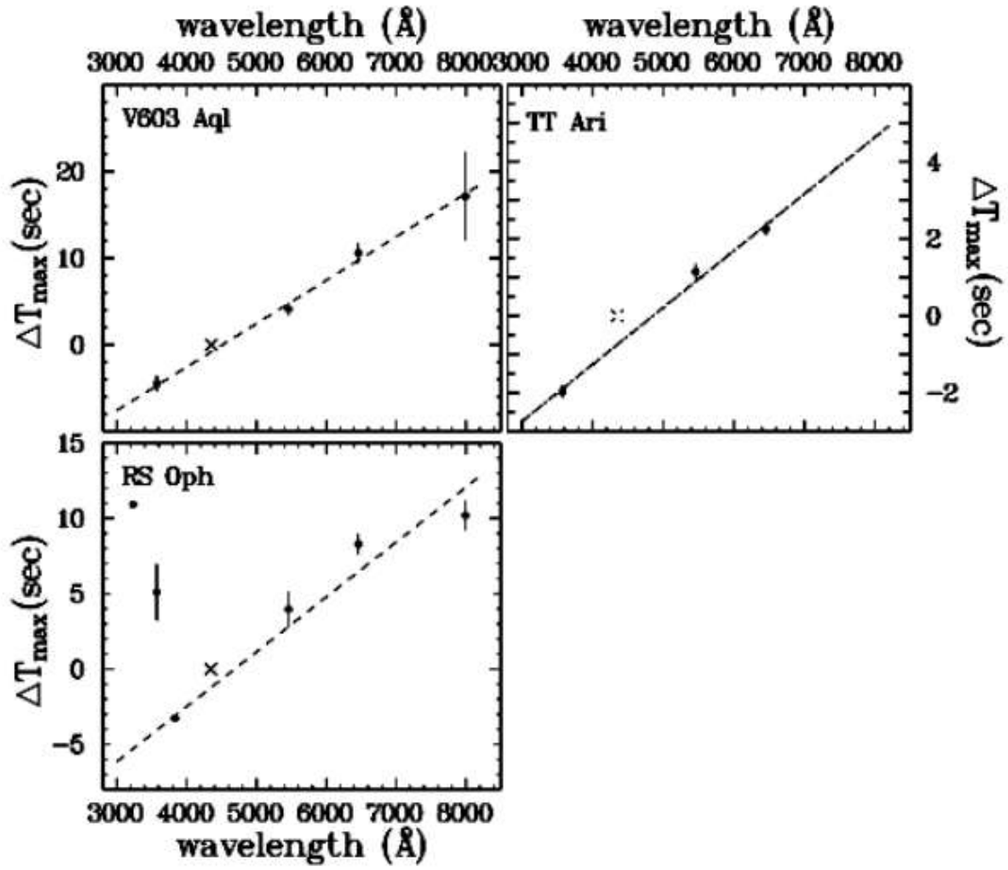

Fig. 4. Average ΔT_{max} derived from high time resolution light curves of V603 Aql, TT Ari and RS Oph as a function of isophotal wavelength of the comparison band. The broken lines are linear least-squares fits to the data points (in the case of RS Oph without considering the points referring to the *W* and *U* bands), weighted by the inverse of their standard deviations. The location of the reference band (*B*) is indicated by a cross. The error bars represent the mean error of the mean.

Title: Time lags of the flickering in cataclysmic variables as a function of wavelength

Authors: Bruch, Albert

Bibliographic Code: 2015A&A...579A..50B

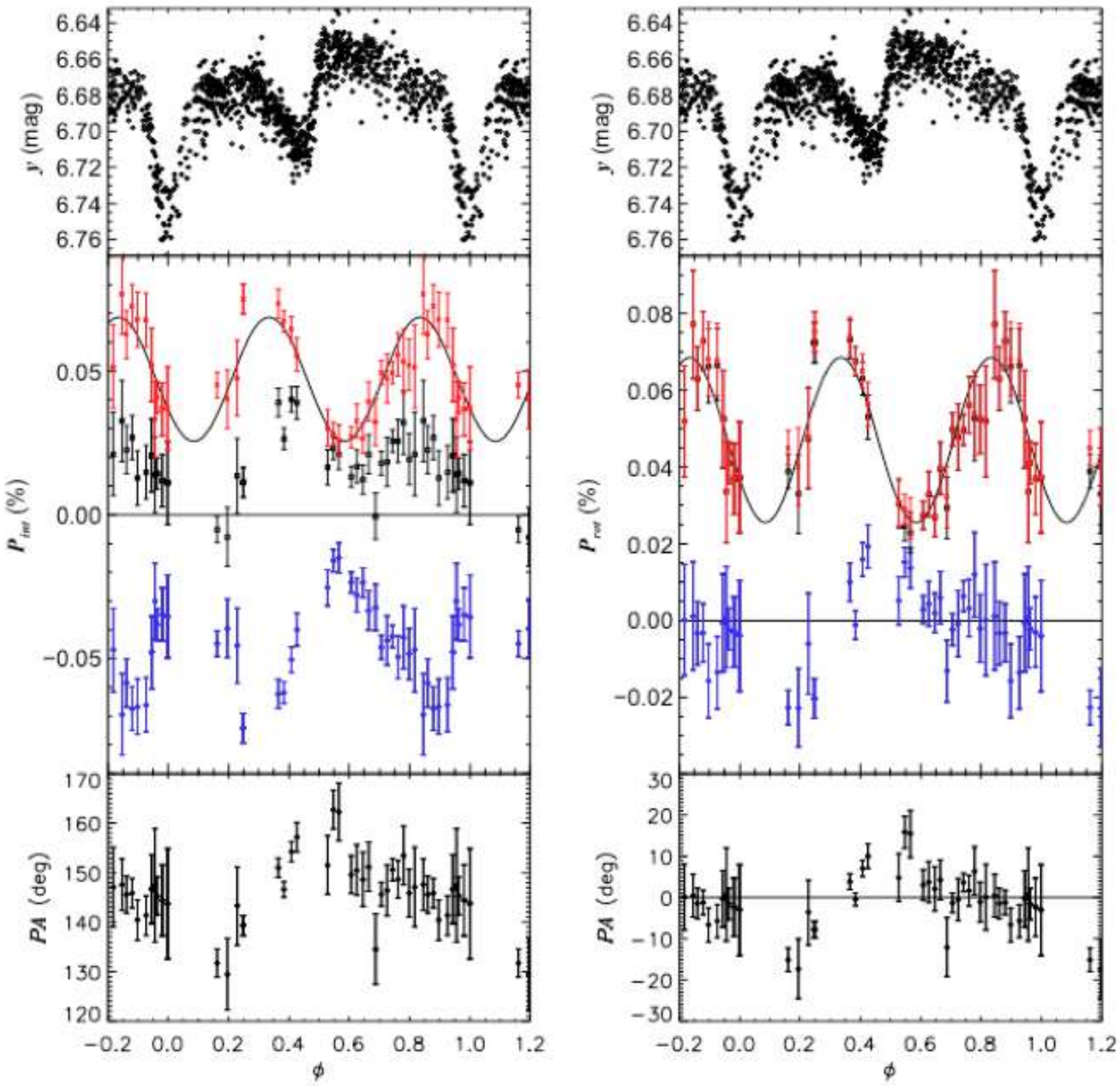

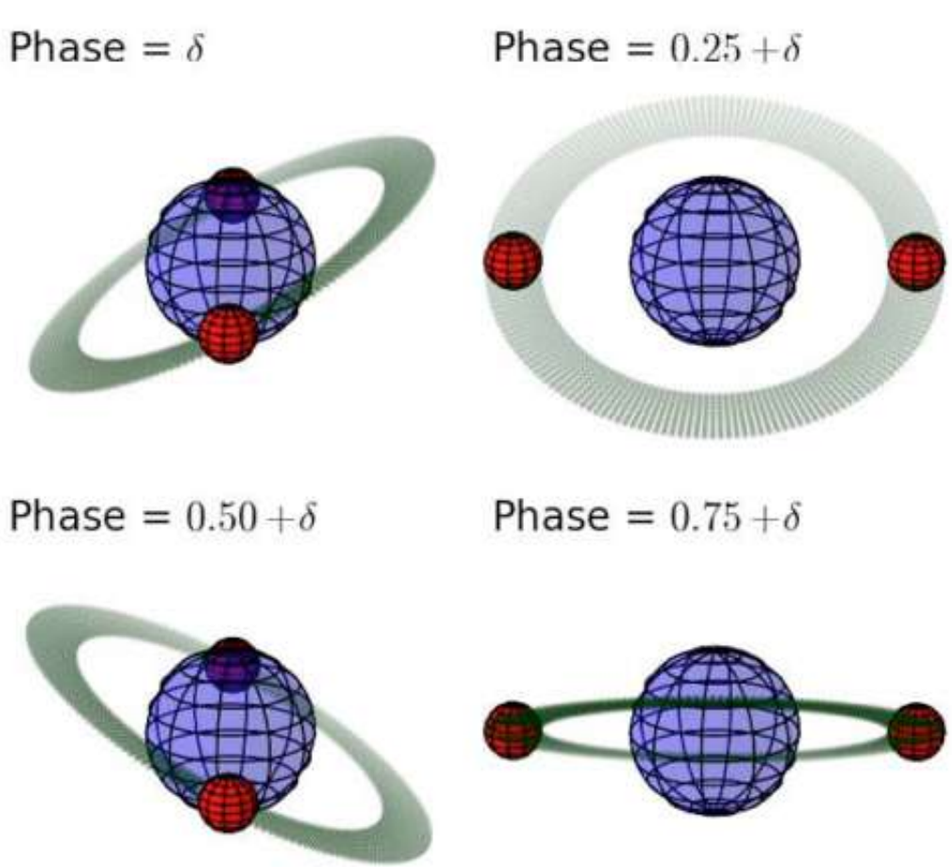

FIG. 3.— Geometric conception of the "dumbbell + disk" model, to scale.

Title: Polarimetric Observations of σ Orionis E

Authors: Carciofi, A. C.; Faes, D. M.; Townsend, R. H. D.; Bjorkman, J. E.

Bibliographic 2013ApJ...766L...9C

Interstellar magnetic field and dust properties

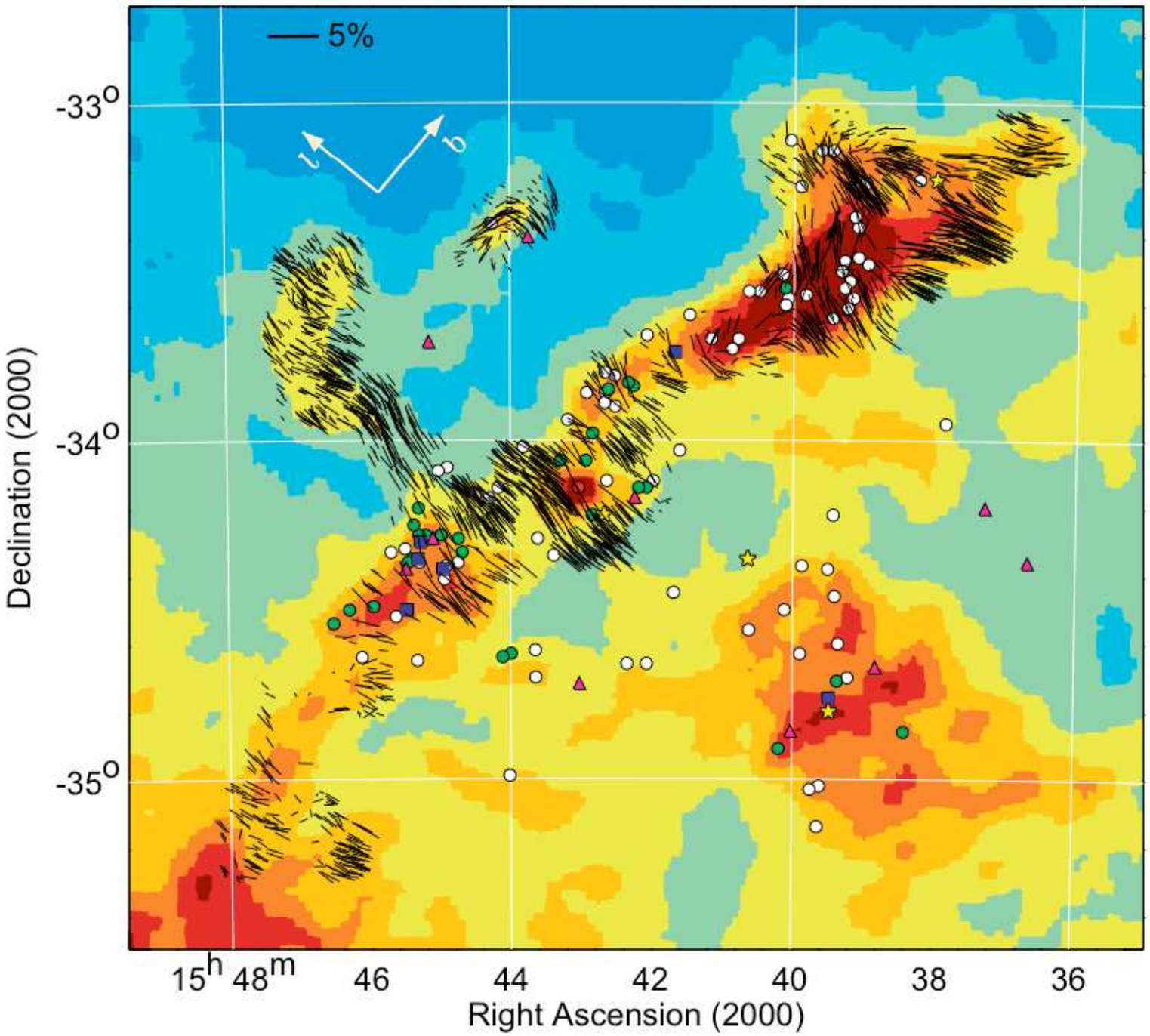

Figure 4. The obtained polarization degree vectors overlaid on the *IRAS* 100 μm emission map of Lupus I and its surrounding region. The length of each vector correlates linearly with the measured degree of polarization according to the scale indicated in the upper left corner, and its orientation gives the direction of the plane-of-sky component of the local magnetic field. The position of different classes of young stellar objects, from Rygl et al. (2013), are indicated according with the following code: unbound cores (white circles), prestellar cores (green circles), class 0 (red circle), class I (triangles), class II (squares), and class III (stars). Directions of increasing Galactic longitude (l) and latitude (b) are shown in the upper left corner.

Title: Tracing the Magnetic Field Morphology of the Lupus I Molecular Cloud

Authors: Franco, G. A. P.; Alves, F. O.

Bibliographic 2015ApJ...807....5F

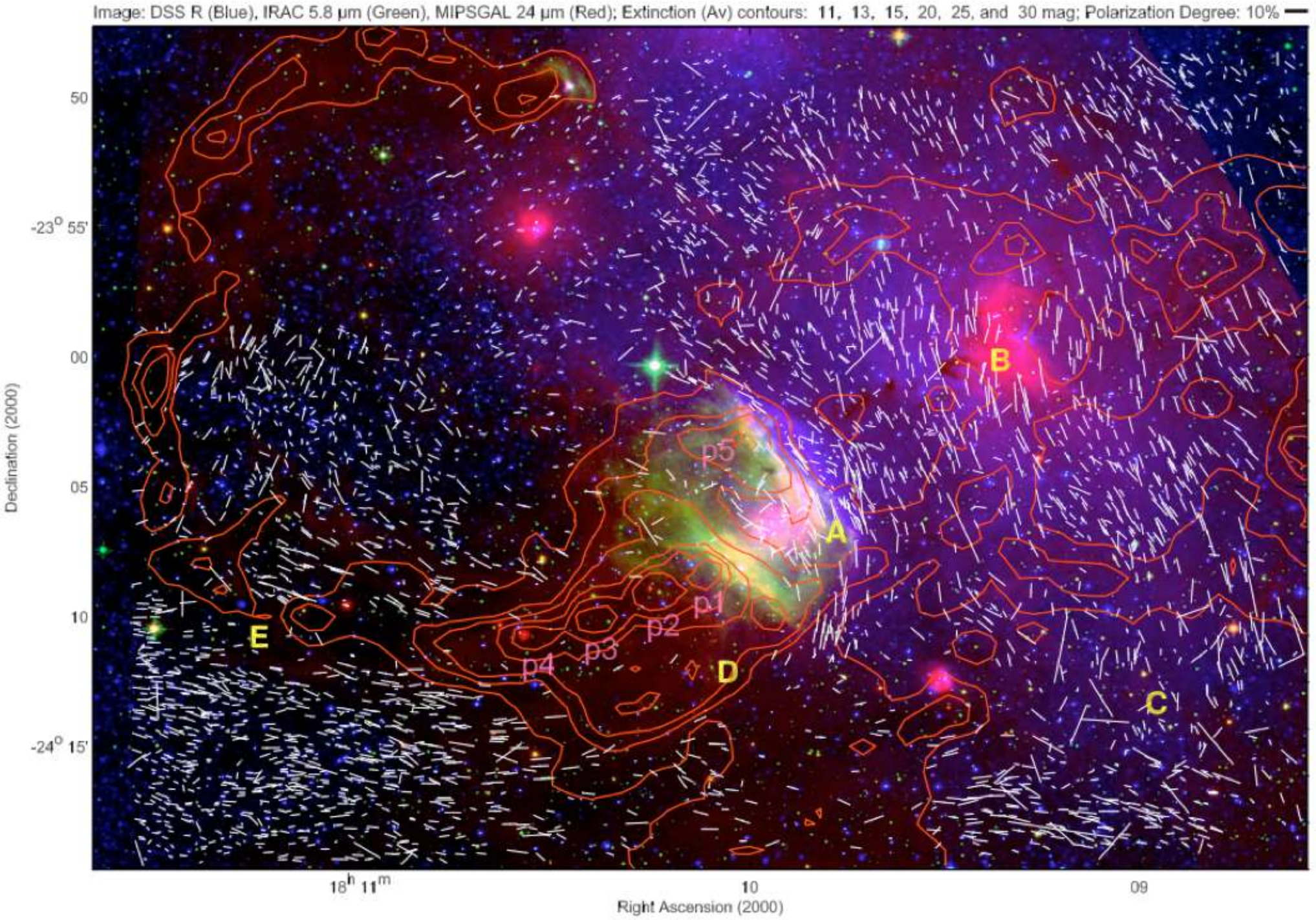

FIG. 4.— R band polarimetric mapping of Sh 2-29. The combined image is composed by the R band (DSS, blue), as well as by the 5.8 and 24 μm bands from *Spitzer* (respectively green and red). The size of each vector is proportional to P (a $P = 10\%$ vector is shown at the upper right). Labels from A to E are used to highlight some of the main features inferred from the polarization vectors' orientation pattern, as discussed in Section 5.1. Indicators p1 to p5 show the location of dense cloud structures around the central cavity, presenting peak extinction values between $A_V = 20$ and $A_V > 35$ (see Section 5.6).

Title: Optical/Near-infrared Polarization Survey of Sh 2-29: Magnetic Fields, Dense Cloud Fragmentations, and Anomalous Dust Grain Sizes

Authors: Santos, Fábio P.; Franco, Gabriel A. P.; Roman-Lopes, Alexandre; Reis, Wilson; Román-Zúñiga, Carlos G.

Bibliographic 2014ApJ...783....1S

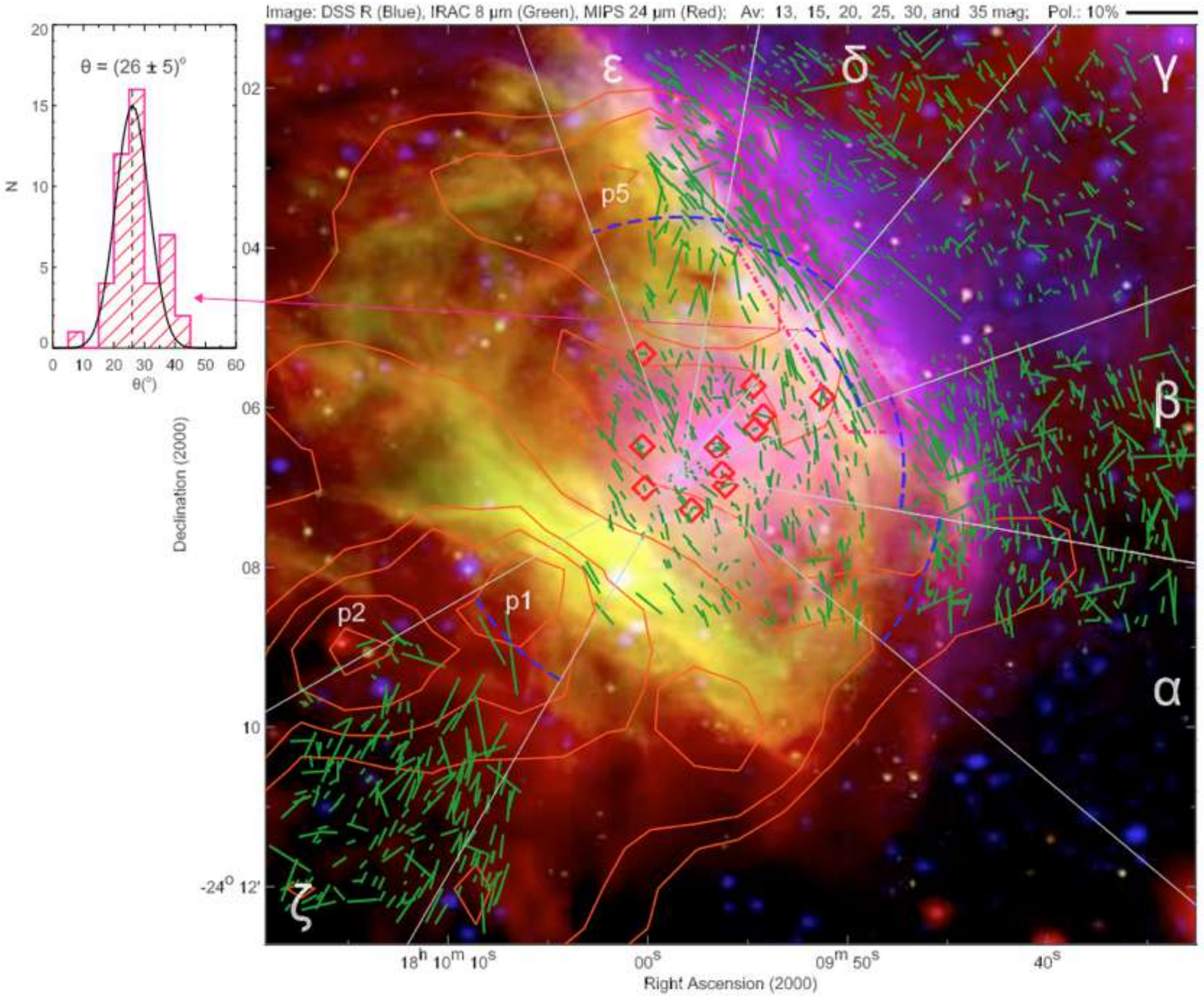

FIG. 5.— Near-IR (H band) polarimetric mapping toward the Sh 2-29 central interstellar cavity. A RGB combined image of this area is used, corresponding to the R-DSS band (blue), as well as the 8 and 24 μm bands from *Spitzer* (respectively green and red). The radial strips labeled from α to ζ are used to study polarization degree as a function of radius (Section 5.5), with the blue dashed lines indicating the positions were a rise in polarization occur. Red diamonds mark the positions of those stars presenting Hα emission (Ogura et al. 2002) that were detected in the polarimetric survey. The dot-dashed pink polygon indicates the area which was used to apply the Chandrasekhar-Fermi method (see Section 5.8). The polarization angle histogram shown at the left is used in this same analysis in order to derive the angle dispersion within this area.

Microlenses

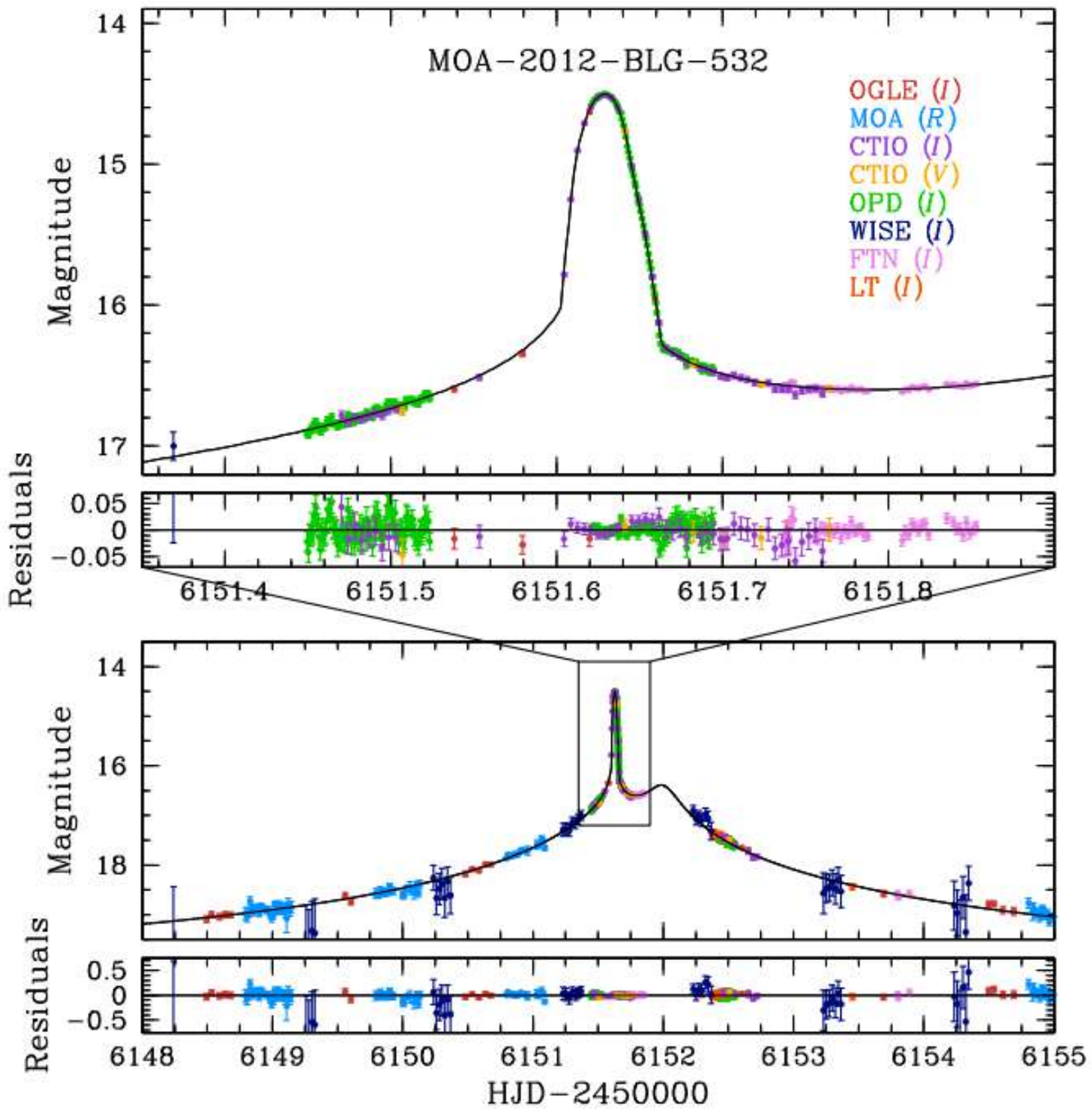

Figure 6. Light curve of MOA-2012-BLG-532. The notations are the same as those in Figure 2.

Title: Candidate Gravitational Microlensing Events for Future Direct Lens Imaging
Publication: The Astrophysical Journal, Volume 794, Issue 1, article id. 71, 11 pp. (2014).

Henderson+

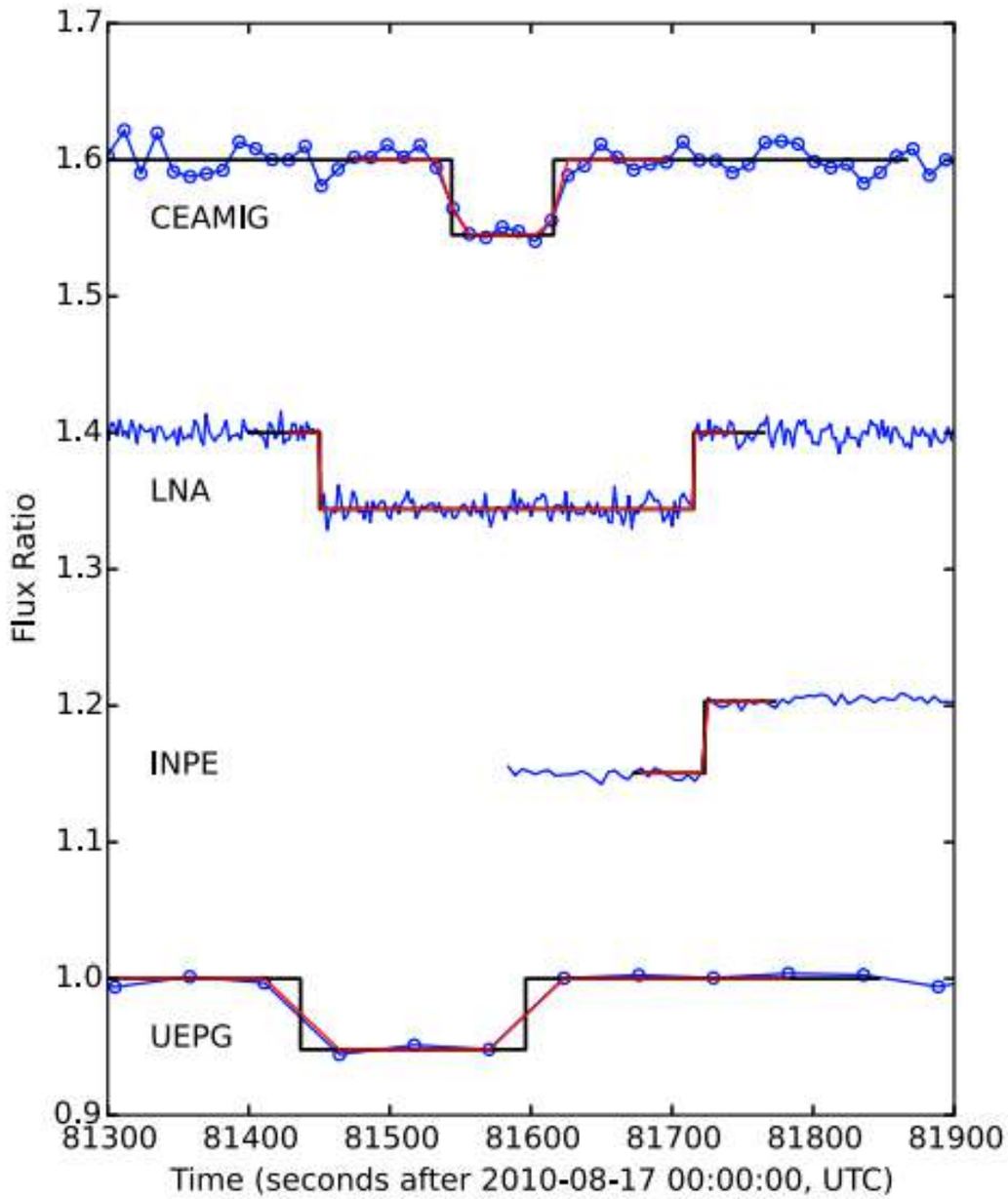

Title: Results of two multichord stellar occultations by dwarf planet (1) Ceres

Authors: Gomes-Júnior, A. R.; Giacchini, B. L.; Braga-Ribas, F.; Assafin, M.; Vieira-Martins, R.; Camargo, J. I. B.; Sicardy, B.; Timerson, B.; George, T.; Broughton, J.; Blank, T.; Benedetti-Rossi, G.; Brooks, J.; Dantowitz, R. F.; Dunham, D. W.; Dunham, J. B.; Ellington, C. K.; Emilio, M.; Herpich, F. R.; Jacques, C.; Maley, P. D.; Mehret, L.; Mello, A. J. T.; Milone, A. C.; Pimentel, E.; Schoenell, W.; Weber, N. S.

Bibliographic 2015MNRAS.451.2295G

Monthly Notices
of the
ROYAL ASTRONOMICAL SOCIETY

MNRAS **451,** 4183–4192 (2015) doi:10.1093/mnras/stv1105

MLS110213:022733+130617: a new eclipsing polar above the period gap

K. M. G. Silva,[1,2★] C. V. Rodrigues,[2★] A. S. Oliveira,[1] L. A. Almeida,[2,3,4] D. Cieslinski,[2] J. E. R. Costa[2] and F. J. Jablonski[2]

[1] *Universidade do Vale do Paraíba (Univap), Av. Shishima Hifumi, 2911 – São José dos Campos – SP, 12244-000, Brazil*
[2] *Instituto Nacional de Pesquisas Espaciais (INPE/MCTI), Av. dos Astronautas, 1758 – São José dos Campos – SP, 12227-010, Brazil*
[3] *Instituto de Astronomia, Geofísica e Ciências Atmosféricas (IAG/USP), Rua do Matão 1226 – São Paulo – SP, 05508-090, Brazil*
[4] *Department of Physics & Astronomy, Bloomberg Center for Physics and Astronomy, Room 520, 3400 N Charles St, Johns Hopkins University, Baltimore, MD 21218, USA*

Accepted 2015 May 12. Received 2015 May 12; in original form 2015 January 8

ABSTRACT

This study confirms MLS110213:022733+130617 as a new eclipsing polar. We performed optical spectroscopic, polarimetric and photometric follow-up of this variable source identified by the Catalina Real Time Transient Survey. Using the mid-eclipse times, we estimated an

An eclipsing polar

Goodman spectra

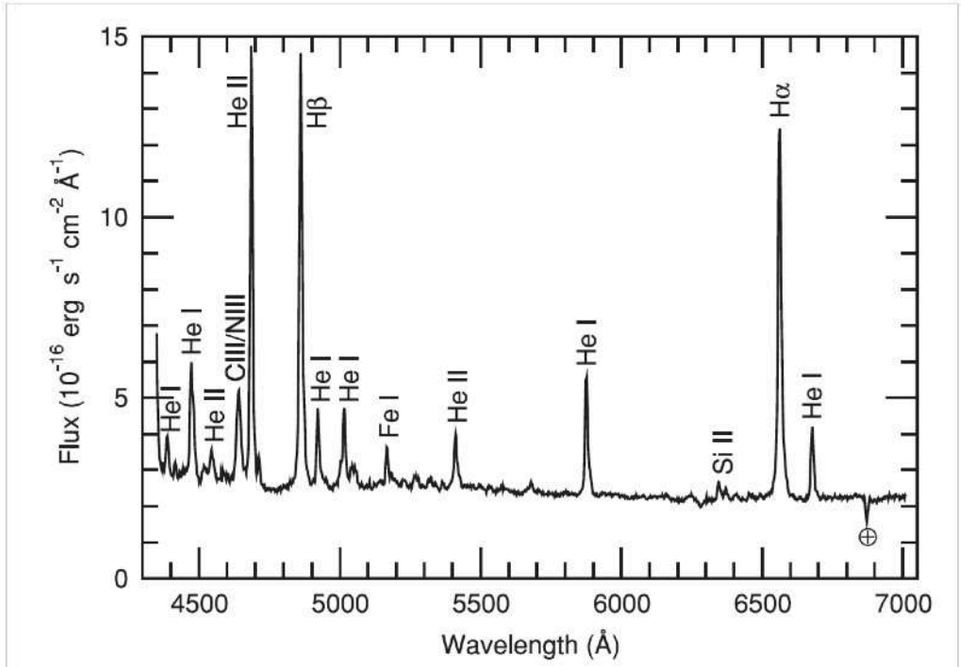

Figure 3. Average spectrum of MLS110213.

OPD photometry and polarimetry

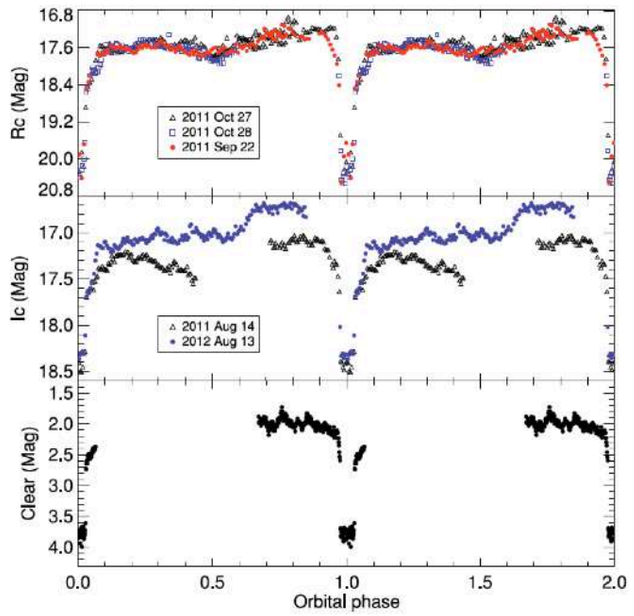

Figure 1. OPD light curves of MLS110213 folded with the ephemeris estimated in Section 3.1. From top to bottom: R_C band, I_C band and white light. White light magnitudes are not calibrated.

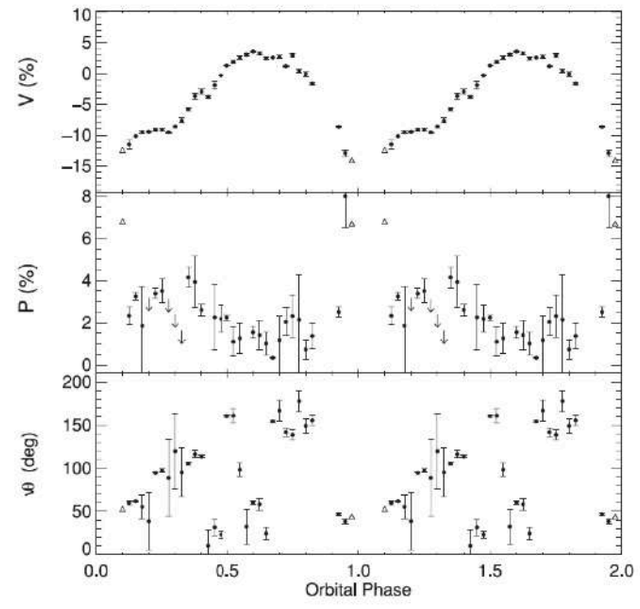

Figure 2. Polarimetry of MLS110213 in R_C band. The data points were grouped in 40 orbital phase bins. The lack of points around phase 0 corresponds to the eclipse in which we had no signal to measure the polarization. From top to bottom, the panels show the circular polarization, linear polar-

Geometry from data modelling

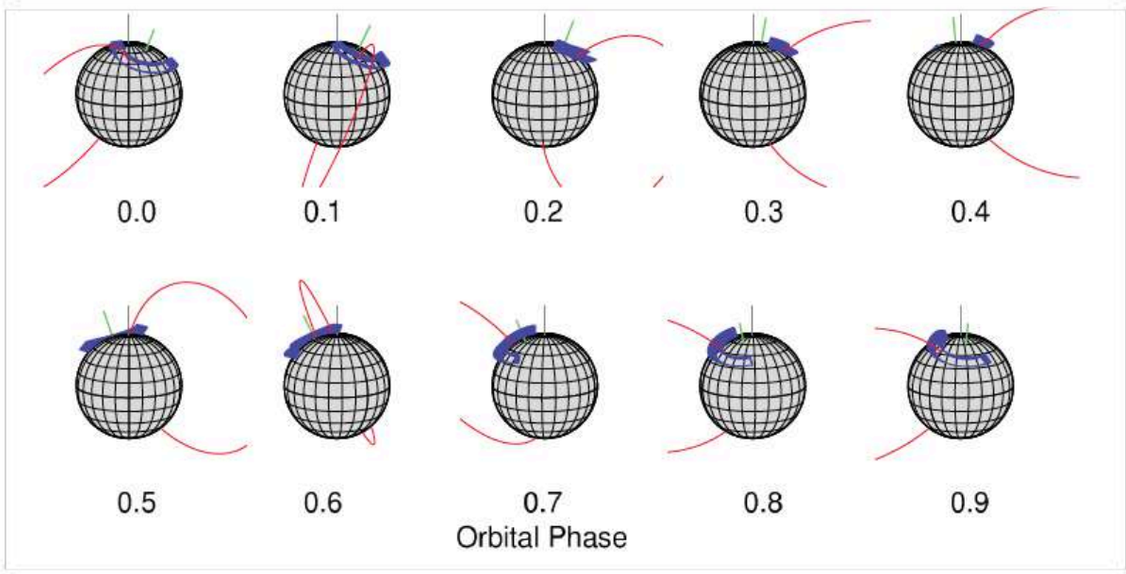

Silva+2015

The Astronomical Journal, 153:144 (18pp), 2017 April https://doi.org/10.3847/1538-3881/aa610d

Exploratory Spectroscopy of Magnetic Cataclysmic Variables Candidates and Other Variable Objects*

A. S. Oliveira[1], C. V. Rodrigues[2], D. Cieslinski[2], F. J. Jablonski[2], K. M. G. Silva[3], L. A. Almeida[4], A. Rodríguez-Ardila[5], and M. S. Palhares[1]
[1] IP&D, Universidade do Vale do Paraíba, 12244-000, São José dos Campos, SP, Brazil; alexandre@univap.br
[2] Divisão de Astrofísica, Instituto Nacional de Pesquisas Espaciais, 12227-010, São José dos Campos, SP, Brazil
[3] Gemini Observatory, Casilla 603, La Serena, Chile
[4] Instituto de Astronomia, Geofísica e Ciências Atmosféricas, Universidade de São Paulo, 05508-900, São Paulo, SP, Brazil
[5] Laboratório Nacional de Astrofísica LNA/MCTI, 37504-364, Itajubá MG, Brazil
Received 2016 July 6; revised 2017 February 14; accepted 2017 February 14; published 2017 March 9

Abstract

The increasing number of synoptic surveys made by small robotic telescopes, such as the photometric Catalina Real-Time Transient Survey (CRTS), provides a unique opportunity to discover variable sources and improves the statistical samples of such classes of objects. Our goal is the discovery of magnetic Cataclysmic Variables (mCVs). These are rare objects that probe interesting accretion scenarios controlled by the white-dwarf magnetic field. In particular, improved statistics of mCVs would help to address open questions on their formation and evolution. We performed an optical spectroscopy survey to search for signatures of magnetic accretion in 45 variable objects selected mostly from the CRTS. In this sample, we found 32 CVs, 22 being mCV candidates, 13 of which were previously unreported as such. If the proposed classifications are confirmed, it would represent an increase of 4% in the number of known polars and 12% in the number of known IPs. A fraction of our initial sample was classified as extragalactic sources or other types of variable stars by the inspection of the identification spectra. Despite the inherent complexity in identifying a source as an mCV, variability-based selection, followed by spectroscopic snapshot observations, has proved to be an efficient strategy for their discoveries, being a relatively inexpensive approach in terms of telescope time.

Key words: binaries: close – novae, cataclysmic variables – stars: dwarf novae – stars: variables: general – techniques: spectroscopic

Supporting material: data behind figure, machine-readable table

SOAR spectra

Search of mCVs

- First sample of 45 CRTS objects (Oliveira+2017)
  - ✓ 32 CVs
    - 22 mCVs: confirmed or strong candidate
  - ✓ interesting extragalactic objects in the sample (see Ardila's talk)

Table 1
List of Observed Targets

Object name	Abbreviation	R.A. (J2000)	Decl. (J2000)	Date Obs.	Telesc.	Exp. Time (s)	Type[a]
CSS091009:010412-031341	CSS0104-03	01:04:12	−03:13:41	2012 Aug 25	SOAR	3600	D/IP
CSS091215:021311+002153	CSS0213+00	02:13:11	+00:21:53	2012 Sep 09	SOAR	8100	E
MLS110213:022733+130617	MLS0227+13	02:27:33	+13:06:17	2012 Sep 09	SOAR	3600	P
CSS071206:031525-014051	CSS0315-01	03:15:25	−01:40:51	2012 Nov 13	SOAR	8100	E
CSS090922:032603+252534	CSS0326+25	03:26:03	+25:25:34	2012 Nov 20	SOAR	3600	D
CSS091109:035759+102943	CSS0357+10	03:57:59	+10:29:43	2012 Nov 12	SOAR	8100	P
MLS101203:045625+182634	MLS0456+18	04:56:25	+18:26:34	2012 Nov 13	SOAR	8100	P
XMMSL1 J063045.9-603110	XMM0630-60	06:30:45	−60:31:13	2012 Nov 12	SOAR	8100	N
MLS101226:072033+172437	MLS0720+17	07:20:33	+17:24:37	2012 Nov 12	SOAR	1440	P
1RXS J072103.3-055854	1RXS0721-05	07:21:03	−05:59:20	2012 May 01	SOAR	1440	HA
MLS120127:085402+133633	MLS0854+13	08:54:02	+13:36:33	2012 Dec 15	SOAR	8100	P
1RXS J100211.4-192534	1RXS1002-19	10:02:11	−19:25:36	2012 May 30	SOAR	360	P
CSS120324:101217-182411	CSS1012-18	10:12:17	−18:24:11	2012 May 30	SOAR	3600	D/IP

Polarimetry

- The polarimetry is done as explained in Magalhães et al. (1986).

- The retarder can be a half-wave plate or a quarter-wave plate, so linear and circular polarimetry can be performed

- All the polarimetric elements can be removed from the beam to perform standard imaging

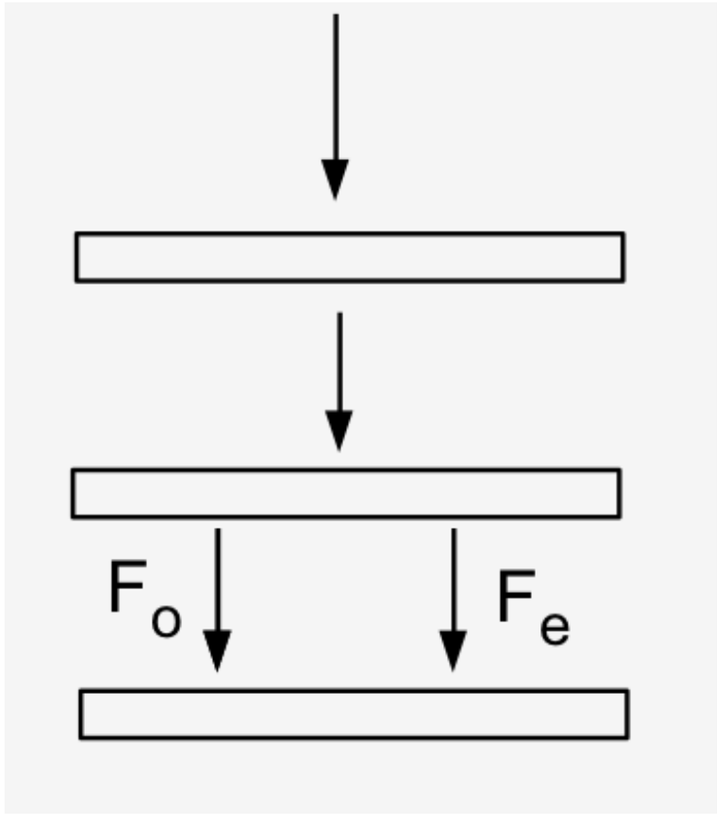

Rotating retarder

Savart Prism

Ordinary and extraordinary beams at the detector

SENSOR DETAILS

Manufacturer / Model No.	Pixels	Description
E2V / CCD201-20-1-179	1024x1024, 13µm x 13µm	Back-illum., Fringe Suppression, Dual AR-coated

WINDOW VARIANT

Window Variant	VIS-NIR Enhanced Wedged

SUMMARY OF SYSTEM TEST DATA

SENSITIVITY & READOUT NOISE

System Readout Rate	Preamp setting	CCD Sensitivity ♦1 (electrons per A/D count)	Single Pixel Noise ♦2 (electrons)
30 MHz, 16-bit Single, EM amplifier	1	17.6	188
	2	5.38	111
20 MHz, 16-bit Single, EM amplifier	1	16.8	148
	2	4.51	67.5
10 MHz, 16-bit Single, EM amplifier	1	16.2	78.6
	2	4.00	39.2
1 MHz, 16-bit Single, EM amplifier	1	16.1	25.1
	2	3.92	12.2
1 MHz, 16-bit Single, Conventional amplifier	1	3.36	6.55
	2	0.800	4.65
0.1MHz, 16-bit Single, Conventional amplifier	1	3.37	8.43
	2	0.800	3.21